

**Characterization of the nodulation phenotype of
E151, a pleiotropic pea (*Pisum sativum L.*) mutant**

by

MICHAEL CHLUP

A thesis

presented to the University of Waterloo

in fulfilment of the

thesis requirement for the degree of

Master of Science

in

Biology

Waterloo, Ontario, Canada, 2007

© Michael Chlup 2007

I hereby declare that I am the sole author of this thesis. This is a true copy of the thesis, including any required final revisions, as accepted by my examiners.

I understand that my thesis may be made electronically available to the public.

Abstract

Characterization of the nodulation phenotype of E151, a pleiotropic pea (*Pisum sativum L.*) mutant.

Michael Chlup
University of Waterloo, 2007

Co-Advisors:
Professor F.C. Guinel
Professor T.C. Charles

E151 (*sym15*) is characterized as a pleiotropic pea (*Pisum sativum L.*) mutant. It has been described as having short lateral roots, a short primary root, and a shorter epicotyl than that of the wild type Sparkle. Furthermore, after 4 weeks of growth it was described as a low nodulator since nodulation was rare (Kneen et al., 1994). My main objective is to further characterize the nodulation phenotype of this mutant. Inoculated of the mutant with two separate strains of *Rhizobium leguminosarum* biovar *viciae* caused E151 to develop more nodules when infected with 8401 (*lacZ*) than with 128C53K. These results suggest that E151 exhibits different levels of susceptibility to infection with different strains. Nodule organogenesis was studied by inoculating E151 with a rhizobial strain that constitutively produces β -galactosidase and then staining cleared whole root sections with the X-Gal substrate. The substrate produced a blue colour and allowed the rhizobial path to be visualized. It was found that nodule organogenesis in the mutant line is delayed at stage C (i.e., IT associated with cortical cell division) and eventually mature nodules form. The rates of N_2 fixation ($\mu\text{mol } N_2/\text{hr}$)/nodule dry weight (g) were found to be similar between Sparkle and E151 at 14, 21, and 28 days after inoculation. When comparing the nodulation defect of E151 to other pea mutants summarized by Guinel and Geil (2002), it appears that the nodulation phenotype of E151 is unique.

Acknowledgements

I am extremely grateful to my supervisor Dr. Frédérique Guinel (Department of Biology, Wilfrid Laurier University). Her feedback, support, and encouragement were greatly appreciated and helped me become a better researcher. I would like to thank my committee members, Dr. Trevor Charles, Dr. Barbara Moffatt, and Dr. Simon Chuong, all from the Department of Biology at the University of Waterloo, for their helpful suggestions and insight. Furthermore, I would like to thank Dr. Wayne Hawthorne for being part of my proposal committee and providing positive feedback.

I thank Dr. Tom LaRue for providing the Sparkle and E151 seeds used in our lab. I am grateful for the assistance that Dr. Stephen Hunt and Jason Curtis (Qubit Systems, Kingston, ON) provided to me with the setup of the Qubit System. I would like to acknowledge Dr. Neil Emery (Department of Biology, Trent University) for providing me with advice regarding nitrogen fixation. From the WLU Department of Biology, I would like to thank Dr. Lucy Lee, Dr. Bruce Wolff, and Gena Braun for the use of their equipment and supplies, and advice. A thank you also goes out to Michael Allen (Department of Chemistry, WLU) for helping me with the initial setup of the Qubit System. Finally, I would like to thank the faculty and staff members of both UW and WLU for their support.

Throughout the time that I have spent on my Masters, many colleagues have assisted me in the laboratory. I would like to give a special thanks to Scott Clemow for helping me with the etiolation study and Sean Delanghe for helping me count numerous

nodules. Also a thank you goes out to Mark Held, Alicia Pepper, and Andrew Morse for helping me keep my plants watered and providing useful feedback regarding my research. I would like to acknowledge my fellow graduate students at UW and WLU for their support during these past two years.

Special thanks go out to my family and friends who supported me throughout my Masters and kept my spirits high. Financial support was provided by the Natural Science and Engineering Research Council of Canada (operating grant to Dr. F.C. Guinel) and the University of Waterloo Graduate Scholarships (to MC).

Table of Contents

Author's declaration.....	ii
Abstract.....	iii
Acknowledgements.....	iv
Table of Contents.....	vi
List of Figures.....	ix
List of Tables.....	xi
List of Appendixes.....	xii
I. INTRODUCTION.....	1
A. Importance of the association.....	1
B. Use of model plants to study the association.....	3
C. Organogenesis of the Nodule.....	6
<i>A. Pre-infection events.....</i>	<i>6</i>
<i>B. Infection events.....</i>	<i>15</i>
<i>C. Late infection events.....</i>	<i>21</i>
D. Nodule physiology and regulation of nodulation.....	23
<i>A. Nodule physiology.....</i>	<i>23</i>
<i>B. Regulation of nodulation.....</i>	<i>30</i>
<i>B1. Auto-regulation mechanism.....</i>	<i>31</i>
<i>B2. Other factors involved.....</i>	<i>35</i>
<i>B3. Techniques used to study the problem.....</i>	<i>36</i>
<i>C. Differences of physiology and regulation noted between determinate and indeterminate nodules.....</i>	<i>37</i>
<i>C1. Physiological differences.....</i>	<i>37</i>
<i>C2. Anatomical differences.....</i>	<i>38</i>
E. Use of mutants.....	39
<i>A. Bacterial mutants.....</i>	<i>39</i>
<i>B. Plant mutants.....</i>	<i>40</i>
F. Objectives.....	42
II. MATERIALS AND METHODS.....	43
A. Physiological characterization.....	43
<i>A1. Analysis of the embryonic plant; the seed.....</i>	<i>43</i>

<i>A2. Etiolation</i>	43
<i>A2a. Plant growth conditions</i>	43
<i>A2b. Parameters measured</i>	46
<i>A3. Pigmentation</i>	51
<i>A3a. Plant growth conditions</i>	51
<i>A3b. Measurement of chlorophyll a, b, xanthophylls and carotenoids, and total chlorophyll</i>	51
B. Nodulation characterization	53
<i>B1. Bacterial Culture</i>	53
<i>B2. Study of nodule organogenesis</i>	53
<i>B2a. Plant growth conditions</i>	54
<i>B2b. LacZ strain description</i>	54
<i>B2c. Preparation of root segments</i>	55
<i>B3. Nodule formation on plants of different ages</i>	56
<i>B4. Nitrogenase activity experiments</i>	57
<i>B4a. Plant growth conditions</i>	57
<i>B4b. Calibration of the Qubit apparatus</i>	58
<i>B4c. Nitrogenase activity determination for individual plants</i>	61
<i>B5. Grafting</i>	65
C. Statistics	68
III. RESULTS	71
A. Physiological characterization	71
<i>A1. Analysis of the embryonic plant; the seed</i>	71
<i>A2. Etiolation</i>	72
<i>A2a. Sparkle plants</i>	72
<i>A2b. E151 plants</i>	75
<i>A2c. Sparkle and E151 compared</i>	75
<i>A3. Pigmentation</i>	75
<i>A3a. Qualitative observations</i>	75
<i>A3b. Quantitative analysis</i>	76
B. Nodulation characterization	76
<i>B1. Nodule organogenesis</i>	76
<i>B1a. LacZ Protocol</i>	76
<i>B1b. Sparkle and the different events</i>	81
<i>B1c. E151 and the different events</i>	84
<i>B1d. Sparkle and E151 compared</i>	84
<i>B2. Nodule formation on plants of different ages</i>	103
<i>B2a. LacZ strain</i>	103

<i>B2b. 128C53K strain</i>	104
<i>B2c. Comparison of the number of nodules formed with the 2 bacterial strains on each of the plant lines</i>	111
<i>B3. Nitrogenase activity</i>	111
<i>B3a. Qubit system protocol and problems encountered</i>	111
<i>B3b. Nitrogen fixation in Sparkle</i>	113
<i>B3c. Nitrogen fixation in E151</i>	113
<i>B3d. Comparison of nitrogen fixation between both lines</i>	115
<i>B4. Grafting</i>	115
IV. DISCUSSION	117
A. Nodule organogenesis in the two plant lines	118
B. Plant behaviour towards different rhizobial strains	126
C. Nodulation control	129
D. Model	133
<i>D1. Zone of Susceptibility</i>	133
<i>D2. Auto-regulation signal</i>	134
<i>D3. The Model</i>	137
REFERENCES	139

List of Figures

Figure 1.1. Structure of determinate (A) and indeterminate (B) nodules.....	4
Figure 1.2. The chemical structures of the pea flavonoids hesperetin and naringenin (from Begum et al., 2001).....	7
Figure 1.3. The structure of the Nod factor compound produced by <i>Rhizobium</i> <i>leguminosarum</i> bv. <i>viciae</i>	10
Figure 1.4. My depiction of reverse-fountain streaming occurring in growing root hairs.....	16
Figure 1.5. Simplistic diagram depicting the infection process leading to nodule formation.....	18
Figure 1.6. Cross section of a nodule and vascular bundles (VB) surrounding the central, infected zone.....	24
Figure 1.7. Nitrogen compounds synthesized in infected cells are exported by indeterminate and determinate nodules via the xylem.....	28
Figure 1.8. Long-distance autoregulation signaling.....	32
Figure 2.1. Dormant seed of <i>Pisum sativum</i> . (from Finch-Savage and Leubner-Metzger, 2006).....	44
Figure 2.2. Apical hook angles of etiolated pea plants.....	47
Figure 2.3. Morphological features on pea seedlings.....	49
Figure 2.4. Configuration of the Qubit System during calibration.....	59
Figure 2.5. Configuration of the Qubit System during nitrogenase activity measurement.....	62
Figure 2.6. Method of grafting plants.....	66
Figure 2.7. Diagram of a “hot house.” Used to produce hot and humid conditions so That proper vascular connections occurred between grafted plants. (from Zettler, 1998).....	69
Figure 3.1. Sparkle (A) and E151 (B) plants grown till 9 DAP.....	77
Figure 3.2. Nodule organogenesis observed in Sparkle.....	82

Figure 3.3. Total number of infection events at each day of observation tallied per cm of lateral root.....	85
Figure 3.4. Number of infection events at each developmental stage tallied per cm of lateral root 3 DAI.....	87
Figure 3.5. Number of infection events at each developmental stage tallied per cm of lateral root 6 DAI.....	89
Figure 3.6. Number of infection events at each developmental stage tallied per cm of lateral root 9 DAI.....	91
Figure 3.7. Number of infection events at each developmental stage tallied per cm of lateral root 12 DAI.....	93
Figure 3.8. Number of infection events at each developmental stage tallied per cm of lateral root 15 DAI.....	95
Figure 3.9. Number of infection events at each developmental stage tallied per cm of lateral root 18 DAI.....	97
Figure 3.10. Number of infection events at each developmental stage tallied per cm of lateral root 21 DAI.....	99
Figure 3.11. Nodule organogenesis observed in E151.....	101
Figure 3.12. Number of nodules formed on Sparkle and E151 roots at specific days after inoculation with <i>R. leguminosarum</i> strain 8401.....	105
Figure 3.13. Sparkle (A) and E151 (B) 28 DAI. The plants were inoculated with strain 128C53K (HUP ⁺).....	107
Figure 3.14. Number of nodules formed on Sparkle and E151 roots at specific days after inoculation with <i>R. leguminosarum</i> strain 128C53K.....	109
Figure 4.1. Nodulation pea mutants in Dr. Guinel's collection, their defects, and E151's location amongst the mutants.....	120
Figure 4.2. A model proposed by Guinel and Geil (2002) depicting nodule organogenesis, specifically the epidermal and cortical cell programs.....	123
Figure 4.3. A model explaining the root and shoot auto-regulatory signal interactions occurring in Sparkle and E151 during nodule formation.....	135

List of Tables

Table 3.1. Dry weights (g) and fresh weights (g) of Sparkle and E151 seeds.....	73
Table 3.2. Epicotyl height (cm), epicotyl radial thickness (mm), and apical hook angle (°) of Sparkle and E151 9 DAP grown in the light and dark.....	74
Table 3.3. Concentration (mg g ⁻¹ fresh weight) of chlorophyll a (chl a), chlorophyll b (chl b), xanthophyll (x) and carotenoid (c), and total chlorophyll (T chl) pigmentations in Sparkle and E151 14 and 22 DAP.....	79
Table 3.4. Number of nodules formed on Sparkle and E151 roots at specific days after inoculation when plants are inoculated with <i>R. leguminosarum</i> strain 128C53K or 8401.....	112
Table 3.5. The rate of N ₂ fixation (μmol N ₂ /hr)/nodule dry weight (g) in Sparkle and E151 plants harvested at various days after inoculation (DAI).....	114
Table 3.6. Number of nodules formed on grafted plants of Sparkle and E151 21 DAI.....	116
Table 4.1. Examples of some root-controlled and shoot-controlled pea mutants, along with the genes responsible for the mutation, their orthologs, and gene products.....	130

List of Appendixes

Appendix A- Chlorophyll pigment raw data and calculations.....	154
Appendix B- Nodule organogenesis raw data.....	160
Appendix C- Nitrogenase activity raw data.....	163
Appendix D- Grafting raw data.....	169

I. INTRODUCTION

A symbiosis refers to a close physical association between two different organisms and can be organized into mutualism, parasitism, commensalism, and amensalism. There are many examples of mutualism occurring between bacteria and plants (e.g. *Frankia* and alder, *Nostoc* and *Azolla pinnata*) (Taiz and Zeiger, 1998). Mutualistic interactions occur also between leguminous plants and bacteria of the genera *Rhizobium*, *Bradyrhizobium*, and *Azorhizobium*. The one interaction that will be focused on in this thesis occurs between pea and *Rhizobium*. When these two organisms form an association, a bi-directional exchange of nutrients occurs between the symbionts within a structure known as a root nodule. Specifically, the bacteria provide the plants with a useable form of atmospheric nitrogen (N₂), while the plants supply the bacteria with an energy source for their N₂-fixing activity and the production of nitrogenous compounds (Lambers, Chapin, and Pons, 1998; Raven et al., 1999). This association is of great importance for many reasons.

A. Importance of the symbiotic association

Nodulated legumes are important because of their agricultural (Graham and Vance, 2003; Thomas and Sumberg, 1995), ecological (Reich et al., 2001), economical (Morris, 1997; Paetau, Chen, and Jane, 1994; Russell, 2001), and nutritional benefits (Vance, Graham, and Allen, 2000; Wattiaux and Howard, 2001). In both Western and Eastern countries, legumes are used heavily because of the role they play in soil improvement and fertilizer reduction. In order to prevent soil degradation and nutrient depletion, countries in Asia and Africa for example have been known to use tree-fallow and alley cropping systems (Sanchez, 2002). In tree fallows, woody tree legumes

such as *Sesbania* spp. are interplanted with crops (e.g., corn) and grown as dry-season or longer-term fallows. Subsequently, the wood is harvested for timber and the N-rich materials (e.g., leaves, pods, and stem material) are hoed into the soil (Sanchez, 1999). According to Gathumbi et al. (2002), this procedure significantly increases crop yields and total N accumulation in the soil. Similarly, alley cropping, whereby crops (e.g., beans) are grown between hedgerows of woody tree legumes such as *Erythrina* spp., has been known to increase crop yields from 15% to 50% (Henriksen et al., 2002 as in Graham and Vance, 2003). The farming practices mentioned above demonstrate that crops and legumes can act synergistically with one another, and help reduce the use of fertilizers.

Nodulated leguminous plants also play an important role in colonizing disturbed ecosystems, especially those areas that are prone to fire (Arianoutsou and Thanos, 1996; Reich et al., 2001). Thus, when legumes such as *Lupinus perennis* (sundial lupine) are introduced into fire-prone areas such as long-grass prairies, the percentage of plant N derived from rhizobial fixation can increase from 36% to almost 100% (Graham and Vance, 2003). The introduction of legumes into these disaster-stricken areas helps improve the soil quality and paves the way for the colonization of other vegetative species.

It has been determined by Smil (1999) that legumes in association with rhizobia used for agricultural purposes fix approximately 40 to 60 million metric tons (Mt) of atmospheric N₂ annually; additionally, approximately 3 to 5 million Mt are fixed by legumes in natural ecosystems. The ability of legumes to fix “free” N₂ allows U.S. farmers to save \$7 to 10 billion dollars annually on fertilizer N as long as legumes are rotated in with their crops (Peterson and

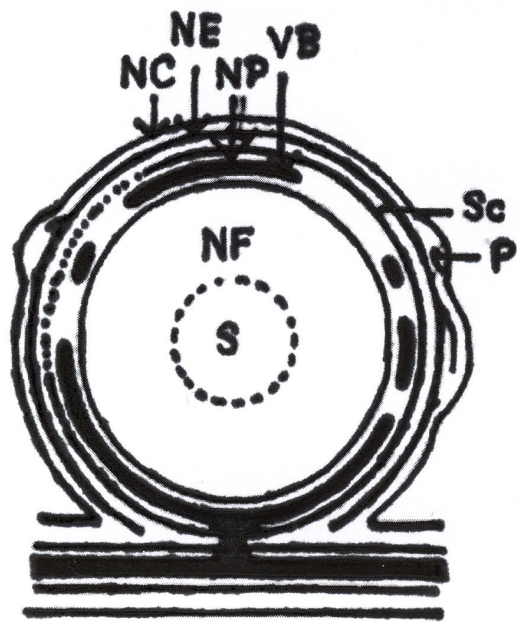
Russell, 1991). And last, but not least, legumes are known to be nutritionally beneficial. They are a useful component in diets because they are low in fat and provide a rich source of protein, fibre, minerals, and vitamins (Simpson and Conner-Ogorzaly, 2001 in Reid, 2005).

B. Use of model plants to study the association

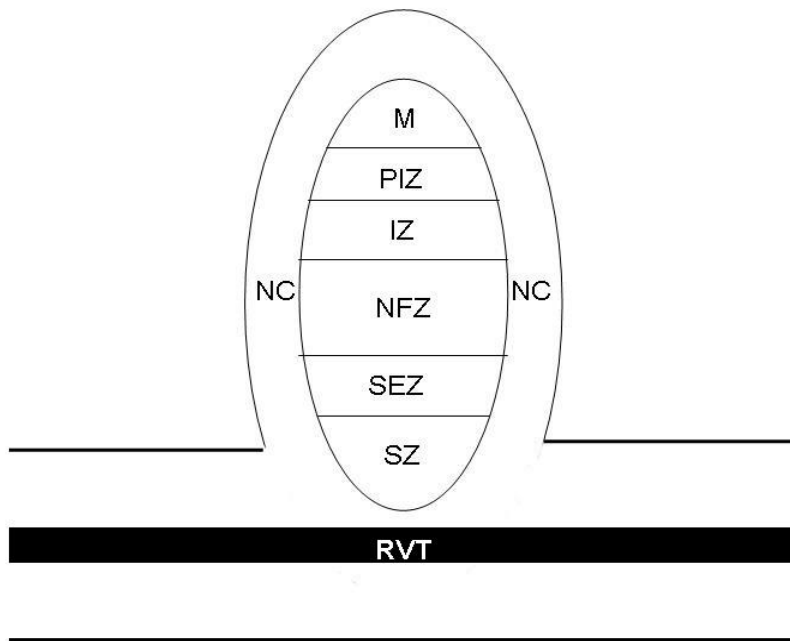
In order for scientists to understand better the development, physiology, and regulation of the nodule, mutants of the model legumes *Medicago truncatula* (barrel medic) and *Lotus japonicus* have been generated and compared to the wild-type species. Barker et al. (1990) produced mutants of the barrel medic, and researchers such as Cook et al. (2002) and Oldroyd et al. (2003) have been using these mutants to study the development of indeterminate nodules. Handberg and Stougaard (1992) produced mutants of *L. japonicus*, the model legume used by researchers such as Nishimura et al. (2002), to study determinate nodule formation. These mutants are created using mutagens which are either chemical (e.g., ethyl methyl sulphonate) or physical (e.g., gamma radiation) in nature. To date, mutants of the two model legumes mentioned above have increased our understanding of indeterminate and determinate nodule formation.

The types of nodules that form in leguminous plants are for the most part determined by the host plant (Mergaert et al., 2006). Plants, such as *Glycine max* L. (i.e., soybean) and *Vigna unguiculata* L. (i.e., cowpea), form determinate nodules (Fig. 1.1 A), which are spherical in shape and have a non-persistent meristem. In these nodules, the rhizobia colonize cells that are still mitotically active and developing (Brewin, 1991). When it comes to the structure of the

Figure 1.1. Structure of determinate and indeterminate nodules. The different parts of a mature determinate (A) nodule (from Hirsch, 1992) are as follows: NC, nodule cortex; NE, nodule endodermis; NF, nitrogen-fixing zone; NP, nodule parenchyma; P, periderm; S, senescent zone; Sc, sclerenchyma; VB, vascular bundle. A mature indeterminate (B) nodule consists of several histological layers listed here: IZ, infection zone; M, meristematic zone; NC, nodule cortex; NFZ, nitrogen-fixing zone; PIZ, pre-infection zone; RVT, root vasculature; SEZ, senescent zone; SZ, saprophytic zone.



A.



B.

nodule, there are no distinct layers present (Provorov et al., 2002). *Medicago sativa* L. (i.e., alfalfa) and *Pisum sativum* L. (i.e., pea) form indeterminate nodules (Fig. 1.1B), which are generally cylindrical in shape (Cohn et al., 1997). In these nodules, the apical meristem remains uninfected during the early stages of development and thus its cells are able to undergo continuous division (Brewin, 1991). Indeterminate nodules are composed of distinct histological layers (Fig. 1.1B) (Timmers et al., 2000).

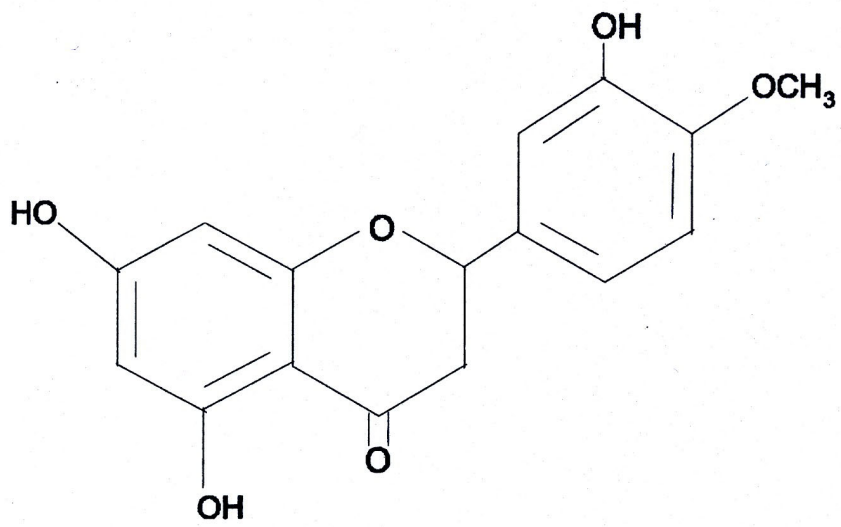
C. Organogenesis of the Nodule

The process of nodule formation is complex and a number of pre-infection and infection events (early and late) need to occur before a mature nodule can function. In the following sections, the interactions that occur under natural conditions between the rhizobia found in the rhizosphere and the host legume will be described with respect to the model systems. However, whenever possible, pea will be focused upon as it is the plant used in my experiments. The focus will primarily be on the anatomical alterations occurring to the inoculated root, and molecular results will be touched upon on occasion.

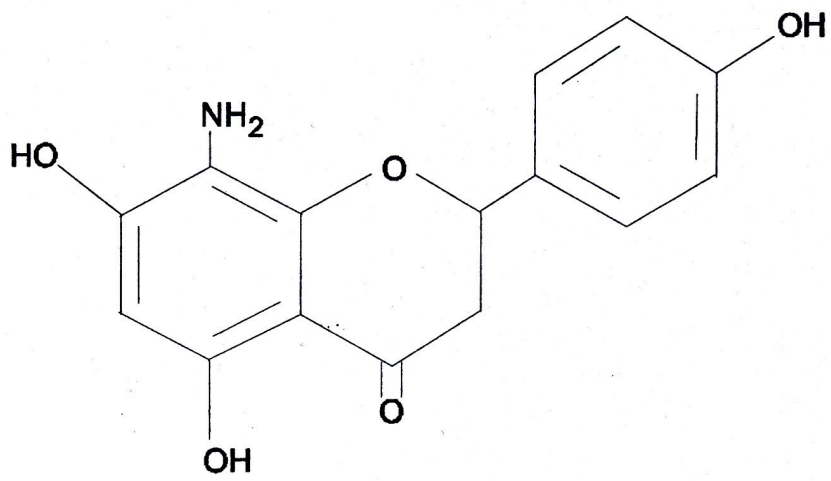
A. Pre-infection events

Nodulation is initiated by chemical compounds called flavonoids, such as hesperetin and naringenin (Fig. 1.2) which are secreted by the pea plant (Begum et al., 2001). In the pea system, these flavonoids attract specifically *R. leguminosarum* biovar *viciae* towards the roots and trigger the transcription of the bacterial genes which are required for nodulation (*nod* genes),

Figure 1.2. The chemical structures of the pea flavonoids hesperetin and naringenin (from Begum et al., 2001).



Hesperetin



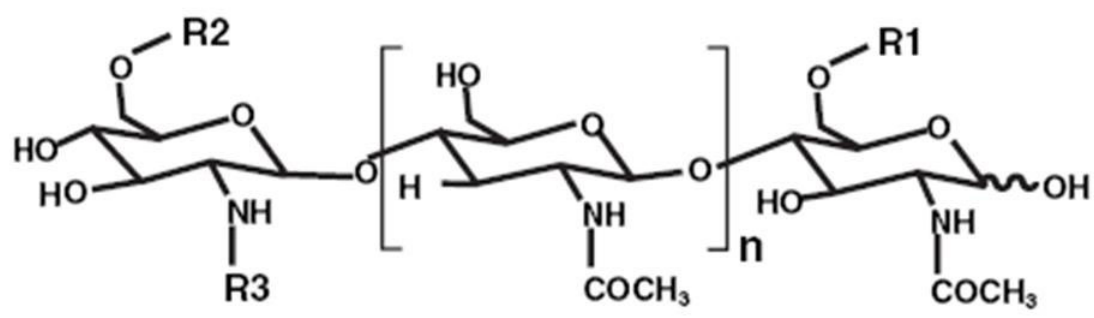
Naringenin

specifically the *nod D* gene. The product of this gene (i.e., NodD protein; Peck et al., 2006) activates the transcription of other *nod* genes (e.g., *nod A*, *B*, and *C*) that code for the enzymes responsible for the synthesis of Nod factors (Fisher and Long, 1992). These factors are lipochito-oligosaccharides composed of β -1-4 linked N-acetylglucosamine residues; their side chains determine the host range of the bacteria (Bras, Spaink, Stuurman, 2000; D’Haeze and Holsters, 2002). In pea (Fig. 1.3), the Nod factors (NF) have a backbone which can be four or five units long and their length affects the host range of the bacterium (Fisher and Long, 1992).

Researchers have suggested two hypotheses for the perception of NF by receptors. Mylona et al. (1995), in the 1st hypothesis, proposed that there are 2 NF receptors, one located on the plasma membrane (PM) of the epidermis, and the other on the PM of the pericycle. The binding of the NF to the epidermal receptor would cause the root hair (RH) to undergo deformation, and interaction between the NF and the pericycle receptor would trigger division in the cortical cells (Mylona et al., 1995).

In the 2nd hypothesis, Ardourel et al. (1994) proposed as well that 2 receptors are needed for proper nodulation to occur; however, both receptors would be located on the epidermis but they would differ in their affinity towards the NF (Ardourel et al., 1994 as in Lhuissier et al., 2001). A variety of NFs (i.e., NFs with various side groups) would be able to bind to the first receptor (signaling receptor) as it would not be very specific (Lhuissier et al., 2001). The binding of the NF to this receptor would induce RH deformation, pre-infection thread formation, and cortical cell divisions (Lhuissier et al., 2001). Only host-specific NFs would be capable of

Figure 1.3. The structure of the Nod factor compound produced by *Rhizobium leguminosarum* bv. *viciae*. The side-chain groups are as follows: R₁, -H; R₂, -COCH₃; R₃, C18:1 or C18:4 and the number of glucosamine monomers is usually 4 (i.e., n=2) (from Oláh et al., 2005).



binding to the second receptor (uptake receptor) (Lhuissier et al., 2001). The uptake receptor main roles would be to induce RH curling, IT formation and nodule tissue infection; in addition, it would be responsible for coordinating the infection events occurring after bacterial entry. Whereas the former alterations linked to the signaling receptor can occur either in the presence of NFs that are released by bacteria or by the exogenous application of NFs, the latter linked to the uptake receptor are possible only in the presence of bacteria.

Studies conducted on alfalfa spp. *varia* allowed for the identification of two NF-binding sites (NFBS1 and NFBS2) (Niebel et al., 1997 as in Lhuissier et al., 2001). The two sites exhibited different levels of affinity for NFs, with NFBS1 having a low affinity and NFBS2 a high affinity (Lhuissier et al., 2001). The NF-binding sites exhibited thus the same varying affinity as the receptors proposed by Ardourel et al. (1994); however, to date only one epidermal receptor has been found by Madsen et al. (2003) and Ben Amor et al. (2003) in *L. japonicus* and *M. truncatula*, respectively. The other potential receptor, whether it be located on the epidermis or pericycle, has not been found and might not even exist.

The NF receptor was identified as a transmembrane serine/threonine receptor-like kinase and was located at the epidermis. In *Lotus*, Madsen et al. (2003) identified it as *L. japonicus* NF receptor 5 (*LjNFR5*); they found it to be homologous to the *SYM10* gene in pea. In barrel medic, Ben Amor et al. (2003) called it *M. truncatula* NF perception (*MtNFP*). In the model legumes, the binding of NF to the receptor is thought to trigger the early steps of nodule formation (Ben Amor et al., 2003; Madsen et al., 2003). Once the binding has been initiated, a number of events occur at the cellular level, the first of which is the depolarization of the plasma membrane. This

is triggered by a decrease in the $[Ca^{2+}]$ around the RH zone when Ca^{2+} ions enter the RH (Felle et al., 1998). Shortly thereafter, the influx of calcium causes the opening of anion channels and the flow of Cl^- ions outwards into the rhizosphere (Felle et al., 1998). The movement of Cl^- ions depolarizes the plasma membrane; however, the membrane is repolarized with the efflux of K^+ ions from the RH (Felle et al., 1998).

Another event resulting from the binding of the NF to its receptor is RH deformation. Before RH deformation is described, the steps involved in usual RH growth will be discussed. During typical RH growth, the exocytotic vesicles which contain cell wall materials are transported to the tip of the RH by reverse-fountain streaming (Fig. 1.4) (Emons and De Ruijter, 2000), whereby the cytoplasm carries the vesicles to their destination and then reverses direction (Miller et al., 1997). This movement is aided by the actin-myosin complex (Miller et al., 1997). The actin filaments act as a route along which cytoplasmic streaming occurs; they also provide some support to the developing RH since they are a component of the cytoskeleton (Miller et al., 1997). In order for exocytosis to occur in the growing RH, Ca^{2+} influx at the tip is required (Schiefelbein et al., 1992). When Ca^{2+} influx occurs, the vesicles fuse with the PM and the contents of the vesicle are discharged adding to the length of the RH (Miller et al., 1997). Studies have shown that when calcium channel blockers (e.g., nifedipine and verapamil) are applied to RHs, they act on the PM and cause the influx of Ca^{2+} to stop, thus halting RH growth (Miller et al., 1997). During RH deformation induced by NF, the RH tip swells and new growth is initiated from the swollen region because the exocytotic vesicles are diverted towards the side of the cell where the NFs are being perceived (Miller et al., 1997).

Shortly after depolarization of the RH plasma membrane and the deformation of the RH, a different type of event involving Ca^{2+} occurs. This event is called calcium spiking and it is considered to be an essential element of the signal transduction pathway leading to nodulation (Ehrhardt, Wais, and Long, 1996). During calcium spiking, cytoplasmic inositol 1, 4, 5-triphosphate (IP_3) binds to a receptor (IP_3 -R) located on the membranes of organelles important in intracellular Ca^{2+} storage such as the endoplasmic reticulum or plastids (Ehrhardt, Wais, and Long, 1996; Cárdenas et al., 1998). The binding of IP_3 to its receptor causes the release of calcium in short waves or pulses from the organelle stores (Ehrhardt, Wais, and Long, 1996). Recently, Imaizumi-Anraku et al. (2005) used *L. japonicus* mutants to study plastid proteins involved with bacterial entry into the root, and it was determined that these organelles contain two closely related proteins called CASTOR and POLLUX, which are localized in their outer membrane (Udvardi and Scheible, 2005). Analysis of the protein structures of CASTOR and POLLUX revealed that they are similar to calcium-gated potassium channels such as those found in *Methanobacterium thermoautotrophicum* (Imaizumi-Anraku et al., 2005). It is suggested by Edwards et al. (2007) that these proteins are responsible for inducing a change in membrane polarization which activates the opening of an unknown Ca^{+2} channel, and triggers calcium spiking. As proposed by Oldroyd, Harrison, and Udvardi (2005), calcium spiking from plastids then acts on the DMI3 protein kinase which is discussed in greater detail below. According to Edwards et al. (2007), the ortholog of *POLLUX* is *SYM8* in pea, and *SYM8* is an ortholog of *M. truncatula* *DMI1*. The orthologs of *CASTOR* in Medicago or pea have not yet been found.

Levy et al. (2004) and Mitra et al. (2004) studying *M. truncatula* found that spiking is very important for nodulation to occur as the gene responsible for calcium spiking (*DMI3*) is

essential for RH curling. DMI3 is a calcium/CaM-dependent protein kinase (CCaMK) that is located in the nucleus of the plant cell (Mitra et al., 2004). The proposed ortholog of the *DMI3* gene in pea is the *SYM9* gene (Mitra et al. 2004) and in *L. japonicus* it is the *CCaMK* gene (Tirichine et al., 2006). In a model proposed by Oldroyd, Harrison, and Udvardi (2005), NFs induce calcium spiking whereby the calcium released from the stores (e.g., plastids) acts on DMI3 which perceives and transduces the calcium spiking signal; the end result of this pathway is root hair deformation.

B. Infection events

All of the pre-infection events (i.e. RH depolarization, RH swelling, and calcium spiking) can happen in the presence of NFs alone; however, without the presence of bacteria, further RH deformation and infection cannot occur (Catoira et al., 2001; Lhuissier et al., 2001) .

For the RH to curl, the host-specific bacteria must bind or attach close to its tip while continuously producing NFs (Goedhart et al., 1999). The attachment of the bacteria to the side of the RH triggers a shift in its cytoskeleton because the microtubules reorganize themselves at the site of infection. This results in the asymmetric growth of the RH which curls around the bacteria that are constantly dividing. The bacterial colony thus becomes entrapped in a tight curl known as the shepherd's crook (Fig. 1.5A) (Timmers, Auriac, and Truchet, 1999; Catoira et al., 2001). Once the legume and the bacteria have recognized each other, a series of morphological changes is initiated in the legume root. The bacteria enter the RH using mechanical pressure and

Figure 1.4. My depiction of reverse-fountain streaming occurring in growing root hairs. Vesicles containing plant cell materials are transported by reverse-fountain streaming to the tip of the RH. There the vesicles are exocytosed, and their contents become part of the RH wall.

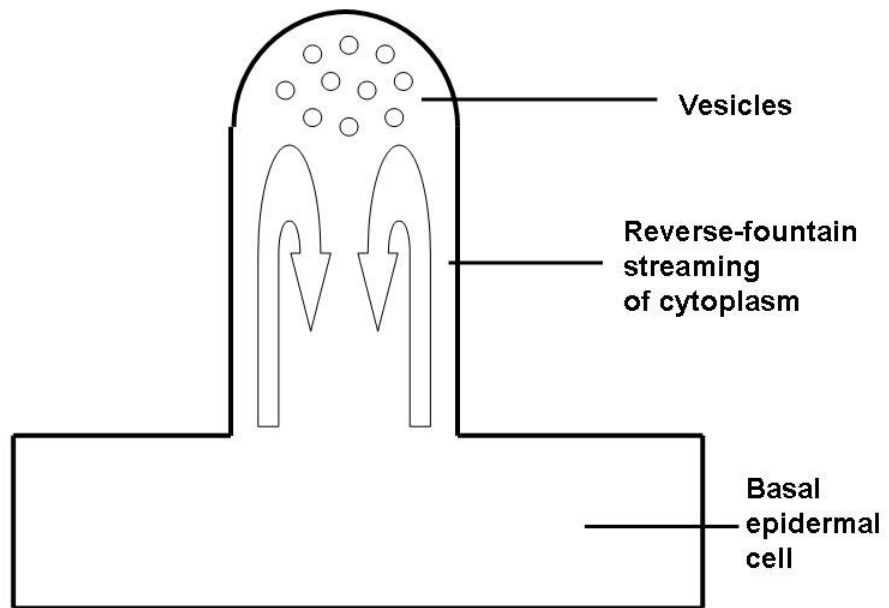
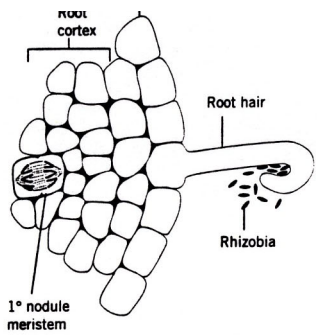
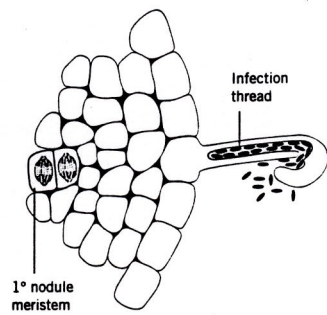


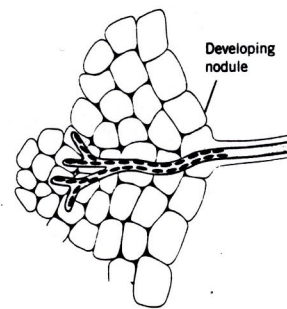
Figure 1.5. Simplistic diagram depicting the infection process leading to nodule formation. (A) Flavonoid-elicited Nod factors act on the RHs and the cortex; rhizobia attach to the RH and become entrapped in a curl. (B) Rhizobia enter the RH and form an infection thread (IT). The IT progresses along the RH length and the rhizobia continue to multiply within the IT. While the IT advances through the RH towards the cortex, the inner cortical cells undergo division and the nodule meristem forms. (C) Eventually, the IT penetrates the inner cortical cells and releases rhizobia into the cells while the nodule, via its meristem, continues to develop outwards. The rhizobia which were released into the cells differentiate into bacteroids and are able to undergo nitrogen fixation (not depicted in diagram) (from Hopkins, 1999).



A.



B.



C.

enzymatic digestion (Mateos et al., 2001); an infection thread (IT) then forms that acts as a passage way for the bacteria, and leads them towards the dividing cortical cells (Fig. 1.5B).

The formation of the IT causes a few cellular rearrangements to occur inside the infected RH. Initially, helically-organized microtubules of the cytoskeleton are slowly replaced by endoplasmic microtubules; the nucleus which is usually close to the RH tip then moves down and positions itself against the cell wall from which the new growth started (Timmers, Auriac, and Truchet, 1999). The nucleus further moves down to the inner periclinal wall of the basal epidermal cell, thus clearing a route for the IT. The development and expansion of the IT from the point of infection to the cortex are controlled partly by the plant cell (Fig. 1.5B). The cell is responsible for coordinating the secretion of the luminal matrix of the IT, the plasma membrane, and wall components (i.e. cellulose, xyloglucan, and pectin) (Rae, Bonfante-Fasolo, and Brewin, 1992). Without this synchronization the IT would not form properly.

A number of changes occur to the pericycle and cortical cells while the bacteria are entering the RH. First, the pericycle cells are activated and undergo anticlinal cell divisions (i.e. which add cells left and right) (Beveridge et al., 2007; Timmers, Auriac, and Truchet, 1999). Second, the nodule progenitor cells (the inner cortical cells) partake in anticlinal divisions followed by periclinal divisions (i.e. which add cell layers upwards towards epidermis) which form a second cell layer (Beveridge et al., 2007; Timmers, Auriac, and Truchet, 1999). Once the second cell layer arisen from the nodule progenitor cells is laid down, the nodule primordium is considered to be formed. Shortly after the primordium is set, non-activated inner cortical cells located beside the outer periclinal wall of the primordial cells become activated (Timmers,

Auriac, and Truchet, 1999). These cells, which initially have a square shape, differentiate, undergo anticlinal and periclinal divisions and form the nodule meristem; by continuously dividing, they expand towards the middle of the cortex (Fig. 1.5C) (Timmers, Auriac, and Truchet, 1999).

While all these cell divisions are occurring in the inner cortex, the outer cortical cells prepare themselves for infection. The cells do this by forming a pre-infection thread (PIT) (van Brussel et al., 1992) whereby cytoplasmic reorganization occurs in individual cells (Timmers, Auriac, and Truchet, 1999). This results in a centrally positioned cytoplasmic bridge which joins the outer and inner periclinal sides of the outer cortical cells (Timmers, Auriac, and Truchet, 1999). The PITs in the individual cells are orientated and aligned in such a way that they provide a path across the entire outer cortex (Timmers, Auriac, and Truchet, 1999).

Once the bacteria within the IT have reached the basal epidermal cell, they will take the direction of the PIT in the outer cortex (Brewin, 1991). Van Spronsen et al. (1994) proposed that as the bacteria located in the IT follow the pathway paved out by the PIT, the periclinal walls of the encountered cortical cells undergo degradation. They suggested that bacteria inside the IT release NF that cause the periclinal wall of the cortical cells to weaken, and that the actual presence of the rhizobia allows the wall of the cell to be broken down (Van Spronsen et al., 1994).

C. Late infection events

Most studies that have focused on late infection events have been done on pea; the following section will summarize what is known for this species. Eventually the growing IT reaches the inner cortical cells that have undergone divisions (Fig. 1.5C). It breaches the surface of the nodule meristem region because the cells in this area are thin and newly formed; it grows in many directions (Newcomb, 1976) and it was found that ITs undergo branching (Gage, Bobo, and Long, 1996). The host cell membrane is lining the surface of the IT separating the cytoplasm from the wall of the IT (Newcomb, 1976). Cells which have been penetrated by the IT are distinct from non-penetrated cells by having numerous free ribosomes, plastids, and Golgi. Also, they have large vacuoles, condensed chromatin, and lack endoplasmic reticulum (Newcomb, 1976). The IT (which is devoid of a closure at its tip) infects cells by releasing droplets containing bacteria into the cell cytoplasm by way of endocytosis (Newcomb, 1976). In the case of pea, a single bacterium is released in the symbiosome, i.e. the droplet which is surrounded by the peribacteroid membrane (Mylona, Pawlowski, and Bisseling, 1995).

Once infected, a cell undergoes a number of changes. One of the first things to occur is that the cell increases in volume, then new endoplasmic reticulum forms, less condensed chromatin appears in the nucleus, and the single nucleolus enlarges (Newcomb, 1976). As the cell structure alters, the bacteria in the symbiosome undergo changes too. They increase in size slowly and change their morphology from rod-shaped to branched, Y-shaped cells; in pea they lose their ability to divide (Newcomb, 1976). The differentiated bacteria are referred to as bacteroids and are capable of nitrogen fixation (Mylona, Pawlowski, and Bisseling, 1995). Infected cells containing bacteroids look different from newly infected cells (i.e. those in which the rhizobia have not yet differentiated into bacteroids); they have a lobed nucleus, less

endoplasmic reticulum, and rectangular-shaped starch grains found in the amyloplasts (Newcomb, 1976). As the bacteria mature and change into bacteroids in the infection zone (IZ in Fig. 1.1B), the nodule continues to develop until it breaches the epidermis (Provorov et al., 2002; Timmers et al., 2000).

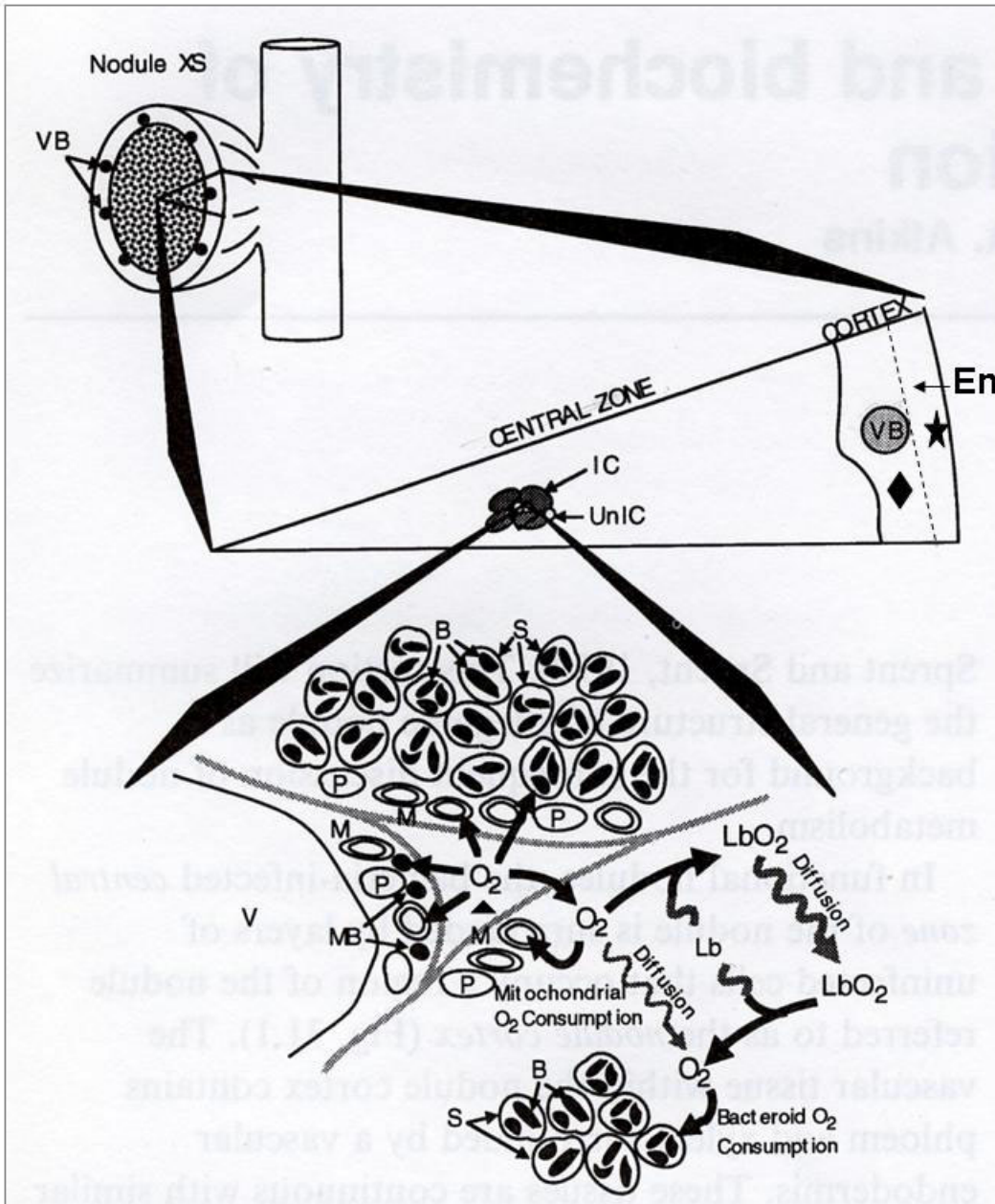
Pea mature nodules can be separated into six regions (Fig. 1.1B): an apical meristematic zone allowing the nodule to continue growing, a pre-infection zone where ITs penetrate cells; an infection zone composed of cells in which bacteria differentiate into bacteroids; a nitrogen-fixation zone which has nitrogen-fixing (i.e. bacteroids inside) and non-fixing cells (Fig. 1.6); a senescent zone in which the infected cells degrade; and a saprophytic zone that contains senescing cells in which bacteria, which have never differentiated into bacteroids, are kept so that they will be released back into the soil when the plant dies (Timmers et al., 2000). The nodules of pea have only one point of attachment to the root and possess two vascular strands which connect the nodule to the root vasculature (Pepper, Morse, and Guinel, 2007). The apical meristematic regions of the nodule allow it to form many lobes as it continuously develops.

D. Nodule physiology and regulation of nodulation

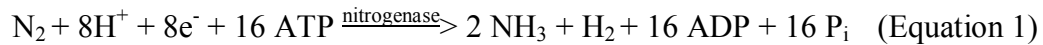
A. Nodule physiology

As the nodule has developed into a mature organ, the bacteroids inside the nodule are able to fix N_2 . The bacteroids break apart the triple bond present in atmospheric N_2 with the aid of the

Figure 1.6. Cross section of a nodule and vascular bundles (VB) surrounding the central, infected zone. In the expanded view of the nodule, both infected (IC) and uninfected (UnIC) cells are shown within the central zone. A VB is shown within the nodule cortex. The nodule cortex is traversed longitudinally by the nodule endodermis (En) which separates the outer (star) and inner (diamond) cortex from each other. The zoomed image of the cells depicts a gas filled space (triangle) along with two infected cells and one uninfected cell. The smaller uninfected cell contains a large central vacuole (V), plastids (P), mitochondria (M) and peroxisomes or microbodies (MB). The larger infected cells lack microbodies, but contain numerous symbiosomes (S) that have bacteroids (B) enclosed within them. The leghemoglobin (Lb)-facilitated O₂ diffusion pathway is depicted in one of the infected cells. Leghemoglobin binds to O₂ and facilitates the diffusion of O₂ from the surface of the infected cell to the bacteroids (modified from Dennis et al., 1997).



complex enzyme nitrogenase; they convert N₂ to ammonia (NH₃) and then to ammonium (NH₄⁺), a form of nitrogen that is consumable by the plant. The enzymatic reaction is as follows:



In order to respire and function properly, the bacteroids inside the nodule require oxygen. However, a tight control of the oxygen levels (between 3-30 nM) within the bacteroid compartment is required because free O₂ damages the nitrogenase (Lambers et al., 1998). The bacteroids obtain their oxygen from the intercellular spaces, formed between infected and non-infected cells, with the aid of the O₂-binding protein called leghemoglobin (Fig. 1.6). The protein is located in the cytoplasm of infected cells and is produced by the plant (Dennis et al., 1997). Besides rapidly supplying O₂ to the highly metabolically active bacteroids, the protein keeps a low free O₂ concentration in the nodule. The flow of oxygen to the bacteroids is further regulated by the plant via a physical barrier located in the nodule inner cortical cell region (Brewin, Ambrose, and Downie, 1993); this region is located between the zone containing the infected cells and the nodule endodermis (Fig. 1.6) (Pepper, Morse, and Guinel, 2007). This barrier is approximately 1-5 cell layers thick and its cells are tightly packed with relatively few intercellular spaces; this type of layout limits gas exchange. It has been proposed by Brewin, Ambrose, and Downie (1993) that legumes alter the rates of O₂ exchange by filling the air-spaces with gel-like extracellular glycoproteins. In a recent study, Wei and Layzell (2006) proposed that certain ions play a role in controlling nodule O₂ permeability by acting as messengers; they would carry information about the status of the infected cells to the inner cortex of the nodule.

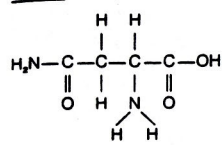
These authors show that K^+ ions move from the infected cell cytoplasm to the apoplast, drawing out water with them (Wei and Layzell, 2006). The water then fills the network of intercellular spaces located in the inner cortex of the nodule, likely reacting with the gel-like glycoproteins and thus blocking the diffusion of O_2 (Wei and Layzell, 2006). N_2 -fixing bacteroids can also regulate O_2 by way of an electron transport chain that terminates with a high-affinity oxidase. This cytochrome oxidase is produced by certain strains of *R. leguminosarum* such as bv. *viciae* when the rhizobia have not yet differentiated into bacteroids; in the infected area, this enzyme helps to capture efficiently the low free O_2 and regulate its concentration (Brewin, Ambrose, and Downie, 1993).

The end-result of N_2 fixation is the production of ammonium which is assimilated later into nitrogenous compounds. These compounds are exported in the xylem to the rest of the plant where they are used to synthesize amino acids, nucleic acids, and other nitrogen-containing compounds needed for proper development (Hunt, 2005). Pea plants, which form indeterminate nodules, transport nitrogen in the form of amides such as asparagine and glutamine (Fig. 1.7) whereas plants such as soybean that form determinate nodules usually transport nitrogen in the form of ureides such as allantoic acid, allantoin, urea, and citrulline (Dennis et al., 1997; Mylona, Pawlowski, and Bisseling, 1995).

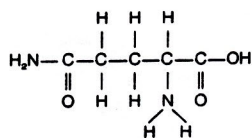
However, none of the building blocks allowed to be created by the process of N_2 fixation could be made without a carbon source; this is because the bacteria require a lot of energy (16 ATP) for the nitrogenase reaction to go to completion. Carbon, in the form of photosynthates, is

Figure 1.7. Nitrogen compounds synthesized in infected cells are exported by indeterminate and determinate nodules via the xylem. Temperate legumes, which form indeterminate nodules, export amides, whereas tropical legumes, which form determinate nodules, export ureides (from Salisbury and Ross, 1992).

amides

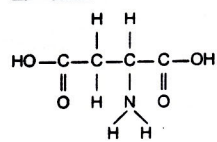


asparagine



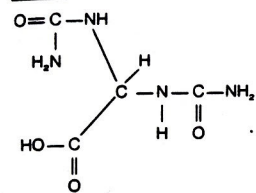
glutamine

amino acid

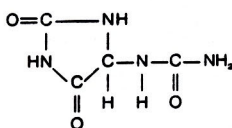


aspartic acid
(parent of asparagine)

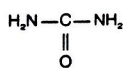
ureides



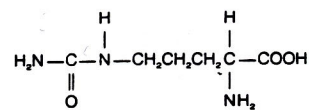
allantoic acid



allantoin



urea



citrulline

supplied via the phloem to the root nodules which contain the N₂-fixing bacteroids (Hunt, 2005). The bacteroids receive the carbon source in a partially metabolized state so that the carbon compounds entering the bacteroids need to be further metabolized to produce ATP (Hunt, 2005). Since fixation requires such a large amount of carbohydrates, nodules are often considered to be sinks for carbon. During the nitrogen fixation process, a large amount of hydrogen is also released by the nitrogenase enzymatic reaction (Equation 1); to ensure that this hydrogen is not wasted, bacteria such as *R. leguminosarum* bv. *viciae* have evolved a hydrogen uptake (*hup*) system to oxidize this hydrogen. An enzyme called uptake hydrogenase is responsible for the oxidation of hydrogen and it therefore reduces the energy losses of the fixation process (Baginsky et al., 2002). Some bacterial strains lack the uptake hydrogenase enzyme; in such a case, when these bacteria fix N₂, hydrogen is released into the soil (Hunt, 2005). The hydrogen is, however, not lost entirely since H₂-oxidizing bacteria such as the gram-positive actinomycetes can use it up (McLearn and Dong, 2002); these bacteria are known to promote the growth of plants.

B. Regulation of nodulation

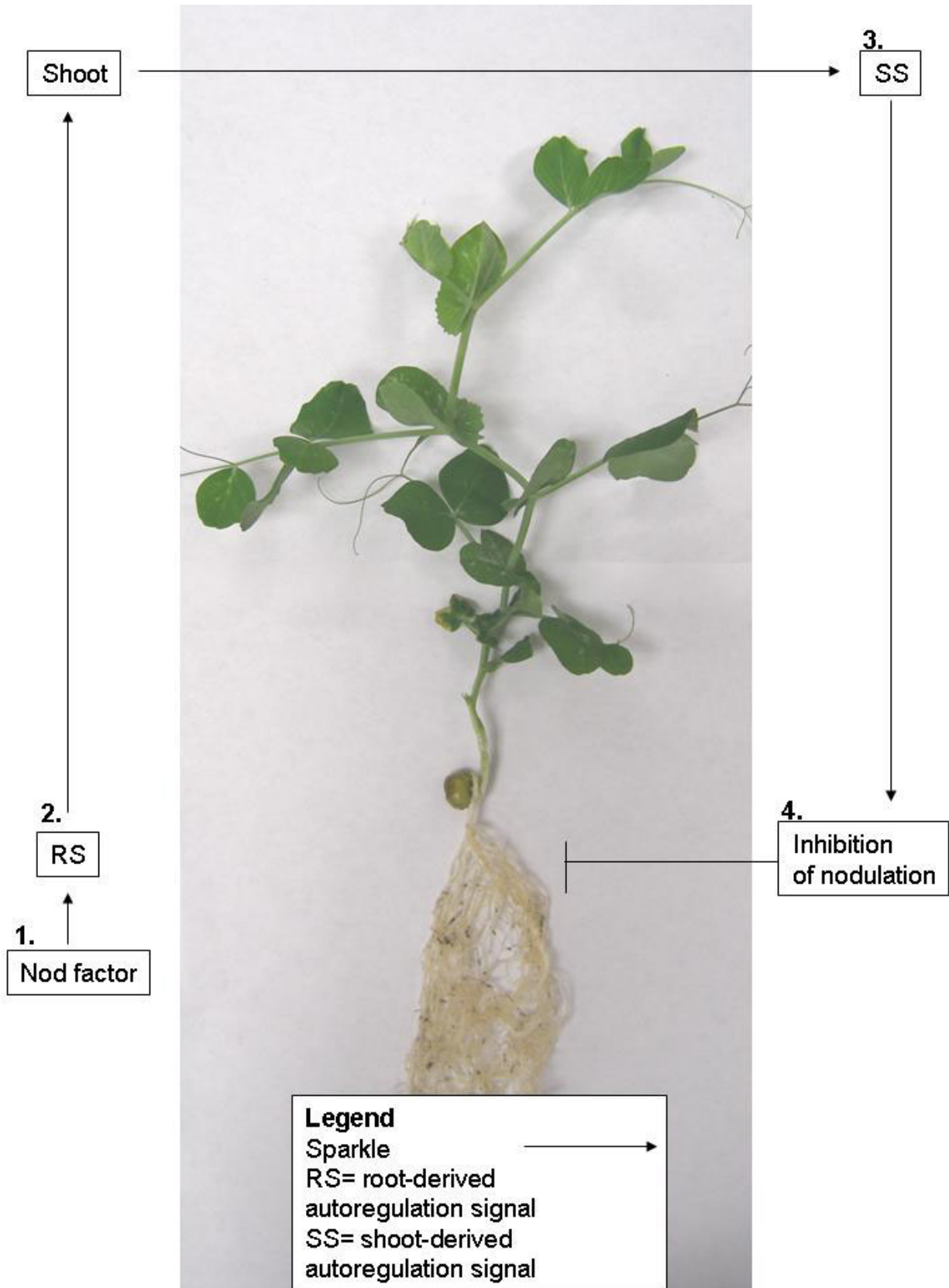
As was mentioned previously, nodulated legumes are agriculturally, ecologically, economically, and nutritionally beneficial; however, the formation of nodules requires an enormous amount of energy (i.e., photosynthates) and thus affects greatly the plant growth. If too much energy were allocated towards the development of nodules and nitrogen fixation, then the plant would not receive enough energy to continue growing. In order to prevent the over-consumption of energy by the nodules and maintain a balance in energy allocation, legumes have

developed a mechanism that autoregulates nodulation. This process controls by way of long-distance signaling the number of nodules that form on the root system and the size of the nodulation zone (Oka-Kira and Kawaguchi, 2006).

B1. Auto-regulation mechanism

The existence of an auto-regulation signal was discovered through the use of four categories of mutants that differed from the wildtype in their nodule production: *nitrogen-tolerant symbiosis (nts)* or supernodulating mutants, ethylene-insensitive mutants, light-insensitive mutants, and the so called auto-regulation mutants (Oka-Kira and Kawaguchi, 2006). As will be discussed in the following sections, the boundaries between these classes of mutants are rather blurred. The perception of specific NFs by the host plant and the development of nodule primordia are believed to trigger auto-regulation (Oka-Kira and Kawaguchi, 2006). To date, it is proposed that an auto-regulation signal from the root system is sent towards the shoot, and causes a shoot-derived auto-regulation signal to be produced. That shoot-signal is transported towards the root system; its perception results in the inhibition of further nodulation (Fig. 1.8) (Oka-Kira and Kawaguchi, 2006). The exact origin of either the root or the shoot auto-regulation signal is not known but Sheng and Harper (1997) showed that when the shoots of the WT soybean plants were defoliated, there was an increase in the number of nodules that formed on the root system; thus, the leaves appear to be one potential source for the auto-regulation signal (Oka-Kira and Kawaguchi, 2006).

Figure 1.8. Long-distance autoregulation signaling. 1. The bacterial Nod factor is perceived by the root system and the autoregulation of nodulation starts. 2. An unknown root-derived signal is transported towards the shoot. 3. Perception of the root-signal in the shoot elicits a shoot-derived autoregulation signal which is sent towards the root system. 4. The autoregulation signal from the shoot inhibits further nodulation.



To attempt the determination of the chemical nature of the signal, various phytohormones have been applied to WT and hypernodulation mutants (i.e. plants which produce more nodules than the WT). It is known that ethylene has an inhibitory role in nodulation as described in a review by Guinel and Geil (2002). For example, Penmetsa and Cook (1997) found that the application of ethylene to the growth medium post-inoculation caused a drastic decrease in infections and the number of developing nodules on the WT barrel medic. Despite this effect, ethylene is probably not involved in regulating nodulation because *sickle*, an ethylene-insensitive hypernodulating barrel medic mutant formed many nodules, especially nodule primordia, when treated with this gas (Penmetsa and Cook, 1997). Suzuki et al. (2004) found that the exogenous application of abscisic acid to the roots of *Trifolium repens* (white clover) and *Lotus japonicus* also greatly reduced the number of nodules. The involvement of brassinosteroids (e.g., brassinolide) was examined by Terakado et al. (2005) who applied this phytohormone to the leaves of a WT soybean and of a hypernodulating soybean (i.e., En6500); as a result, the hypernodulator showed a decrease in nodule production whereas the number of nodules on WT did not change. Finally, the application of methyl jasmonate to the shoot of WT *Lotus* and the hypernodulating mutant *har1* was found to cause a reduction in the number of nodules formed in both plant lines (Nakagawa and Kawaguchi, 2006). Taken together, these studies suggest that a number of different phytohormones have a regulatory role in nodulation. Moreover, it is interesting to note that all the hormones mentioned here are in fact produced in times of stress by the plant and their action is likely linked to excessive bacterial entry and nodule formation.

In the mean time, further studies are being conducted to determine the chemical composition of the long-distance auto-regulation signal produced during nodulation because none of the hormones mentioned above appear to be directly involved in regulation.

B2. Other factors involved

Other factors such as nitrate have been shown to be involved in regulating nodule formation. Ligeró et al. (1991) demonstrated that varying quantities of nitrate present in the soil or applied exogenously to a nodulated root system can greatly reduce and inhibit the number of nodules formed. Furthermore, the supernodulator *nts* mutants (e.g., *har1*, *sun*, *sym29*, and *nark*) can form greater numbers of nodules than the WT under various combinations of nitrogen sources (KNO₃, urea, NH₄Cl, and NH₄NO₃) given at 5 mM levels (Carroll, McNeil, and Gresshoff, 1985). As well, light is known to affect nodulation. Lee and LaRue (1992a) determined that inoculated WT pea roots exposed to dim light exhibited blocks in IT growth in the epidermis or outer cortex of the root. However, light suppression of nodulation could be linked to ethylene because a dark treatment resulted in an increase in ethylene in the roots (Lee and LaRue 1992a). Investigations on the *Lotus* light-insensitive mutant *astray* by Nishimura, Ohmori, and Kawaguchi (2002) revealed that the plant's root system could form nodules when exposed to a light source and its zone of nodulation was greater than that of the WT plants. When typical nodulation inhibitors such as ethylene and nitrate were applied by these authors to the growth medium (i.e. agar plates), the mutant showed sensitivity (i.e. nodulation was reduced). Based on all these studies, it can be concluded that nodulation is probably regulated by a combination of environmental and hormonal factors.

B3. Techniques used to study the problem

The two main techniques used to study auto-regulation are the split-root system and grafting. In the split-root system, the roots of the plant being studied are physically separated by placing half of the roots in one container and the other half in another; this allows each half to be treated and studied independently (Kinkema, Scott, and Greshoff, 2006). Olsson et al. (1989) used this system to investigate how the timing of inoculation affected auto-regulation and nodule suppression. In the WT soybean Bragg, developing nodules that formed on the side of the root system that was inoculated early almost completely suppressed nodule formation on the other side of the root system that was inoculated 7-days later (Olsson et al., 1989). This indicates that nodules developing in one portion of the root system could send signals to the shoot and the shoot in turn sends a signal to the part of the root that was inoculated later; that latter signal appears to regulate nodule formation. The nitrate-tolerant supernodulating mutant (*nts382*) showed only a 30% suppression in nodulation when a similar 7-day delay in inoculation was performed (Olsson et al., 1989). The authors suggested that the *nts382* mutant has a possible deficiency in the production of the auto-regulation signal and that is why the mutant exhibits a reduced suppression of nodulation.

Another technique used to study auto-regulation is grafting. The grafting technique helps elucidate whether nodulation is root- or shoot-controlled. In this technique, shoots from mutant plants such as hypernodulators are joined to the roots of wild-type plants, and this results usually in wild-type roots exhibiting a hypernodulation phenotype (Kinkema, Scott, and Greshoff, 2006).

In reciprocal grafts, whereby the wild-type shoot is grafted onto the hypernodulation mutant roots, a normal quantity of nodules form (Kinkema, Scott, and Greshoff, 2006). These results suggest that nodulation in hypernodulator mutants is shoot-controlled. For example, Oka-Kira et al. (2005) performed a grafting experiment between a WT *L. japonicus* (Gifu) and a hypernodulating mutant called *klavier* (*klv*) in order to study autoregulation. The *klv*/Gifu and *klv/klv* grafts formed a notably higher number of nodules than that of the Gifu/*klv* and Gifu/Gifu grafts. Based on the results of the grafts, Oka-Kira et al. (2005) suggest that the aberrant leaf veins that develop in the hypernodulating *klv* mutant are the likely cause of the hindrance in the long-distance auto-regulatory signal pathway responsible for nodulation because these abnormal veins do not allow the proper transmission of the signal from the root to the shoot. Also, it is suggested that *KLV* is found in the shoot and roots, and may be expressed in the shoot apical meristem (SAM) (Oka-Kira et al., 2005). It should be noted that there appear to be no orthologues of *KLV* in barrel medic or pea. Mutants which are root-controlled are generally found in the classes exhibiting defects in nodule organogenesis. The exception to the shoot-controlled hypernodulators and root-controlled low nodulators are low nodulation mutants such as E132 (Markwei and LaRue, 1997) and E107 (Resendes, Geil, and Guinel, 2001) which both have shoot-controlled nodulation.

C. Differences of physiology and regulation noted between determinate and indeterminate nodules

C1. Physiological differences

For some time, it has been thought that plants forming indeterminate and determinate nodules may be regulated differently by hormones. Thus Lee and LaRue (1992b) were able to distinguish soybean and pea; while the former was not too sensitive to C₂H₄, the latter responded to a minute amount of the gas. Van Spronsen et al. (2003) demonstrated similar findings with the hormone salicylic acid (SA). SA inhibited vetch nodulation (indeterminate) whereas *Lotus* (determinate) was not affected (Van Spronsen et al., 2003). Recently, Schmidt et al. (1999) and Stacey et al. (2006) have shown that the distinction based on hormonal response was perhaps too simplistic. Schmidt et al. (1999) found that ethylene-insensitive mutants of soybean were able to nodulate as well as the WT when it was expected that the mutant line would form significantly more nodules. As well, transgenic plants of *Lotus japonicus* and barrel medic over-expressing the bacterial gene *nahG* (i.e, responsible for encoding salicylate hydroxylase, an enzyme which prevents the accumulation of SA) were studied by Stacey et al. (2006). Since there was no SA being produced, according to the previous findings of Van Spronsen et al. (2003), the barrel medic (indeterminate) should have shown an increase in nodules but *Lotus* (determinate) should not be affected. However, in response to the reduced levels of SA, both plants exhibited levels of infection close to those of the WT plants (Stacey et al., 2006), contradicting the findings of Van Spronsen et al. (2003).

C2. Anatomical differences

Differences between indeterminate and determinate nodules can be seen at the cellular level. In pea, IT development or cortical cell divisions are induced earlier than in soybean (Provorov et al., 2002). Gresshoff (1993) found that a second-wave of nodule formation in root

portions already infected is impossible in alfalfa which forms indeterminate nodules due to a complete autoregulatory block, while it still occurs in soybean, the nodules of which are determinate. Strict controls also exist at the sub-cellular level. Thus, within the infected cells of indeterminate nodules, bacterial division is arrested quicker and the differentiation of the bacteria into bacteroids occurs sooner than in those of determinate nodules (Provorov et al., 2002). For example, in pea and alfalfa, each symbiosome contains one highly morphologically and biochemically differentiated bacteroid, whereas in soybean there are 5-10 bacteroids per symbiosome and these are morphologically similar to free-living bacteria (Provorov et al., 2002). Through the use of recombinant *Rhizobium* strains, Mergaert et al. (2006) discovered that legumes that form indeterminate nodules only contain one bacteroid per symbiosome because the bacterial symbionts in response to plant factors are hindered in their cell division; the bacteroid unable to divide is triggered to undergo multiple endoreduplication cycles. These cycles cause cell enlargement by way of genome amplification and steer the bacterium towards a bacteroid state (Mergaert et al., 2006). In determinate nodules, genome amplification does not occur because the plant factors are absent from the nodule and the bacteroids keep the DNA content of free-living bacteria (Mergaert et al., 2006).

E. Use of mutants

A. Bacterial mutants

Even though the main focus of this thesis is on pea and the nodulation phenotype of one specific mutant, it should be mentioned that bacterial mutants have been used extensively to

better understand the plant-rhizobium interaction that results in nodule formation. Indeed, plant-rhizobium interactions require the proper functioning of both symbiotic partners, that of the macrosymbiont but also that of the microsymbiont. A number of articles and reviews can be found on this topic (Ardourel et al., 1994; Gage, 2004; Gonzalez, York, and Walker, 1996; Leigh and Coplin, 1992; Spaink, 2000). For example, mutations in the common *nodABC* genes, which are present in most rhizobia (Downie, 2007), cause a number of abnormal plant responses such as a lack of RH curling, IT formation, and cortical cell divisions (Fisher and Long, 1992). In particular, Ardourel and colleagues (1994) created *nodL*, *nodFE*, and double *nodF/nodL* mutants of *R. meliloti* to see whether any of the strain-specific *nod* genes were required for nodulation. They found that the *nodL* and *nodFE* mutants were unable to form proper ITs, and the double *nodF/nodL* mutants were incapable of penetrating the legume host RHs (Ardourel et al., 1994). Furthermore, as seen in Gage 2004, studies done on *S. meliloti* demonstrated the importance of the rhizobial exopolysaccharides (i.e. succinoglycan (EPS I), EPS II, K antigen, lipopolysaccharide, and β -glucans) in nodulation. *exo* mutants, deficient in succinoglycan production, were unable to form ITs in inoculated alfalfa and barrel medic plants; in some plants, ITs formed but these were grossly misshaped and did not progress past the basal epidermal cell (Gage 2004).

B. Plant mutants

The production of leguminous mutant plants has also shed much light on nodule formation. Leguminous mutants, specifically those that have had their ability to nodulate altered, can be broken down into a few main classes: non-nodulators (*nod*-), low-nodulators (*nod*-/+), mutants

with ineffective nodules (nod+ fix-), mutants with low-efficient nodules, mutants with variable numbers of nodules and variable efficiency, hyper-nodulators, and super-nodulators (Sidorova and Shumnyi, 2003). These mutants are represented in the two model plants already mentioned; however the findings found in the model legumes are not always relatable to the vast varieties of other legumes. Therefore, it is important to try and expand scientific findings by using other diverse leguminous species. Mutant legumes of *Glycine max* (soybean) (i.e., nod49, nod772; Mathews, Carroll, and Gresshoff, 1992), *Phaseolus vulgaris* (white bean) (i.e., R69 and R99; Shirtliffe et al., 1996), *Melilotus alba annua* (sweetclover) (i.e., BT62, BT70; Utrup, Cary, and Norris, 1993), *Cicer arietinum* (chickpea) (i.e., ICC 435M; Singh, Vanrheenen, and Rupela, 1992), *Medicago sativa* (alfalfa) (i.e., MN-1008; Endre et al., 2002), and especially *Pisum sativum* (pea) (i.e., R50; Pepper, Morse, and Guinel, 2007), have allowed for a better understanding of the function of many genes involved in the process of nodule formation (Guinel and Geil, 2002). By studying pea plants, it was determined that *SYM10* and *SYM9* code for a serine/threonine kinase-like receptor and calcium/CaM-dependent protein kinase, respectively (Madsen et al., 2003; Mitra et al., 2004).

The advent and use of both physical and chemical mutagens, and the continuous funding into pea research have enabled labs from such countries as Russia (i.e., Tsyganov et al., 1998), France (i.e., Duc and Messenger, 1989), U.S.A. (i.e., Kneen, Weeden, and LaRue, 1994), and Czech Republic (i.e., Novak, 2003) to study mutant varieties of this plant. These mutants have allowed researchers to dissect microscopically the symbiosis that occurs between the rhizobia and the host plant. Specifically, symbiosis (*sym*) genes have been linked to specific steps of, and potential roles in, nodule organogenesis (see Guinel and Geil, 2002, for extensive review).

My thesis focuses on the nodulation of the pea mutant E151 which was compared to the wild-type Sparkle. E151 was mutagenized using ethyl methyl sulfonate; it carries a single recessive mutation on symbiosis gene 15 (*sym15*) (Weeden et al., 1990; Kneen, Weeden, and LaRue, 1994). The pea genome is composed of seven chromosomes, and the *sym15* gene can be found on chromosome 7, linkage group 7 (Kneen, Weeden, and LaRue, 1994; Ellis and Poyser, 2002). In a previous study conducted by Kneen, Weeden, and LaRue (1994), E151 was described as a pleiotropic mutant. Its epicotyl was significantly shorter than that of Sparkle, based on the height of the third internode. In addition, its primary root length was reduced and it had shorter lateral roots; it was also characterized as a low nodulator.

F. Objectives

The objective of this thesis was to perform an observational investigation of E151 and to determine how its nodulation phenotype differs from that of the WT Sparkle. *LacZ* staining, measurement of nitrogenase activity, and grafting were techniques employed to characterize any differences seen in nodulation. Furthermore, some morphological characteristics (i.e., pigmentation, embryo size and weight) were studied to determine whether any other phenotypic differences exist between the two plant lines.

II. MATERIALS AND METHODS

A. Physiological characterization

A1. Analysis of the embryonic plant; the seed

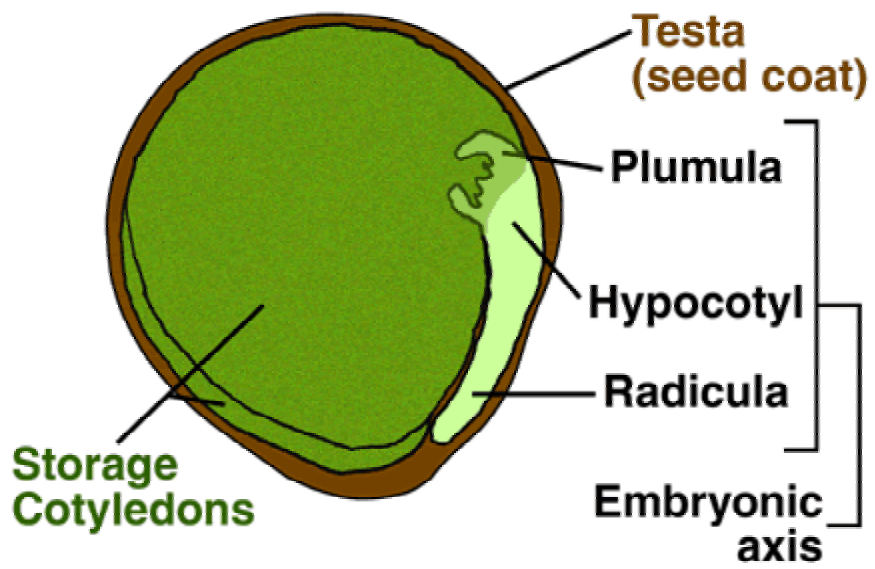
Individual seeds (45 for each line) were chosen randomly from previous harvests. Each seed was weighed to obtain its dry weight and then placed individually into a glass vial (volume: 25 mL). The seeds were surface-sterilized for 5 min with 8% (v/v) household bleach (5.25% NaOCl), rinsed three times (1 min each) with sterile deionized water, and left to imbibe in the dark for 14-16 h. The imbibed seeds were then weighed to obtain their fresh weight. Using a pair of forceps, the seed coat was removed and the embryo dissected. The fresh weights of the embryo and the cotyledons were taken for each seed (Fig. 2.1). In order to obtain their dry weights, the plant structures were dried in an oven for 72 h at 65° C and weighed individually.

A2. Etiolation

A2a. Plant growth conditions

Seeds (9 seeds per line, 2 replicates) were surface-sterilized and imbibed as above. Then individual seeds were planted in conetainers™ (dimensions: 3 cm diameter, 16.5 cm height, 50 mL capacity, Stuewe and Sons, Inc., Corvallis, OR) filled with sterilized medium grade Holiday vermiculite (Hydro-Garden, Toronto, ON). All conetainers™ were arranged inside Nalgene™ plastic beakers (1000 mL) which were filled to a 500 mL mark on the beaker with water and

Figure 2.1. Dormant seed of *Pisum sativum*. Plumula= Plumule. Radicula= Radical.
(from [Finch-Savage and Leubner-Metzger, 2006](#)).



Pisum sativum

then placed inside a growth chamber (SANYO Canada Inc., Concord, ON, Model No. MLR-350) (continuous temperature= 23°C) with no lights on. The controls were placed inside another growth chamber (Lab-line® Instruments Inc., Melrose Park, ILL, Cat. No. 850H, Serial No. 0400-002) with the lights on (light intensity of 380 $\mu\text{E m}^{-2} \text{s}^{-1}$; 23°C/18°C, 16h/8h, light/dark regime).

A2b. Parameters measured

Nine days after planting (DAP), plants were harvested and the following parameters were measured: angle (°) of the apical hook, radial thickness (mm) and height of the epicotyl (cm).

The angle of the apical hook was measured with a protractor as soon as the plants were removed from the growth chamber in order to avoid any angle changes that might occur as a result of light exposure. The protractor was placed flat on the measuring surface with the 0 ° pointing downwards and 180 ° pointing upwards (Fig. 2.2). The plant was placed parallel to the 0 ° to 180 ° axis and the angle formed between the axis of the plant and the hook was measured (Fig. 2.2).

When measuring the radial thickness of the epicotyl with the digital caliper, the midpoint of internode 0 was chosen because it is the first internode to develop, whereas internodes 1 and 2 may not have fully developed (Fig. 2.3). The height of the epicotyl was measured using a ruler, from the point just above the cotyledons to the top of the epicotyl where the apical hook formed (Fig. 2.3).

Figure 2.2. Apical hook angles of etiolated pea plants. 180° refers to a straight seedling, i.e., no apical hook. 0° indicates an acute apical hook.

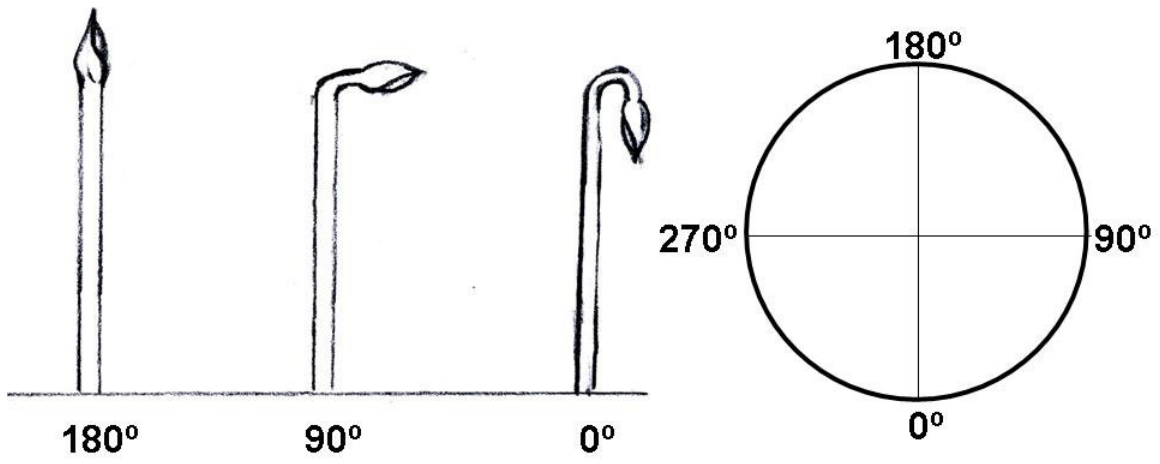
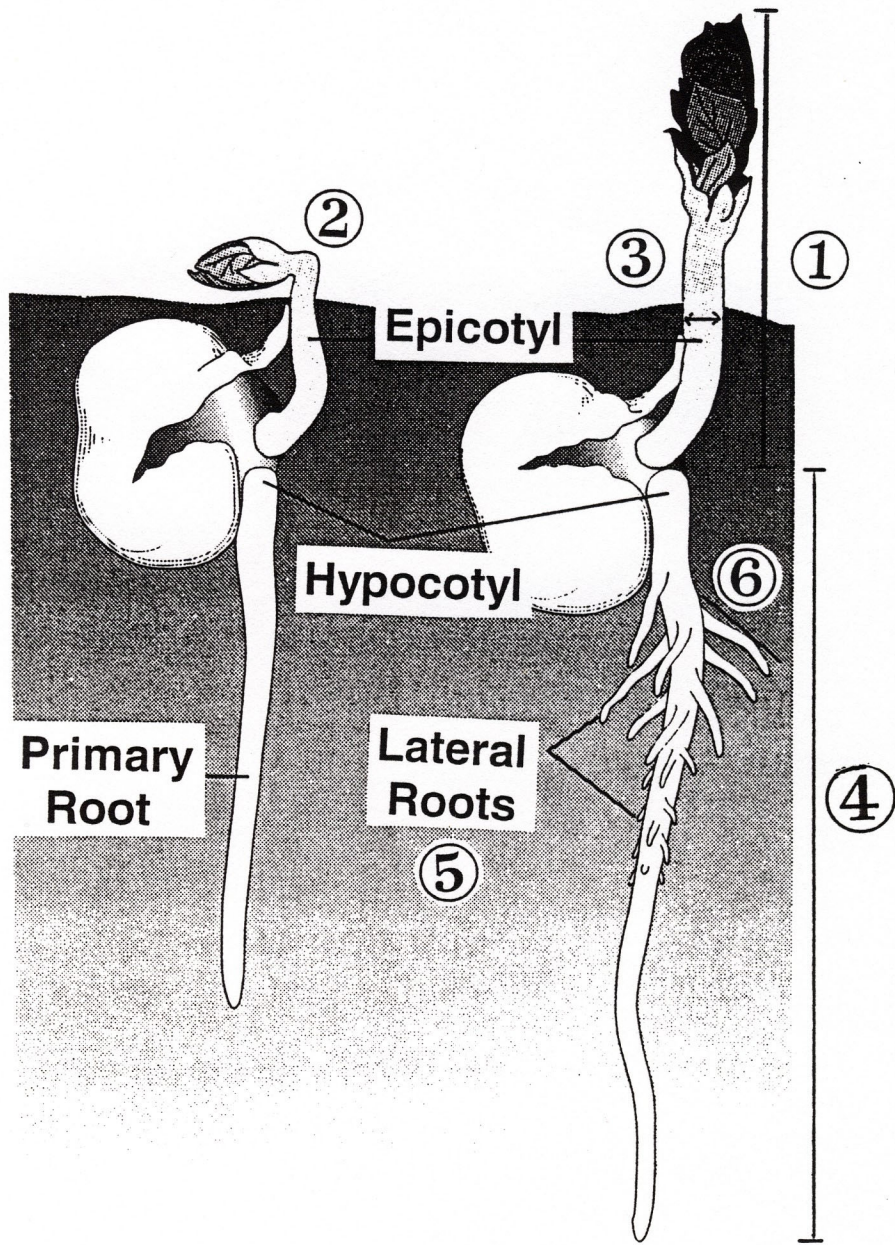


Figure 2.3. Morphological features on pea seedlings. 1. Epicotyl height. 2. Apical hook. 3. Diameter of the mid-point of internode 0. 4. Length of the primary root. 5. Lateral roots. 6. Length of lateral root(s) (Modified from Hopkins, 1999).



A3. Pigmentation

A3a. Plant growth conditions

Seeds (24 from each line) were surface-sterilized and imbibed as above. They were planted (4 seeds per pot) in large green pots (dimensions: 15.2 cm diameter, 11.9 cm height, 1300 mL) filled with 50%:50% mixture of sterilized turface[®] (TURFACE MVP, Profile Products LCC, Buffalo Grove, IL, USA) and peat (ASB Greenworld Ltd., Mount Elgin, Ont., Canada).

The plants were grown in a controlled growth-room with a 23/18°C, 16/8 h, light/dark regime and under high pressure sodium lights (400 watts, P.L. Light Systems) and metal halide lights (400 watts, P.L. Light Systems) (light intensity on growth room bench, 132 to 150 $\mu\text{E m}^{-2} \text{ s}^{-1}$). Plants were watered by irrigation with deionized water for the first 10 DAP, and then with nutrient solution or deionized water every other day (Guinel and Sloetjes 2000). Whenever the plants exhibited signs of wilting, additional water was given to them. The nutrient solution was made of 2 mM KH_2PO_4 , 2.5 mM $\text{Ca}(\text{NO}_3)_2$, 2 mM K_2SO_4 , 1 mM $\text{MgSO}_4 \cdot 7\text{H}_2\text{O}$, 0.2 mM Fe III EDTA, with 1 ml 1^{-1} micronutrient solution (0.05 mM KCl, 0.025 H_3BO_3 , 0.002 mM $\text{ZnSO}_4 \cdot 7\text{H}_2\text{O}$, 0.002 mM $\text{MnSO}_4 \cdot \text{H}_2\text{O}$, 0.0005 mM $\text{CuSO}_4 \cdot 5\text{H}_2\text{O}$, 0.0005 mM $\text{Na}_2\text{MoO}_4 \cdot 2\text{H}_2\text{O}$). Plants were harvested 14 and 22 DAP.

A3b. Measurement of chlorophyll a, b, xanthophylls and carotenoids, and total chlorophyll

Leaflets (0.5 g fresh weight) from the 4th node at 14 DAP and from the 4th and 6th nodes at 22 DAP were homogenized using a mortar and a pestle. The pigments were extracted by grinding the leaflets in 80% acetone and filtering the homogenate through cheesecloth into a beaker (Arnon, 1949). For quantitative analysis, the absorbances (Abs) of the diluted (3 ml extract: 1 ml 80% acetone) pigment extracts were read at 470, 647, 663, and 710 nm wavelengths with a Cary-Win UV Spec (Varian PVT Ltd., Mississauga, ON, Canada). Eighty percent acetone was used as the blank. Three readings were taken at each absorbance and their average was calculated; the average absorbance at 710 nm was then subtracted from the average values at the other absorbances to account for particle scattering. The corrected values were inserted into Lichtenthaler's equations (Lichtenthaler, 1987) to obtain chlorophyll *a* (chl *a*), chlorophyll *b* (chl *b*), xanthophyll and carotenoid (x + c), and total chlorophyll concentrations. The chlorophyll *a/b* ratio was determined by dividing chlorophyll *a* by chlorophyll *b*. Lichtenthaler's equations are:

$$(A) \text{ Chlorophyll } a = 12.25\text{Abs}_{663} - 2.79\text{Abs}_{647}$$

$$(B) \text{ Chlorophyll } b = 21.50\text{Abs}_{647} - 5.10\text{Abs}_{663}$$

$$\text{Xanthophyll and carotenoid} = (1000\text{Abs}_{470} - 1.82A - 85.02B)/198$$

$$\text{Total chlorophyll} = 7.15\text{Abs}_{663} + 18.71\text{Abs}_{647}$$

$$\text{Chlorophyll } a/b \text{ ratio} = \text{chl } a / \text{chl } b$$

The final concentrations obtained were multiplied by the dilution factor (4/3) and were then converted to mg g⁻¹ of fresh weight (FW), by multiplying the diluted value by the total volume of extract obtained (40 mL) divided by the gram fresh weight of leaflets used (e.g., 40 mL/leaflet g FW). Finally, the value obtained was divided by 1000 to get mg g⁻¹ of fresh weight (FW). Raw data can be found in Appendix A.

B. Nodulation characterization

B1. Bacterial Culture

The bacterial strains mentioned above were grown on agar slants and stored in a freezer until needed. The *Rhizobium leguminosarum* bv. *viciae* strains (128C53K (HUP⁺), 128C79 (HUP⁻), and 8401 (*lacZ*)) were grown in a sterilized yeast mannitol broth (YMB) solution. The YMB was composed of 1g mannitol, 0.05g K₂HPO₄, 0.02g MgSO₄ (7H₂O), 0.01g NaCl, and 0.04g yeast extract, and made up a final volume of 100 mL. Twenty mL of the YMB were aliquoted into 125 mL Erlenmeyer flasks and autoclaved.

The bacterial culture was prepared in a laminar flow hood. Two loops of the appropriate rhizobial strain were placed into the 125 mL Erlenmeyer flasks containing the YMB solution. Subsequently, the flasks were placed into a water-bath shaker set to 25°C and 100 rpm (rotations per minute) for approximately 2 to 3 days. Once the bacterial culture became slightly cloudy and had an absorbance reading between 0.5 and 1.0 at 600 nm (using the Cary-Win UV Spec), it was at the right growth stage (i.e. stationary phase) to make inoculum. A 5% (v:v) rhizobial inoculum was made by placing the bacterial culture into sterile H₂O. The day that the plant was inoculated was referred to as 0 days after inoculation (DAI).

B2. Study of nodule organogenesis

B2a. Plant growth conditions

Seeds were surface-sterilized in the same manner as in section A1. Imbibed seeds were planted three per pot (15.3 cm diameter, 14.7 cm height, 1600 mL capacity) filled with autoclaved Holiday vermiculite. Five DAP, the seedlings were inoculated with a 5% solution of *R. leguminosarum* bv. *viciae* (strain 8401, pRL1 + constitutive B-Gal, expressor pXLGD4, Strep. R., Tet. R., *lacZ*; obtained as a gift from Allan Downie of the John Innes Centre, Norwich, UK). The plants were grown in a controlled growth-room which had the same temperature and light/dark regime as in Section A3a. Plants were watered as mentioned in Section A3a. However, the nutrient solution contained reduced amounts of nitrogen, specifically with five times less $\text{Ca}(\text{NO}_3)_2$ (0.5 mM). Plants were harvested every 3 days between 0 and 26 DAP (i.e., 0 and 21 DAI).

B2b. LacZ strain description

The strain used for the study of nodule organogenesis was *R. leguminosarum* bv. *viciae* strain A34 (pXLGD4) (Walker and Downie, 2000). Strain A34, a derivative of strain 8401, contains the symbiosis plasmid pRL1JI, and carries chromosomally-encoded streptomycin resistance. The plasmid pXLGD4 is a replicon with an IncP origin of replication. This plasmid carries a tetracycline resistance marker as well as a *S. meliloti hemA-lacZ* fusion that constitutively produces β -galactosidase. This fusion was constructed by cloning a 2.0 kb *Bam*HI-*Hind*III fragment, containing the regulatory region of the *S. meliloti hemA* gene, likely its promoter and

its transcription factor binding sites upstream of the coding region of the *lacZ* gene of the parent vector, pGD499 (Leong et al. 1985).

B2c. Preparation of root segments

Predetermined segments (3 segments per time point per line, each segment from individual plants, 4 replicates) cut from the 3rd oldest lateral root 1 cm away from its branching point of the primary root (as in Guinel and LaRue, 1991). The lateral root segments were 1 cm in length and were placed in small glass vials with caps (6.7 cm height and 12 mL capacity). Once the segments were in vials, they underwent a series of treatments as follow:

The segments were fixed for 1 h in a 1.25% (v/v) glutaraldehyde solution. The solution was composed of 1 mL 25% glutaraldehyde (Marivac, Canton de Gore, Québec) into 19 mL of 0.1 M Phosphate Buffer (5.3 g KH₂PO₄, 13.9 g K₂HPO₄, 1 L distilled H₂O, pH 7.0). Then they were rinsed two times in 0.1 M phosphate buffer (15 min per rinse) and stained in an X-gal (5-bromo-4-chloro-3-indolyl-β-D-galactopyranoside (substrate)) solution overnight, at room temperature, in a dark location. The X-gal solution was composed of 3.2 ml 0.1 M phosphate buffer, 200 μl of 100 mM K₄Fe(CN)₆, 200 μl of 100 mM K₃Fe(CN)₆, 120 μl of 2% 5-Bromo-4-chloro-3-indolyl-beta-D-galactoside (X-gal) (Fermentas Canada Inc.) in dimethyl formamide (DMF). In order to make an X-gal stock solution 20 mg X-gal powder was dissolved in 1 mL DMF). During the staining process, the substrate reacted with the enzyme beta-galactosidase that was produced by the rhizobia and the end product was blue (i.e. 4-chloro-3-brom-indigo). The next day the segments were rinsed once again in a buffer three times (10 min per rinse) and in deionized

water (dH₂O) two times (5 min per rinse). They were cleared in a 30% bleach solution for 6 min and rinsed two times in dH₂O for 5 min. Following the clearing, the segments were vacuum-infiltrated for 1 h in a 30% and then a 60% glycerine solution. In order to preserve the segments for later use, they were stored in 60% glycerine.

It should be mentioned that the root segments were fixed in glutaraldehyde in order to inactivate the indigenous β -galactosidase of the plant, as this might interfere with the visualization of the ITs in the segments (Chovanec and Novak, 2005).

The root segments were observed with a Carl Zeiss Axiostar light microscope equipped with phase-contrast optics (objective 40X; Ph; NA= 0.64) for the presence of any one of the six nodulation events described by Guinel and Sloetjes (2000): (A) infection threads (IT) in root hair or epidermis, (B) IT in cortex and not associated with cortical cell divisions, (C) IT in cortex but associated with divisions, (D) nodule primordium, (E) emerging nodule, and (F) mature nodule. The presence of any one of these nodulation events was scored on a tally sheet. The number of nodulation events (i.e., A-F) per 1 cm of 3rd lateral root for each time point was determined. Also, the total number of infection events per 1 cm of 3rd lateral root was determined for every day studied, from 3 DAI to 21 DAI. Raw data can be found in Appendix B.

B3. Nodule formation on plants of different ages

Seeds were surface-sterilized in the same manner as noted in section A1; however, there were 2 seeds planted per large green pot (15.3 cm diameter, 14.7 cm height, 1600 mL capacity) filled

with autoclaved Holiday vermiculite. Seedlings were inoculated with 5 mL of a 5% solution of *Rhizobium leguminosarum* bv. *viciae*, strain 128C53K (HUP⁺, the wild-type with hydrogenase uptake; obtained from Nitragin Inoculants, Liphatech Inc., Milwaukee, WI) 5 DAP. The plants underwent the same watering regime as in Section B2a., and were grown in a controlled growth-room under the same day/night cycle as in Section A3a. The plants were harvested 26, 33, 40, and 47 DAP (i.e., 21, 28, 35, and 42 DAI).

Six plants from each line (Sparkle and E151) were used at each time point and the study was replicated 4 times. The nodule lobes found on the root system were tallied and the average number of nodule lobes found per plant line was determined. The study was replicated with *R. leguminosarum* strain 8401 (*lacZ*).

B4. Nitrogenase activity experiments

B4a. Plant growth conditions

Seeds were surface-sterilized as previously mentioned in Section A1. They were planted in Qubit plant growth pots (dimensions: 8.8 cm diameter, 14.4 cm height, and 550 mL capacity; Qubit Systems, Kingston, ON) filled with a 50%:50% mixture of sterilized Holiday vermiculite and grade 16 silica sand (Bell and MacKenzie, Hamilton, ON). Five DAP, seedlings were inoculated with 5 mL of a 5% solution of *R. leguminosarum* strain 128C79 (HUP⁻, with no hydrogenase uptake; obtained from Dr. R. Stewart Smith, Nitragin Inoculants, Liphatech Inc., Milwaukee, WI). The control seedlings were never inoculated. The plants were grown in a controlled growth-

room which had the same temperature and light/dark regime as in Section A3a. Plants were watered as mentioned in Section B2a.

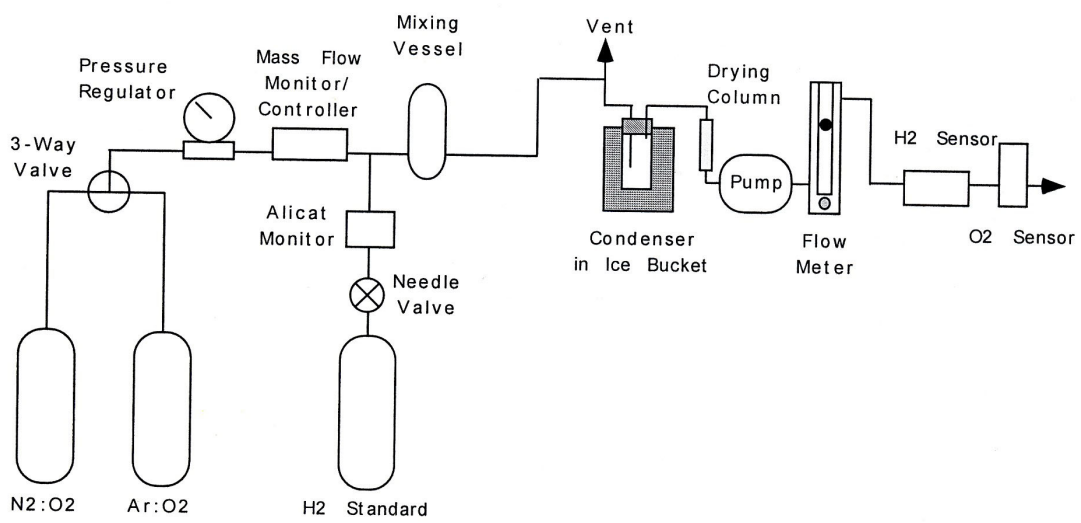
B4b. Calibration of the Qubit apparatus

Before the rate of nitrogen fixation could be calculated, the Qubit apparatus (Qubit Systems, Kingston, ON) was set-up for calibration mode (Fig. 2.4). In order to be calibrated, the Qubit apparatus was initially exposed to a high concentration of H₂ (2000 ppm H₂) for 60 seconds in order to condition the H₂ sensor (Fig. 2.4). Then the Qubit apparatus was exposed to two carrier gases (Praxair Canada, Inc., Kitchener, ON, Canada).

1. The first carrier gas was a mixture of N₂ and O₂; it was used as a representative of the atmosphere. It flowed at the source (tank) at a constant rate (1000 mL/min). As the H₂ concentration was increased by manipulation of the Alicat Monitor (Fig. 2.4), the concentration of the N₂:O₂ mixture was altered depending on the H₂ released, and ranged between 0 and 50 ppm. This carrier gas allowed for the Apparent Nitrogenase Activity (ANA) of nodules to be calculated. ANA represents the minimum number of electrons used to produce H₂, the rest of the electrons are used to reduce N₂ to ammonia (NH₃) (Hunt, 2005).

2. The second carrier gas mixture used was made up of Ar and O₂; it allowed for the measurement of an accurate rate of hydrogen evolution from the nodule. It was released from the source (tank) at a constant rate (1000 mL/min). As above, because the Ar:O₂ gas mixture carried the H₂, its concentration was altered by that of the H₂; this resulted in a range of Ar:O₂ varying

Figure 2.4. Configuration of the Qubit System during calibration. The carrier gases of $\text{N}_2:\text{O}_2$ and $\text{Ar}:\text{O}_2$ are used to measure the Apparent Nitrogenase Activity (ANA) and Total Nitrogenase Activity (TNA), respectively. A H_2 standard provides the hydrogen source (from Hunt, 2005).



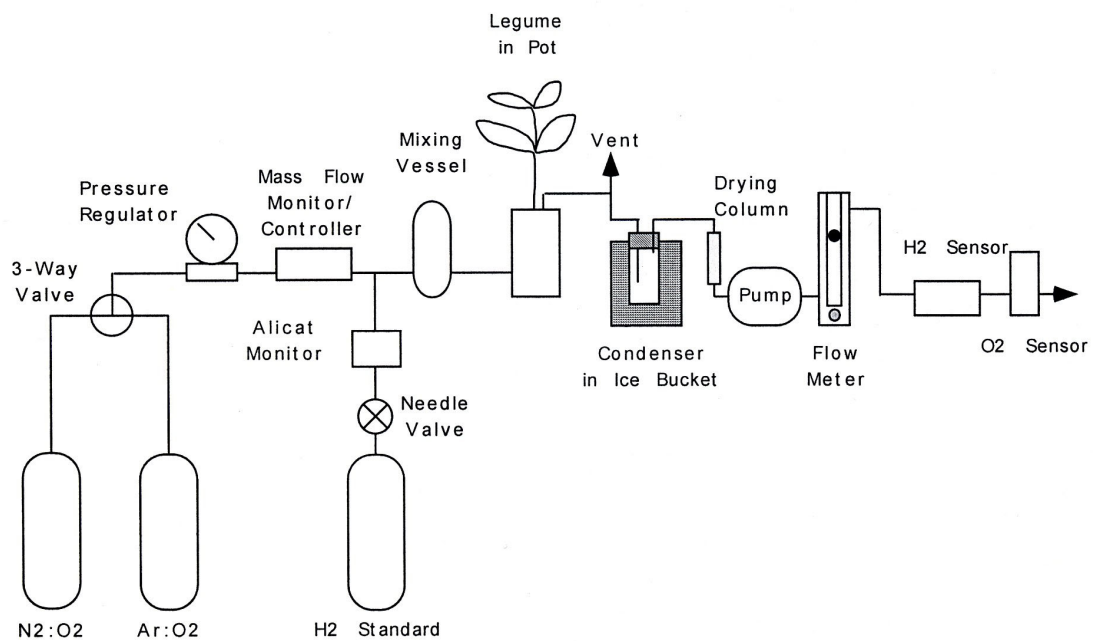
between 0 and 200 ppm. This inert carrier gas was used to calculate the Total Nitrogenase Activity (TNA) of nodules. TNA represents the maximum rate of H₂ evolution because all the electrons are being allocated towards H₂ production instead of N₂ reduction (Hunt, 2005). The flow rates of the H₂ standard carried by either N₂:O₂ or Ar:O₂ were calculated to produce 10 different gas mixtures representing different levels of H₂ in the carrier gases, at even increments across the determined concentration range. Data collection started when the apparatus was being flushed with the N₂:O₂ carrier gas in the absence of H₂, representing point 0 on the calibration curve. As was recommended by the manufacturer, the flow rate was set-up at 200 ml/min through the H₂ sensor using the sub-sampling pump and flow meter (Fig. 2.4). Once the voltage output of the H₂ sensor reached a steady state, the value was recorded for that particular carrier gas.

B4c. Nitrogenase activity determination for individual plants

Once the gas exchange system was calibrated using either the N₂:O₂ or Ar:O₂ carrier gas, the H₂ tank was shut off, and the apparatus was set-up to measure nitrogenase activity in nodulated root systems (Fig. 2.5). Before the plants were hooked up to the Qubit system, the pots were drained of any water because water affects the diffusion of the carrier gases through the soil medium and the interaction of the carrier gases with the H₂ gas being released from the nodules (Dong et al., 2000).

To measure the H₂ gas being released under ANA and TNA conditions, plants were flushed first with the N₂:O₂ carrier gas. The carrier gas picked up the H₂ gas being released from the nodules

Figure 2.5. Configuration of the Qubit System during nitrogenase activity measurement. During this setup a plant inoculated with HUP⁺ rhizobium is attached to the system. The nodules release hydrogen into the soil medium and this H₂ gas is picked up by either N₂:O₂ or Ar:O₂ carrier gases and taken to the H₂ sensor (from Hunt, 2005).



of the plant and carried it to the H₂ sensor. The sensor measured the amount of H₂ being evolved from the plant and relayed this information back to the computer. The peak in hydrogen was recorded for the N₂:O₂ carrier gas. The same procedure was followed with the Ar:O₂ carrier gas. The rates of H₂ [ppm] in ANA (N₂:O₂) and TNA (Ar:O₂) were determined using the polynomial equations obtained from the calibration data and by inserting the hydrogen voltage output of the plants into these polynomial equations (Dong et al., 2000; Jason Curtis, personal communication, Qubit Systems, Kingston, ON). Once [H₂] (ppm) in ANA and TNA were determined for each individual plant, the rates of ANA and TNA were calculated using Equation 2 and Equation 3. In Equation 2 or 3 the abbreviation P was representative of atmospheric pressure, ANA ΔH₂ or TNA ΔH₂ represented any changes in H₂ concentration when calculating ANA or TNA, R was a constant, and T symbolized the room temperature. The rate of nitrogen fixation (μmol N₂/hr) was determined by inserting the ANA and TNA rates into Equation 4.

$$R = 8314.5 \text{ mL kPa K}^{-1} \text{ mol}^{-1}$$

$$P = 101.325 \text{ kPa}$$

$$T = 291.5 \text{ Kelvin}$$

$$\text{ANA rate: ANA flow mL/min} \times P \times \text{ANA } \Delta H_2 \text{ ppm} \times 60 \text{ mins/hr} / R \times T \quad (\text{Equation 2})$$

$$\text{TNA rate: TNA flow mL/min} \times P \times \text{TNA } \Delta H_2 \text{ ppm} \times 60 \text{ mins/hr} / R \times T \quad (\text{Equation 3})$$

$$\text{N}_2 \text{ fixation rate } (\mu\text{mol N}_2/\text{hr}): (\text{TNA}-\text{ANA})/3 \quad (\text{Equation 4})$$

The number three was used as the denominator because the reduction of N₂ to NH₃ requires 3 electron pairs. Also, once the rate of H₂ evolution was determined, the number of nodule lobes found on the plants was recorded. The shoots, roots, and nodules of the plants were dried at 65°C

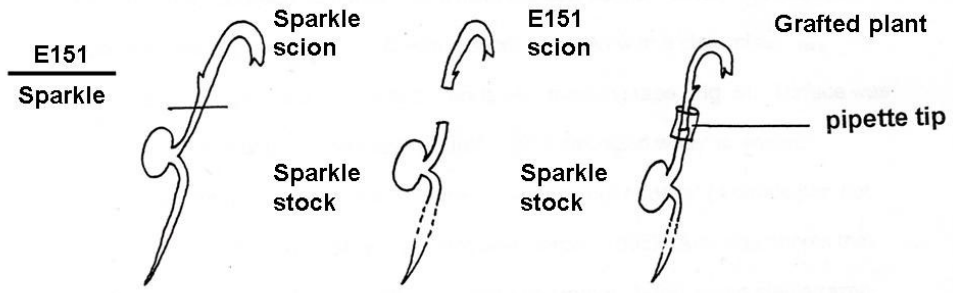
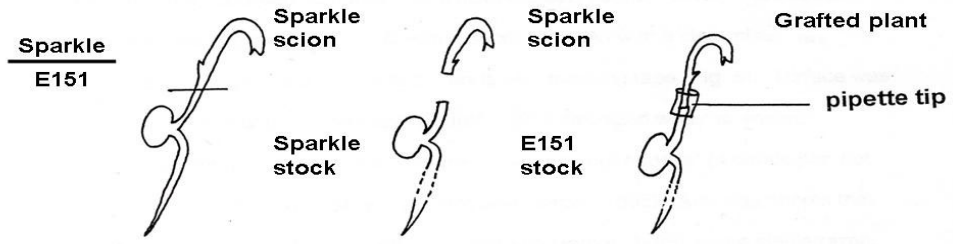
for 3 days, and shoot, root, and nodule dry weights of the individual plants were measured. These parameters were measured so that the rate of nitrogen fixation could be standardized since each individual plant forms varying numbers of nodules, and has a different shoot, root, or nodule dry weight. The rate of N₂ fixation was measured in μmol N₂/hr/nodule DW. Raw data can be found in Appendix C.

B5. Grafting

Sparkle and E151 were surface-sterilized and imbibed as previously mentioned in Section A1. The seeds were planted in small square green pots (dimensions: 8.5cm height, 10.0cm width, 450 mL capacity) that contained turface[®] and peat in a mixture of 75%:25% respectively. The plants were grown for a short period of time in conditions that promoted etiolation; the elongated shoot made it easier to perform the grafts. The pots were placed in black storage bins (dimensions: 32.6 cm width, 43.3 cm length, and 28.2 cm height) on the floor of the controlled growth-room and were watered from the top before the storage bins were closed. It should be noted that the bins were lined with paper towels and filled with water to ensure that the planting medium did not dry out while the bins were closed.

Four DAP, the plants were taken out of the bins and the grafts were performed. The plants were cut transversely halfway between the cotyledons and the first node using a sterile razor blade (Guinel and Sloetjes 2000). The scion of one plant was grafted onto the stock of another plant and the graft was held together with the tip of a disposable pipette (Fig. 2.6) (Guinel and Sloetjes 2000).

Figure 2.6. Method of grafting plants. Grafts of Sparkle/E151 and E151/Sparkle are represented here. Control grafts were produced in the same manner (Modified from Postma, Jacobsen, and Feenstra, 1988).



The disposable pipette was placed around the stock first and then the scion was placed into the pipette tip; this ensured a tight junction between the 2 parts. The following control and reciprocal graft combinations were performed: Sparkle/Sparkle, E151/E151, Sparkle/E151, and E151/Sparkle.

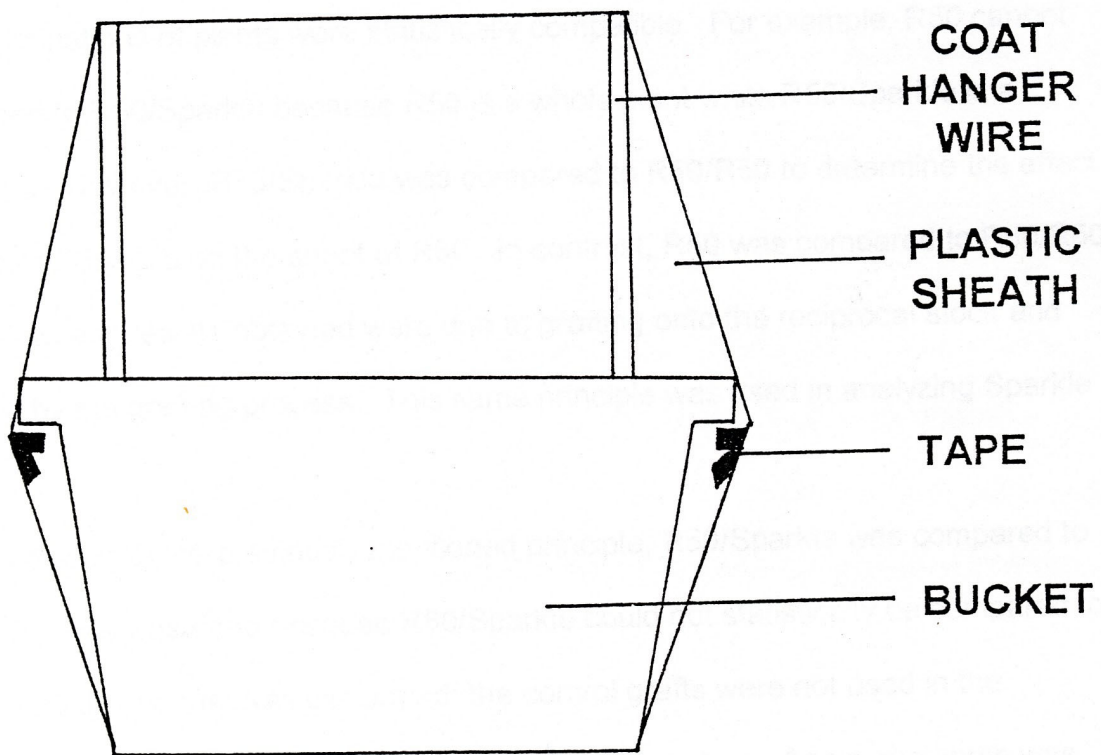
Once the plants had been grafted, they were placed into hot houses (i.e. plastic bins that had turf on the bottom and were covered with plastic; Fig. 2.7). The hot houses were filled with water to ensure that the turf on the bottom remained moist and the humidity in the hot houses was maintained. The plants were checked daily for the growth of lateral shoots from the stock; in the case that a side-shoot had grown, it was removed using a sterile razor blade. This ensured that all of the plant's energy was allocated towards the graft and not towards secondary shoot growth.

Five DAP, the grafted plants were inoculated with 5 ml of a 5% culture of *R. leguminosarum* bv. *viciae*, strain 128C53K (HUP⁺), were grown in the controlled growth-room under day/night regime as mentioned in Section A3a and watered in the same manner as described in Section B2a. The plants were harvested 26 DAP (21 DAI). The number of nodule lobes present on the plants was recorded. Raw data can be found in Appendix D.

B6. Statistics

Descriptive statistics (i.e., mean, standard error) and t-tests were performed on the data using Sigma Stat 2.03. If there was no significant difference between the variables using a Student's t-

Figure 2.7. Diagram of a “hot house.” Used to produce hot and humid conditions so that proper vascular connections occurred between grafted plants. (from Zettler, 1998)



test, then a Mann-Whitney Rank Sum test was performed. When I compared pea lines over a time period, I could not use the original significance value because multiple points were being compared over time. In such a case, the Bonferroni correction was used to reduce the odds of getting significant results that were not truly significant. When using the Bonferroni correction, α/n ($\alpha= 0.05$, $n=$ number of tests) becomes the new significance level.

III. RESULTS

A. Physiological characterization

A1. Analysis of the embryonic plant; the seed

Qualitative analysis showed no obvious differences in the seed size, shape, seed coat or cotyledon colour between the two pea lines used. Sparkle and E151 seeds were approximately 7 mm in size. They were round in shape and their seed coat was smooth. The cotyledons were green in colour.

Because no apparent distinction between the 2 lines was seen based only on the phenotypic characteristics of the seeds, I determined whether the seeds differed in their weight. Dry weight (DW) was first obtained of dormant seeds i.e., seeds which had been harvested several weeks before and kept in a fridge at 4 °C. These seeds were then placed in water for imbibition and weighed several hours later. After careful dissection of the seeds, the embryo and the cotyledon were weighed separately to obtain their fresh weight (FW). The dissected parts of the seed were then dried in an oven for 72 h at 65° C to obtain their DW. Quantitatively there were no

differences in dormant seed DW between the two lines (Table 3.1). In contrast, the FW of E151 imbibed seeds was significantly greater than that of Sparkle imbibed seeds (Table 3.1). When examining the individual parts of the imbibed seed, E151 cotyledons had a significantly greater FW than those of Sparkle, but there were no differences in the embryo FWs between the two lines (Table 3.1). There appeared to be no significant differences in cotyledon and embryo DWs amongst the two lines. Based on the data, E151 seeds appear to have a greater water-holding capacity than Sparkle seeds.

A2. Etiolation

A2a. Sparkle plants

The Sparkle plants were green in colour and variable in size when grown in the light. The apical hook angle was difficult to measure because newly formed leaves were in the way.

The Sparkle seedlings grown in continuous darkness exhibited all of the signs of an etiolated plant (i.e. tall and slender epicotyl, partially closed apical hook, and pale yellow leaves (chlorosis)) (Table 3.2). A comparison was made between light and dark-grown seedlings.

Light-grown Sparkle plants were significantly shorter than the dark-grown plants (Table 3.2). In addition, plants grown in the light had an apical hook angle that was significantly more open than the one on plants grown in the dark (Table 3.2).

Table 3.1. Dry weights (g) and fresh weights (g) of Sparkle and E151 seeds.

Trait	Sparkle	E151
Dormant Seed DW	0.232 ± 0.008	0.250 ± 0.009
Imbibed Seed FW	0.599 ± 0.016	0.679 ± 0.019*
Cotyledon FW	0.522 ± 0.015	0.601 ± 0.018*
Embryo FW	0.012 ± 0.000	0.012 ± 0.000
Cotyledon DW	0.198 ± 0.010	0.219 ± 0.035
Embryo DW	0.003 ± 0.000	0.003 ± 0.000

Values are means ± SE (n=45 for each line). A *t*-test was used. Values marked by an asterisk represent statistically significant differences (95% confidence level). DW= Dry weight. FW= Fresh weight.

Table 3.2. Epicotyl height (cm), epicotyl radial thickness (mm), and apical hook angle (°) of Sparkle and E151 9 DAP grown in the light (control) and dark.

Characteristic	Sparkle		E151	
	Light (Control)	Dark	Light (Control)	Dark
Epicotyl height	4.4 ± 0.2 ^a	12.5 ± 0.9 ^a	4.4 ± 0.3 ^c	10.7 ± 1.0 ^c
Epicotyl radial thickness	2.63 ± 0.05	2.55 ± 0.07	2.63 ± 0.06	2.62 ± 0.05
Apical hook angle	159 ± 5 ^b	115 ± 10 ^b	171 ± 2 ^d	92 ± 10 ^d

Values are means ± SE (n=9 for each of 2 trials). A *t*-test was used. Values marked by different letters represent statistically significant differences (95% confidence level).

A2b. E151 plants

E151 plants that were grown in the light and dark exhibited the same qualitative characteristics as Sparkle. Quantitatively, the light-grown mutants were drastically shorter than the ones grown in the dark (Table 3.2). The apical hook angle was significantly greater in the mutant line when it was grown in the light than in the dark (Table 3.2).

A2c. Sparkle and E151 compared

Upon close inspection with the naked eye, Sparkle and E151 plants grown under the same conditions looked very similar in appearance (e.g. depth of green pigmentation, variable stature). The three characteristics measured (epicotyl height, epicotyl radial thickness, and apical hook angle) did not vary significantly between the WT and mutant lines grown in the light or grown in the dark (Table 3.2).

A3. Pigmentation

A3a. Qualitative observations

The colouration between Sparkle and E151 leaves was visually examined throughout the growth of the plant; no distinguishable differences in pigmentation were ever seen in the younger plants (9 (Fig. 3.1) or 14 DAP). The leaves borne by nodes 4 at 14 DAP and by nodes 4 and 6 at 22 DAP were chosen as representatives of leaves of different ages; my choice was based on the

study of Guinel and Sloetjes (2000). This will allow me to compare my findings to those of Guinel and Sloetjes (2000).

A3b. Quantitative analysis

In Sparkle, there were no significant differences in the concentration of chlorophyll a (chl a), chlorophyll b (chl b), total chlorophyll (T chl), total accessory pigments (xanthophylls and carotenoids), and the chlorophyll a/b ratio when comparing leaves at different nodes (i.e. 4th and 6th at 22 DAP) and in plants of different ages (i.e. leaves of node 4 at 14 and 22 DAP) (Table 3.3). Likewise, when the various pigment concentration and pigment ratios were compared in E151 plants of different ages or leaves of different nodes no significant statistical differences could be found (Table 3.3). In addition, comparisons between Sparkle and E151 at each of the specific ages and at the corresponding nodes revealed no quantitative differences in the pigment concentrations or the chlorophyll a/b ratios. The lack of an easily noticeable trait such as altered leaf colouration makes it difficult to distinguish E151 mutants from WT plants.

B. Nodulation characterization

B1. Nodule organogenesis

B1a. LacZ Protocol

Previous studies in the lab have focused on longitudinal sections of fresh root tissue stained with toluidine blue to examine nodule organogenesis. A major drawback with this method is that only

Figure 3.1. Sparkle (A) and E151 (B) plants grown till 9 DAP. Plants are shown next to each other to demonstrate that no clear differences can be seen at a young age in their pigmentation even though other phenotypic differences such as shoot height are visible. Bar= 1 cm.



Table 3.3. Concentration (mg g⁻¹ fresh weight) of chlorophyll a (chl a), chlorophyll b (chl b), xanthophyll (x) and carotenoid (c), total chlorophyll (T chl), and chlorophyll a/chlorophyll b (chl a/b) pigments in Sparkle and E151 14 and 22 DAP.

Sparkle					E151				
Node 4 (14 DAP)					Node 4 (14 DAP)				
chl a	chl b	x+c	T chl	chl a/b	chl a	chl b	x+c	T chl	chl a/b
1.44 ± 0.11	0.68 ± 0.08	0.46 ± 0.01	2.12 ± 0.18	2.18 ± 0.19	1.28 ± 0.21	0.60 ± 0.09	0.39 ± 0.04	1.88 ± 0.28	2.18 ± 0.21
Node 4 (22 DAP)					Node 4 (22 DAP)				
chl a	chl b	x+c	T chl	chl a/b	chl a	chl b	x+c	T chl	chl a/b
1.59 ± 0.11	0.70 ± 0.07	0.41 ± 0.02	2.29 ± 0.18	2.30 ± 0.11	1.78 ± 0.11	0.79 ± 0.02	0.43 ± 0.02	2.57 ± 0.12	2.26 ± 0.11
Node 6 (22 DAP)					Node 6 (22 DAP)				
chl a	chl b	x+c	T chl	chl a/b	chl a	chl b	x+c	T chl	chl a/b
1.77 ± 0.06	0.72 ± 0.05	0.44 ± 0.01	2.49 ± 0.11	2.49 ± 0.13	1.81 ± 0.10	0.74 ± 0.03	0.45 ± 0.02	2.55 ± 0.11	2.46 ± 0.13

Values are means ± SE (n=8 for each of 4 trials for node 4 and node 6 (14 DAP and 22 DAP), of each of 5 trials for node 4 (22 DAP). A *t*-test was used with the Bonferroni correction and there were no statistical differences within or between the lines of same nodes of different ages.

small segments of the root can be visualized and because sections are taken one has only a two-dimensional view of the process. The technique I used, in contrast, can be applied to the entire system and one can see the whole root cortex of a particular region since the root fragment under observation has been cleared. However, to see simultaneously the IT and the cell divisions in the inner cortex with the protocol generally described in the literature (e.g. Chovanec and Novak, 2005; Karas et al., 2005) was practically impossible. Indeed, when I saw a clear blue IT in the outer cortex, I was unable to distinguish individual cells in the inner cortex. To visualize clearly these inner cortical cells, I had to bleach dramatically the root segment; this was done at the expense of the IT which would then lose its bright colour. Since I was interested in identifying the infection events in the inner cortex I had to find a compromise. Initially it was suggested that root segments should be stained overnight; later, I found that a 24 hour staining period produced the best results. Furthermore, the protocol mentioned that root segments should be cleared using 10% bleach for 1-3 minutes; various trials were run whereby the percentage of bleach and the time used to clear the root segment were modified. It was determined that clearing the segments in 30% bleach for 6 minutes provided a clear view of the inner cortex of the root and did not drastically diminish the intensity of the stain.

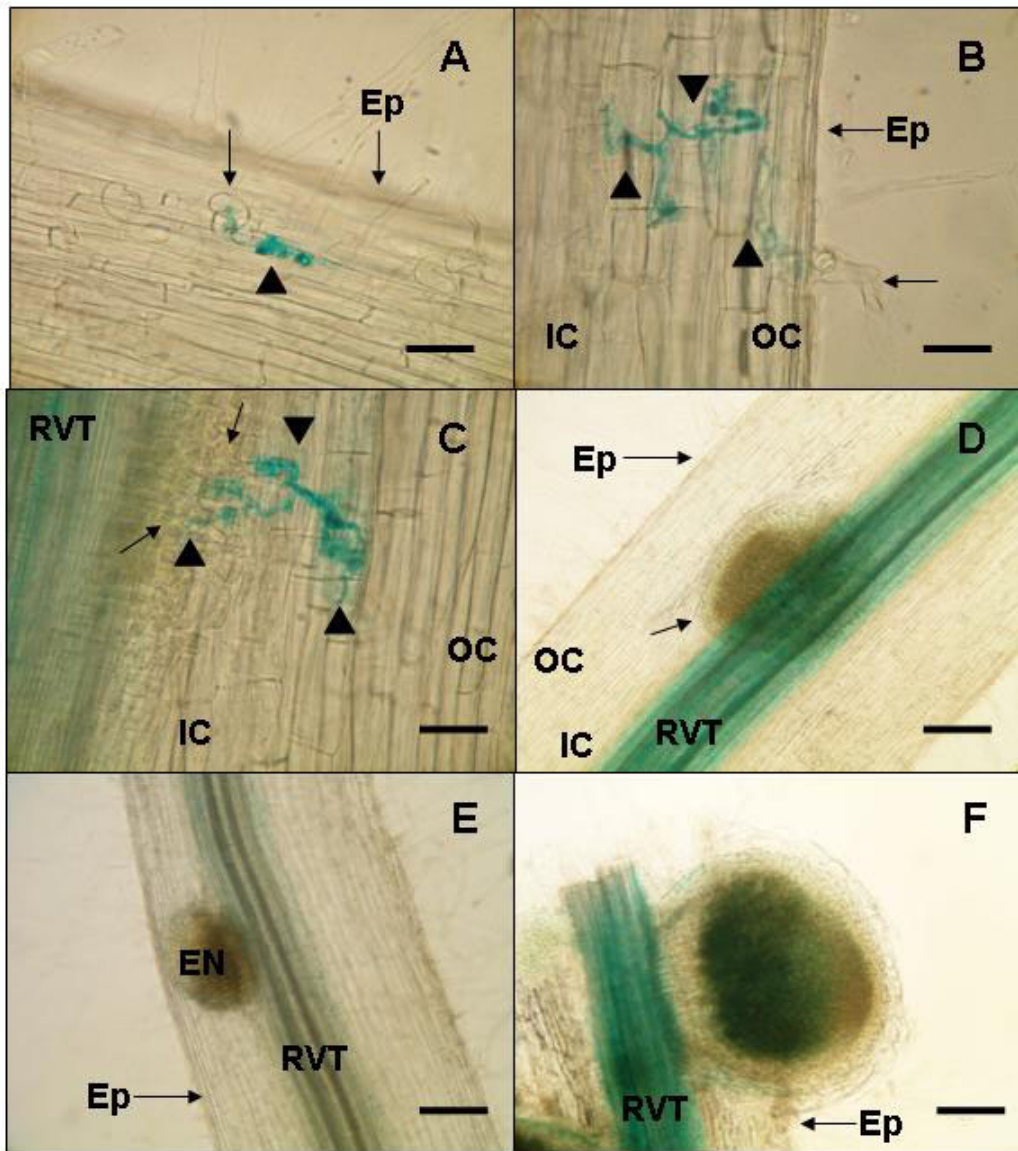
For these experiments, Sparkle and E151 plants were inoculated with *R. leguminosarum* bv. *viciae* strain 8401, which contained a *lacZ* (i.e. encodes beta-galactosidase, an enzyme that cleaves lactose) plasmid. Once the plants reached the appropriate age, they were harvested. One centimetre root segments starting from the 3rd lateral root were used based on the study by Guinel and Sloejtes (2000). This allowed me to compare my findings to the findings of Guinel and Sloejtes (2000).

B1b. Sparkle and the different events

Qualitatively, the six nodulation events described by Guinel and Sloetjes (2000), and mentioned in Materials and Methods section B2, were noted in Sparkle root segments: (A) infection threads (IT) in root hair or epidermis (Fig. 3.2A), (B) IT in cortex and not associated with cortical cell division (Fig. 3.2B), (C) IT in cortex but associated with division (Fig. 3.2C), (D) nodule primordium (Fig. 3.2D), (E) emerging nodule (Fig. 3.2E), and (F) mature nodule (Fig. 3.2F). As a standard, I counted any developing nodules which had not passed the midpoint of the cortex as nodule primordia and any nodules which had passed the midpoint of the cortex but had not breached the epidermis as emerging nodules.

Quantitatively, in Sparkle, the total number of infection events significantly increased from 3 DAI to 6 DAI and then that number remained constant up to my last point of measurement (21 DAI) (Fig. 3.3). In the first few DAI (i.e. 3 and 6), most of the infection events were at stages A to D (Figs. 3.4-3.5) with the majority of the ITs in the RHs or the basal epidermal cells. As time passed, the infection events appeared to progress so that 9 DAI and thereafter, nodule primordia and emerging nodules were visible (Figs. 3.6-3.10). These developing nodules appeared to mature continuously as the number of infection events at stages D and E remained the same whereas those at stage F increased constantly to reach a maximum of 3 at 21 DAI (Fig. 3.10). It is worthwhile to note that over the entire developmental study the highest number of infection events was always found in stage A, indicating that many ITs are probably aborted early in the

Figure 3.2. Nodule organogenesis observed in Sparkle; cleared roots which were inoculated with *R. leguminosarum* strain 8401 (*lacZ*) and stained with X-gal. All roots segments are from plants harvested 9 and 15 DAI. The infections were classified into six different categories: A, IT (arrowheads) either in RH (arrow) or in epidermal cells; B, IT in cortex and not associated with divisions; C, IT in cortex and associated with cortical cell division (arrows); D, nodule primordium (arrow); E, emerging nodule (EN); and F, mature nodule. EN=Emerging nodule, Ep= Epidermis, IC= Inner cortex, OC= Outer cortex, RVT=Root vasculature tissue. Bar= 100 μm for A, B, C. Bar= 220 μm for D, E, F.



nodulation process. These data suggest that Sparkle nodule organogenesis occurs at a constant rate without any delays or blocks in its events.

B1c. E151 and the different events

When nodule organogenesis was inspected in E151, only nodulation events from stages A to E were seen in the root segments (Fig. 3.11). In E151, a significantly increase in the total number of infections was seen from 3 DAI to 12 DAI and then a plateau was reached as time passed (15 DAI to 21 DAI) (Fig 3.3). Three to 6 DAI, most of the infections were at stages A to B with a majority at A (Figs. 3.4-3.5). As the DAI increased (i.e. 9-21), the number of infections increased and more infections were seen at later stages (i.e., C to E) (Figs. 3.6-3.10). However, nodule primordia and emerging nodules rarely formed (Figs. 3.6-3.8), while mature nodules were never seen during the entire study (Figs. 3.4-3.10). Taken together, the data suggest that there is a block in stage C because there is a build-up of infection events at that stage over time up to 18 DAI. The fact that at 21 DAI the number of ITs in stage C decreased in comparison to 18 DAI and the number of ITs in stages D and E increased would indicate that ITs are not entirely blocked but their progression is delayed. As in Sparkle, the number of ITs arrested in stage A is high.

B1d. Sparkle and E151 compared

Qualitatively, the nodules of E151 appear to not develop as fast as the ones of Sparkle because no mature nodules were ever found on E151 (Fig. 3.11). When looking at total number of

Figure 3.3. Total number of infection events at each day of observation tallied per cm of lateral root. Values are means \pm SE (n=3 for each of 4 trials except for E151 15 and 18 DAI where n=11 only). A *t*-test was used with the Bonferroni correction. Letters above columns represent statistically significant differences (99% confidence level) amongst the same plant line.

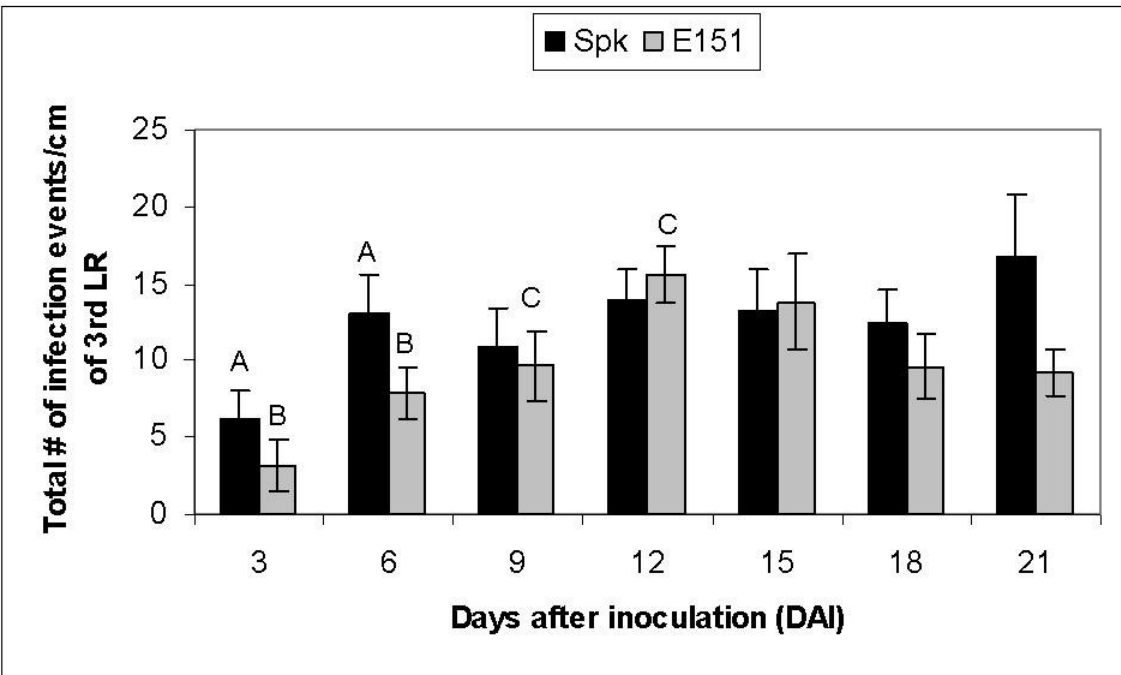


Figure 3.4. Number of infection events at each developmental stage tallied per cm of lateral root 3 DAI. The infections were classified into six different categories: A, IT either in RH or in epidermal cells; B, IT in cortex; C, IT in cortex and associated with cortical cell division; D, nodule primordium; E, emerging nodule; and F, mature nodule. Values are means \pm SE (n=3 for each of 4 trials). A *t*-test was used. The star represents a statistically significant difference (95% confidence level) between the two lines.

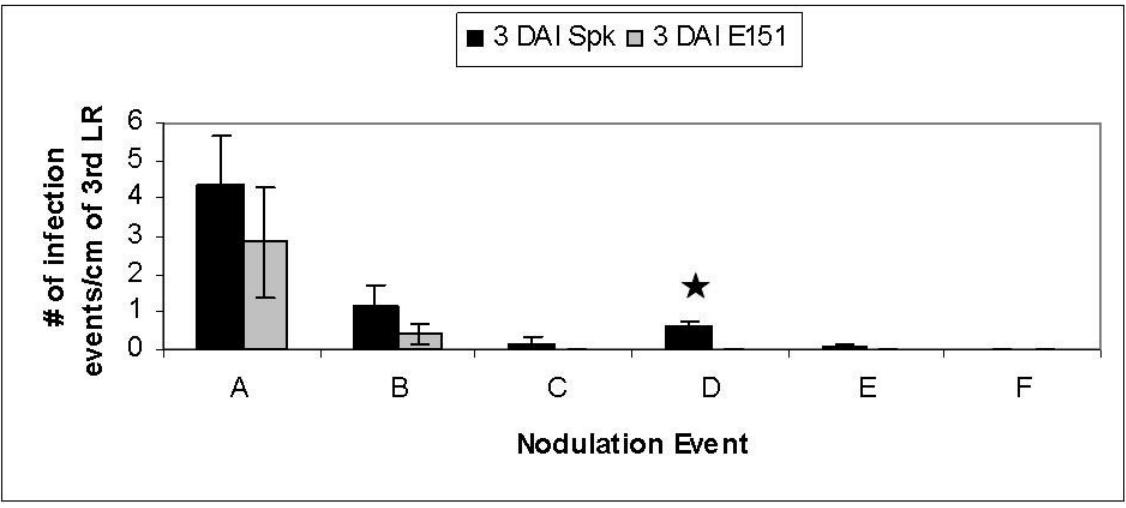


Figure 3.5. Number of infection events at each developmental stage tallied per cm of lateral root 6 DAI. The infections were classified into six different categories: A, IT either in RH or in epidermal cells; B, IT in cortex; C, IT in cortex and associated with cortical cell division; D, nodule primordium; E, emerging nodule; and F, mature nodule. Values are means \pm SE (n=3 for each of 4 trials). A *t*-test was used.

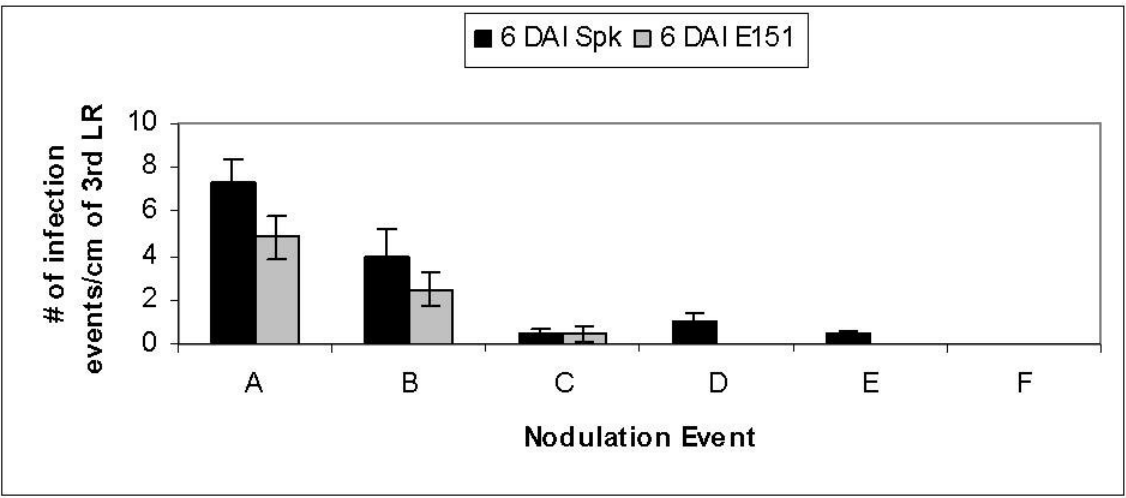


Figure 3.6. Number of infection events at each developmental stage tallied per cm of lateral root 9 DAI. The infections were classified into six different categories: A, IT either in RH or in epidermal cells; B, IT in cortex; C, IT in cortex and associated with cortical cell division; D, nodule primordium; E, emerging nodule; and F, mature nodule. Values are means \pm SE (n=3 for each of 4 trials). A *t*-test was used.

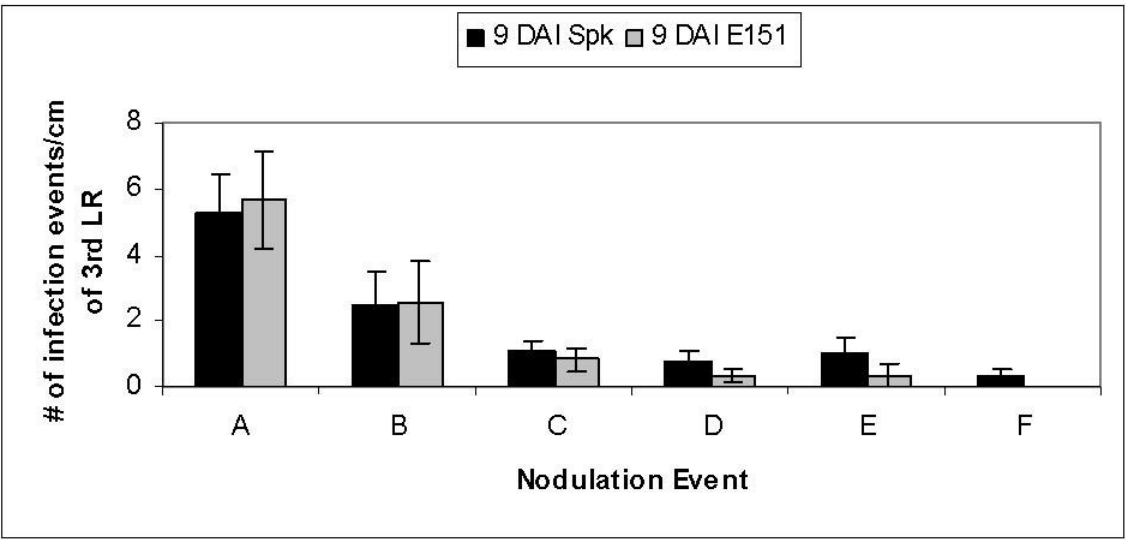


Figure 3.7. Number of infection events at each developmental stage tallied per cm of lateral root 12 DAI. The infections were classified into six different categories: A, IT either in RH or in epidermal cells; B, IT in cortex; C, IT in cortex and associated with cortical cell division; D, nodule primordium; E, emerging nodule; and F, mature nodule. Values are means \pm SE (n=3 for each of 4 trials). A *t*-test was used. Stars represent a statistically significant difference (95% confidence level) between the two lines.

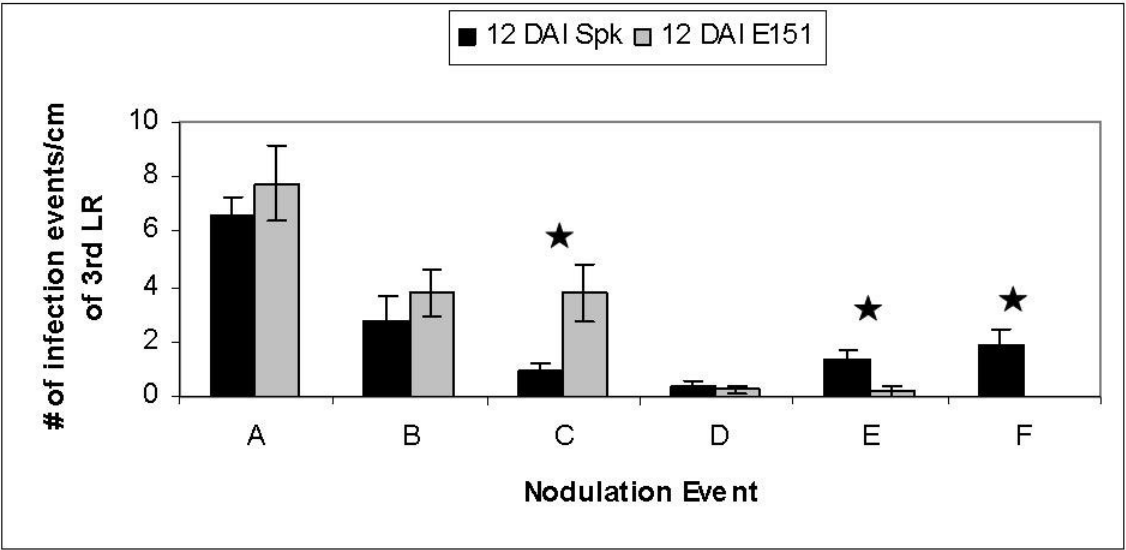


Figure 3.8. Number of infection events at each developmental stage tallied per cm of lateral root 15 DAI. The infections were classified into six different categories: A, IT either in RH or in epidermal cells; B, IT in cortex; C, IT in cortex and associated with cortical cell division; D, nodule primordium; E, emerging nodule; and F, mature nodule. Values are means \pm SE (n=3 for each of 4 trials except for E151 where n=11 only). A *t*-test was used. Stars represent a statistically significant difference (95% confidence level) between the two lines.

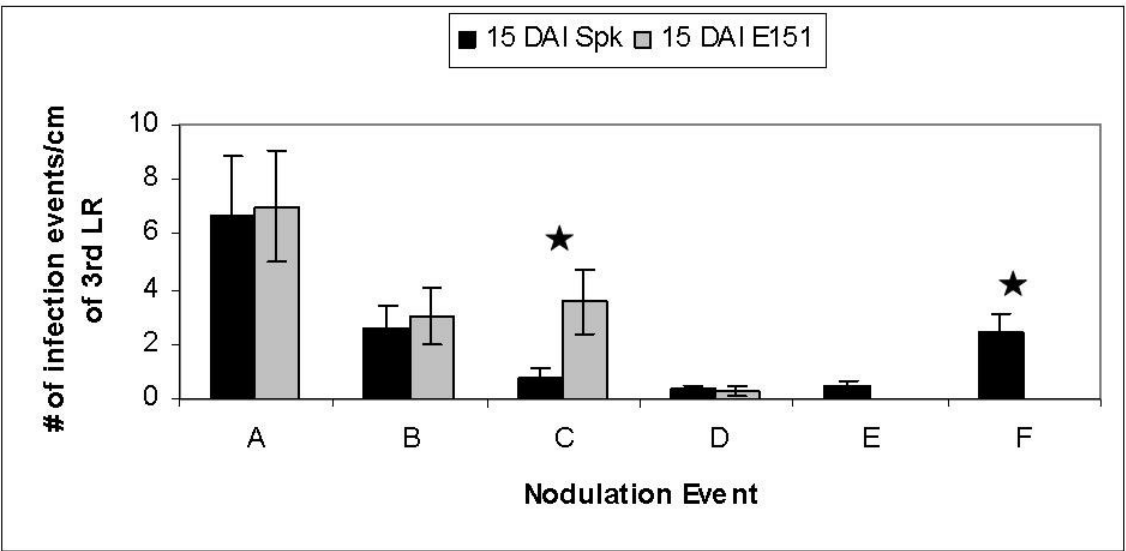


Figure 3.9. Number of infection events at each developmental stage tallied per cm of lateral root 18 DAI. The infections were classified into six different categories: A, IT either in RH or in epidermal cells; B, IT in cortex; C, IT in cortex and associated with cortical cell division; D, nodule primordium; E, emerging nodule; and F, mature nodule. Values are means \pm SE (n=3 for each of 4 trials except for E151 where n=11 only). A *t*-test was used. The star represents a statistically significant difference (95% confidence level) between the two lines.

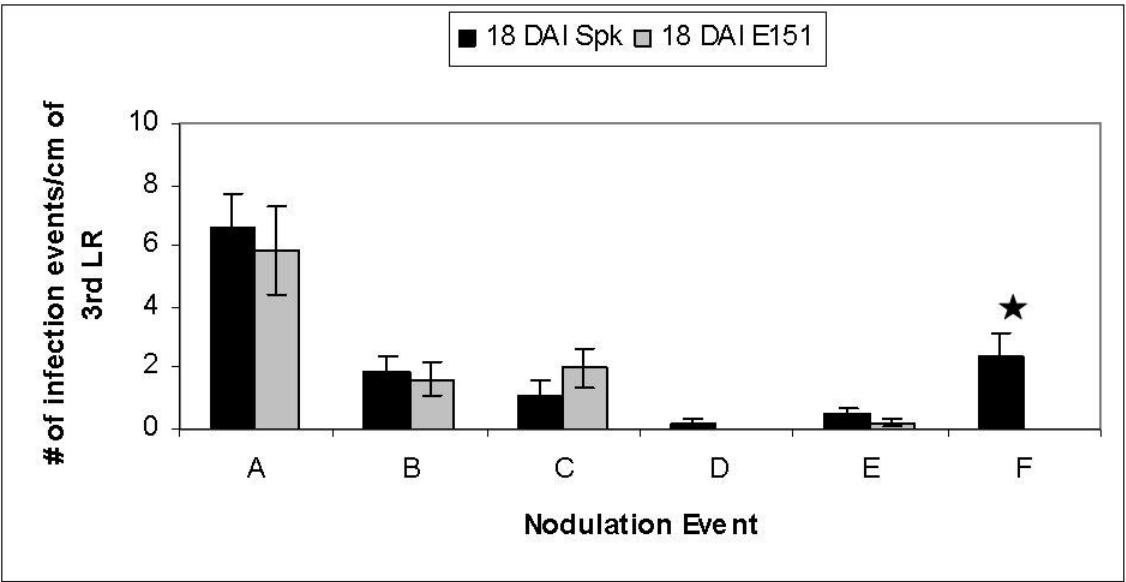


Figure 3.10. Number of infection events at each developmental stage tallied per cm of lateral root 21 DAI. The infections were classified into six different categories: A, IT either in RH or in epidermal cells; B, IT in cortex; C, IT in cortex and associated with cortical cell division; D, nodule primordium; E, emerging nodule; and F, mature nodule. Values are means \pm SE (n=3 for each of 4 trials). A *t*-test was used. The star represents a statistically significant difference (95% confidence level) between the two lines.

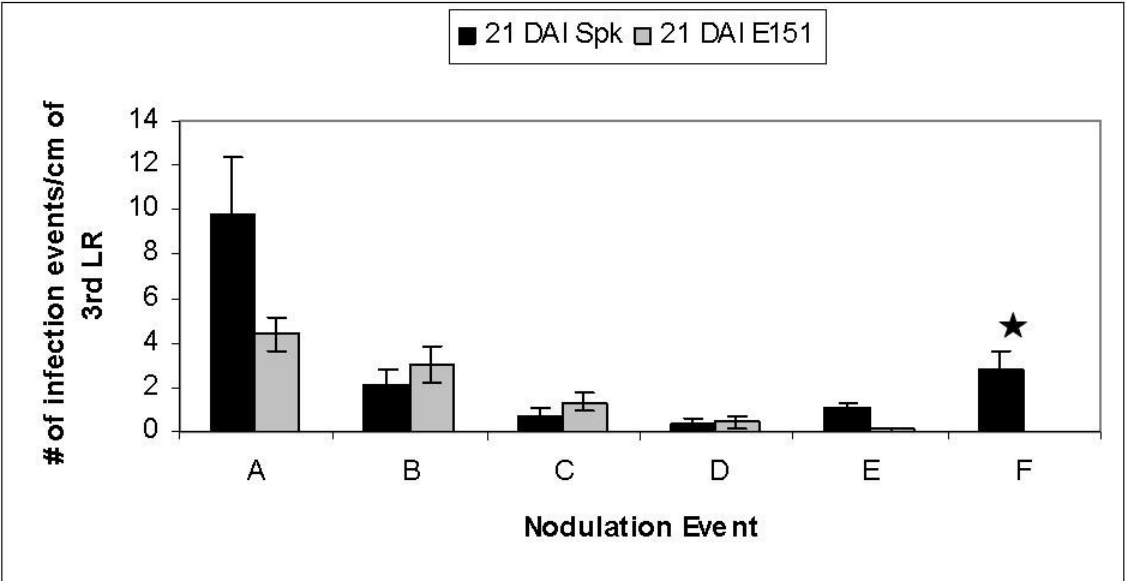
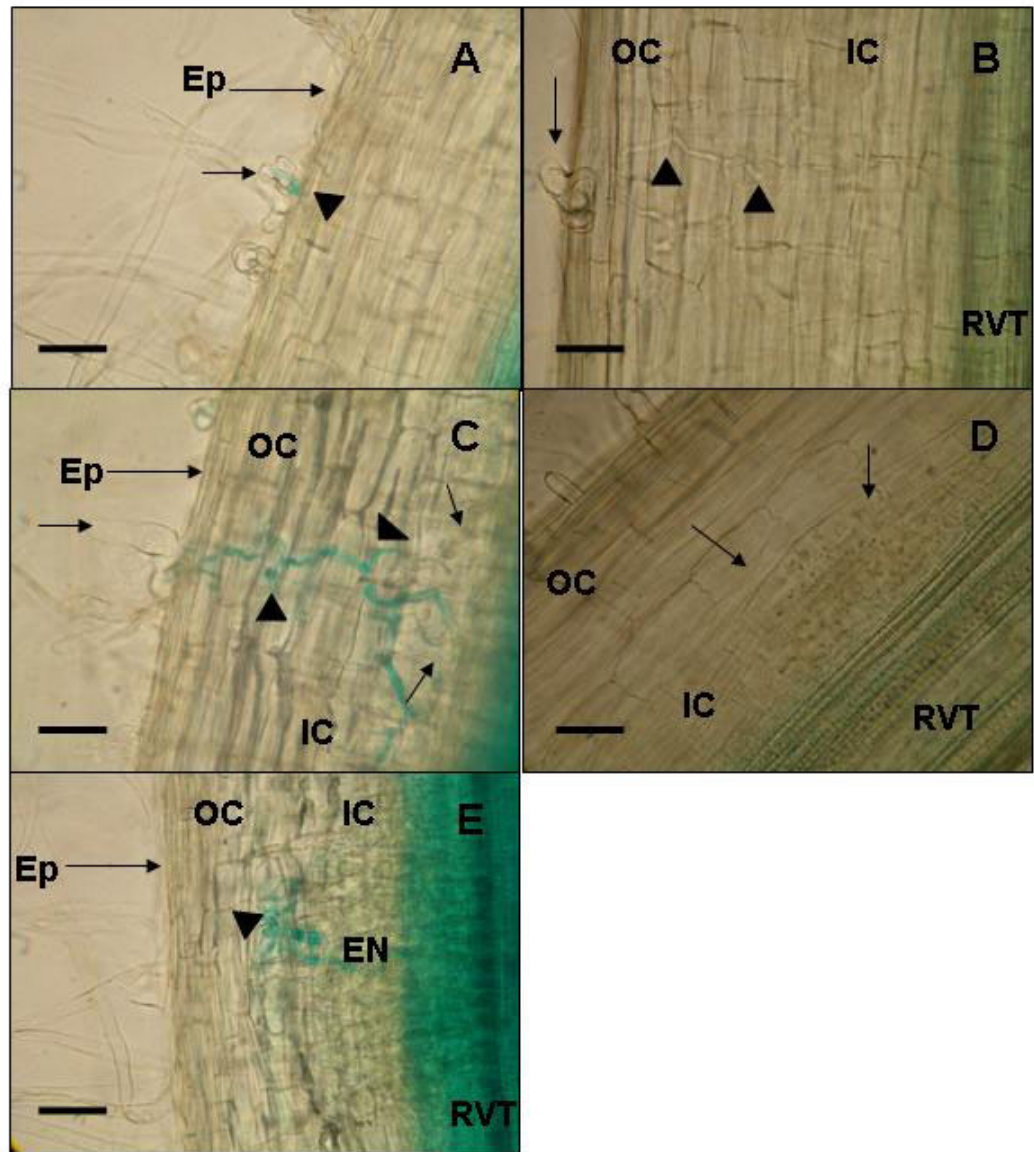


Figure 3.11. Nodule organogenesis observed in E151; cleared roots which were inoculated with *R. leguminosarum* strain 8401 (*lacZ*) and stained with X-gal. All roots segments are from plants harvested 9 and 15 DAI. On these micrographs, the root epidermis is always located on the left side and the root vasculature tissue on the right side. The infections were classified into six different categories: A, IT (arrowheads) either in RH (arrow) or in epidermal cells; B, IT in cortex and not associated with divisions; C, IT in cortex and associated with cortical cell division (arrows); D, nodule primordium (arrow); E, emerging nodule. No mature nodules could be seen. EN=Emerging nodule, Ep= Epidermis, IC= Inner cortex, OC= Outer cortex, RVT=Root vasculature tissue. Bar= 100 μ m for A, B, C, D, E, and F.



infection events between Sparkle and E151 throughout the whole study at each specific day no significant increases or decreases were found (Fig. 3.3). At 3 and 6 DAI, Sparkle exhibited nodulation events up to stage E, whereas in E151 the most developed infections were seen in stage C (Figs. 3.4-3.5). Mature nodules were visible on Sparkle 9 and 12 DAI while few nodulation events were observed past stage C in E151 (Figs. 3.6-3.7). At later time points (i.e. 15-21 DAI), mature nodules were constant in Sparkle, whilst most infection events in E151 did not appear to develop into emerged nodules (Figs. 3.8-10). It could be generalized that in contrast to Sparkle which formed mature nodules (stage F) as soon as 9 DAI when inoculated with strain 8401, E151 never formed any throughout the entire study. Based on these data, I suggest that nodule organogenesis is just hindered but not arrested at stage C in E151, and later on appears to be reinitiated.

B2. Nodule lobe formation on plants of different ages

In the previous section, nodule organogenesis was examined in Sparkle and E151 up to a certain point (i.e. 21 DAI) by looking at only a specific length (i.e. 1cm segment) of a specific lateral root. However, I was interested in a more global picture, and I chose to look at nodulation on entire root systems of plants of different ages (i.e. 21, 28, 35, and 42 DAI). Furthermore, I used different strains of bacteria (i.e. 8401 (*lacZ*) or 128C53K) to inoculate the root system to determine whether one strain of bacteria formed more nodule lobes than the other.

B2a. LacZ strain

In Sparkle, pink nodules formed at all of the ages. However, some nodules at 42 DAI were green and senesced. Also, it was noticed that plant height was positively correlated to nodule number

as plants that were small in stature produced fewer nodules than plants that were taller. In Sparkle, as the plants aged, the number of nodule lobes significantly increased from 35 to 42 DAI (Fig. 3.12). Similar observations were made for the mutant line. Pink nodules formed at all ages, few nodules formed on smaller plants, and some nodules senesced at 42 DAI. The number of nodule lobes formed on E151 was fairly constant across the ages studied (Fig. 3.12). It was not significantly different from that seen on Sparkle roots. These results were surprising because in the previous study E151 formed no mature nodules.

B2b. 128C53K strain

Upon close inspection it was seen that Sparkle formed big pink nodules in the upper region of the root system (Fig. 3.13). As in the previous study, plants with developed shoots produced more nodules than plants with small shoots. In addition, as Sparkle aged, its number of nodule lobes increased to reach a plateau at 28 DAI (Fig. 3.14). On average, Sparkle exhibited 340 nodule lobes (Fig. 3.14). When the roots of the mutant line were observed, there were few large nodules and many small ones; however they were all pink (Fig. 3.13). As in Sparkle, shoot height and nodules were positively correlated in E151. The number of nodule lobes formed on E151 significantly increased up to 35 DAI when it reached a plateau (Fig 3.14). On average, E151 formed 200 nodule lobes (Fig. 3.14). At all ages analyzed, when Sparkle and E151 plants were inoculated with *R. leguminosarum* strain 128C53K, there were significant differences in the number of nodule lobes, with Sparkle having a greater number of nodule lobes than E151 (Fig. 3.14).

Figure 3.12. Number of nodule lobes formed on Sparkle and E151 roots at specific days after inoculation with *R. leguminosarum* strain 8401. Values are means \pm SE (n=6 for each of 4 trials). A *t*-test was used with the Bonferroni correction. Asterisks represent statistically significant differences between Sparkle at each day counted (99% confidence level).

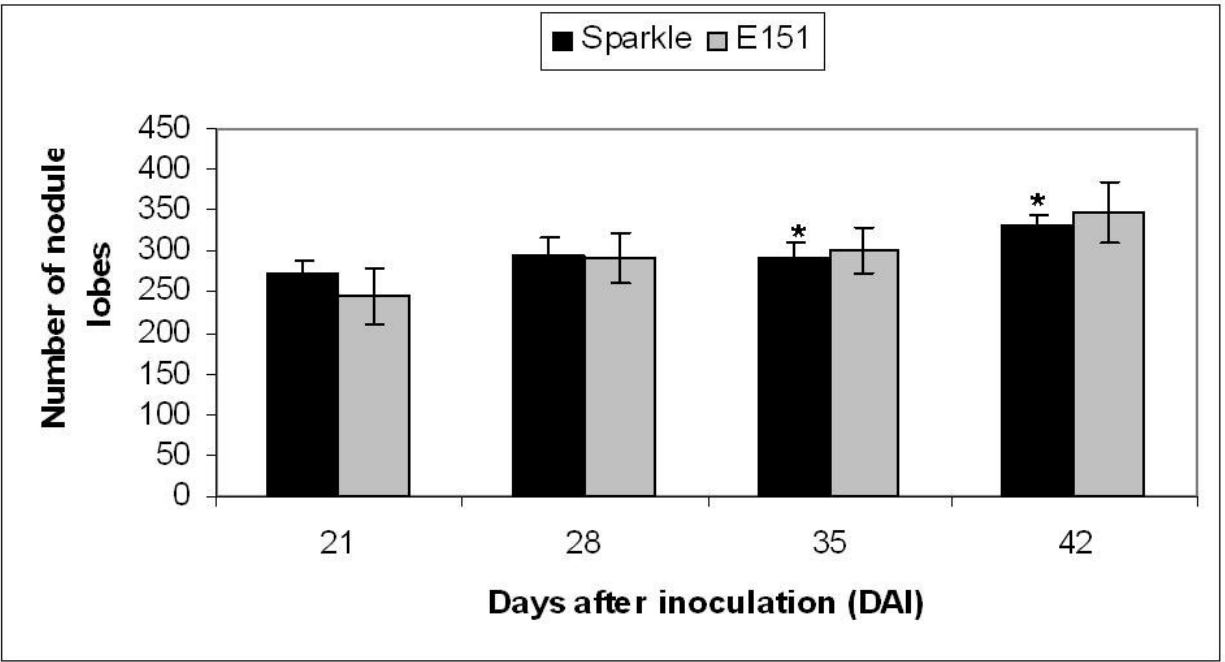


Figure 3.13. Sparkle (A) and E151 (B) 28 DAI. The plants were inoculated with strain 128C53K (HUP⁺). In the upper region of the root system a clear distinction can be seen between the number of nodules (arrowheads) formed on the two plant lines. Sparkle forms significantly more nodules than E151. Dark patches around the roots are water stains.

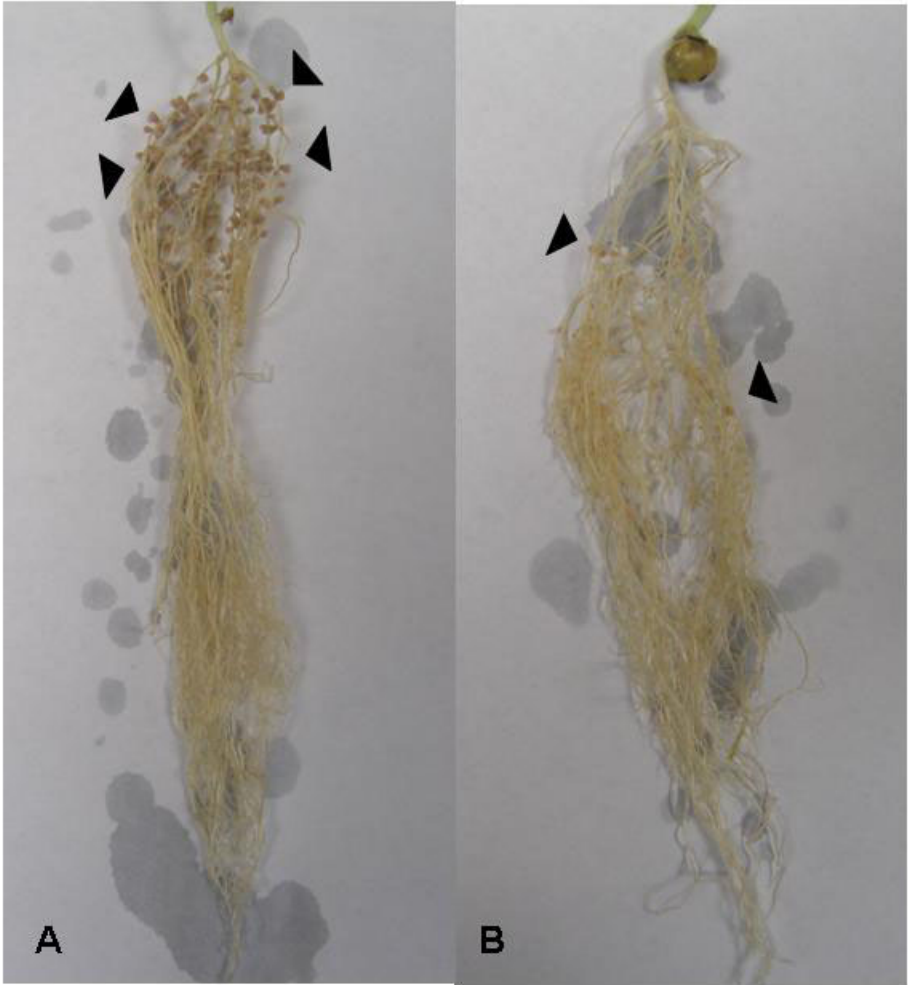
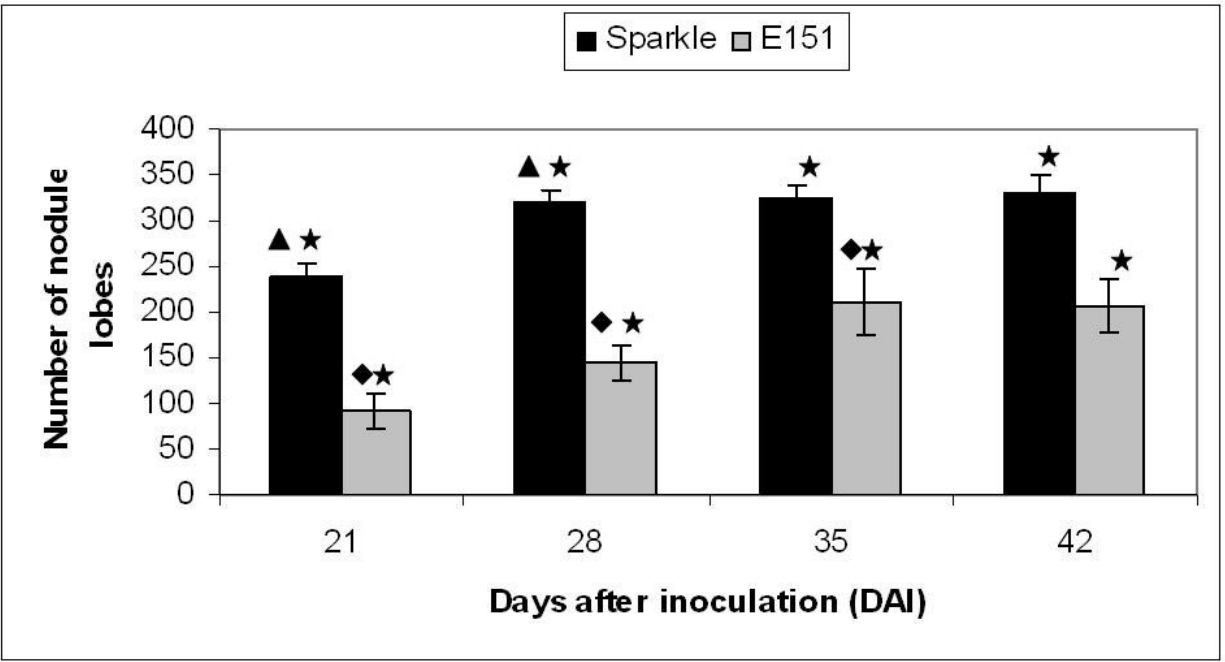


Figure 3.14. Number of nodule lobes formed on Sparkle and E151 roots at specific days after inoculation with *R. leguminosarum* strain 128C53K. Values are means \pm SE (n=6 for each of 4 trials except for 21 DAI, E151 (n=23); 28 DAI, Sparkle (n=23), E151 (n=20); 35 DAI, Sparkle (n=23), E151 (n=20); 42 DAI, Sparkle (n=22), E151 (n=21)). A *t*-test was used with the Bonferroni correction. Stars represent statistically significant differences between Sparkle and E151. Triangles represent statistically significant differences between Sparkle values at each interval and the preceding interval. Diamonds represent statistically significant differences between E151 values at each interval and the preceding interval. Significant differences measured at a 99% confidence level.



B2c. Comparison of the number of nodules formed with the 2 bacterial strains on each of the plant lines

In this experiment the growth conditions and concentration of bacteria used to inoculate the plants lines were the same, the only parameter that differed was the type of bacteria used; thus, the effectiveness of the bacteria in forming nodule lobes could be assessed. Based on the number of nodule lobes, no differences were seen between the 128C53K and 8401 (*lacZ*) strains for Sparkle (Table 3.4). In contrast, E151 plants inoculated with strain 128C53K formed fewer nodule lobes than when inoculated with strain 8401 (Table 3.4). It appears as if E151 responds differently to the 2 bacteria (Table 3.4). In contrast, Sparkle exhibited no differences to bacterial strains (Table 3.4). Therefore, the bacterial strain used appears to be an important factor in nodulation.

B3. Nitrogenase activity

B3a. Qubit sytem protocol and problems encountered

In this experimental setup the plant lines were inoculated with *R. leguminosarum* bv. *viciae* strain 128C79 that lacked HUP⁺ (hydrogenase uptake). Typically, *Rhizobium* with HUP⁺ re-oxidize the H₂ produced during nitrogen fixation however the strain I used released the H⁺ into the soil. The H⁺ was picked up by a carrier gas and allowed me to measure the apparent nitrogenase activity (ANA) and total nitrogenase activity (TNA) of the plants. Once ANA and TNA were known, I was able to use their values to calculate the N₂ fixation rate in the two plant lines (see Section B4c). The Qubit system has not been used frequently by researchers to measure N₂ fixation, instead many researchers have used the acetylene reduction assay whereby

Table 3.4. Number of nodule lobes formed on Sparkle and E151 roots at specific days after inoculation when plants are inoculated with *R. leguminosarum* strain 128C53K or 8401. Values are means \pm SE (n=6 for each of 4 trials). A *t*-test was used with the Bonferroni correction. Asterisks represent statistically significant differences (99% confidence level) between E151 inoculated with either 128C53K or 8401 at the specific time point.

Days after inoculation	Sparkle		E151	
	Bacterial strain		Bacterial strain	
	128C53K	8401	128C53K	8401
21	237.54 \pm 15.23	272.67 \pm 16.46	91.78 \pm 19.16*	245.83 \pm 33.26*
28	318.48 \pm 14.99	294.75 \pm 21.32	144.30 \pm 19.54*	291.54 \pm 32.23*
35	324.39 \pm 13.36	291.88 \pm 19.10	211.10 \pm 37.35	301.46 \pm 27.98
42	331.68 \pm 19.52	331.54 \pm 14.05	206.33 \pm 29.73*	347.79 \pm 36.84*

the reduction by the nitrogenase enzyme of acetylene to ethylene is measured (Hardy et al., 1968). However, the acetylene assay was considered to be dangerous and the acetylene gas that surrounded the infected root system was not representative of the typical gases found in the rhizosphere (Vessey, 1994). I was the first person in our lab to use the Qubit system and a lot of time was spent putting the system together and ensuring that all the equipment was interacting properly with the computer software. During the measurement phase I encountered one major problem, it was the loss of gas flow through the system. This was often caused by the drying column being packed too tightly or the vent valve being closed (Fig. 2.4).

B3b. Nitrogen fixation in Sparkle

The WT control plants that were not inoculated did not form any nodules, and did not undergo N₂ fixation (Table 3.5). Inoculated Sparkle plants harvested at the various ages (14, 21, and 28 DAI) had numerous pink nodules on their roots. The rates of N₂ fixation ($\mu\text{mol N}_2/\text{hr}$)/nodule dry weight (g) did not increase significantly as the Sparkle plants aged (14-28 DAI) (Table 3.5).

B3c. Nitrogen fixation in E151

The uninoculated E151 control plants did not form any nodules, and did not exhibit any N₂ fixation (Table 3.5). At a young age (14 DAI), the E151 line formed few pink nodules or barely any nodules at all. As E151 plants aged (21 and 28 DAI) there were numerous pink nodules present.

Table 3.5. The rate of N₂ fixation (μmol N₂/hr)/nodule dry weight (g) in Sparkle and E151 plants harvested at various days after inoculation (DAI).

Treatment	N ₂ fixation rate	
	Sparkle	E151
14 DAI	115.56 ± 43.05	0.00 ± 0.00
21 DAI	101.81 ± 25.03	33.29 ± 19.18
28 DAI	176.34 ± 36.44	158.79 ± 42.59

Values are means ± SE (At 14 DAI, n=7 for Sparkle and n=3 for E151. At 21 DAI, n=8 for Sparkle and n=5 for E151. At 28 DAI, n=8 for Sparkle and n=6 for E151. For the controls, n=5 for Sparkle and n=6 for E151 only). No control is shown since the N₂ fixation rate is expressed per dry weight of nodule and no nodules were present in the non-inoculated plants (Appendix C). A *t*-test was used with the Bonferroni correction (99% confidence level).

No significant increases or decreases were seen in the rate of N₂ fixation ($\mu\text{mol N}_2/\text{hr}$)/nodule dry weight (g) as the mutant line aged (Table 3.5).

B3d. Comparison of nitrogen fixation between both lines

Qualitatively, at 14 DAI, Sparkle appeared to form more pink nodules than E151, however, as the plants aged (21 and 28 DAI) numerous pink nodules were present in both lines. The rates of N₂ fixation ($\mu\text{mol N}_2/\text{hr}$)/nodule dry weight (g) did not vary significantly between Sparkle and E151 plants of the same ages (Table 3.5).

B4. Grafting

The grafting technique is a classical way of studying regulation of nodulation (e.g. Guinel and Sloejtes, 2000). This method allows the scion of WT plants to be attached to the stock of mutant plants and vice versa. It is used to determine whether the root or shoot controls nodulation. In this study plants were inoculated with strain 128C53K and were harvested 21 DAI. The grafts that I performed proved to be successful as 100% of the control grafts and E151/Sparkle and 75% of the Sparkle/E151 grew properly.

As expected, the Sparkle control grafts (S/S) formed a significantly greater number of nodule lobes than the E151 control grafts (E/E) (Table 3.6). The Sparkle control (S/S) and E/S

Table 3.6. Number of nodule lobes formed on grafted plants of Sparkle and E151 21 DAI.

Graft Type (Shoot/Root)	Nodules formed
S/S	190.58 ± 32.38 ^{a,c}
E/E	27.50 ± 6.91 ^a
S/E	35.56 ± 8.31 ^{b,c}
E/S	155.75 ± 22.46 ^b

Values are means ± SE (n=4 for each of 3 trials except for S/E where n=9 only). A *t*-test was used. Values with similar letters were significantly different (95% confidence level). S= Sparkle. E= E151.

grafts both formed a similar number of nodule lobes (Table 3.6). This was also true when S/E and E/E grafts were compared (Table 3.6). Grafts which had the Sparkle scion (i.e. S/S, E/S) grafted onto either the Sparkle or E151 stock produced more nodule lobes than grafted plants with an E151 stock (i.e. S/E) (Table 3.6). Overall, an abundant number of nodule lobes were formed on grafts with a Sparkle stock and only a few nodule lobes were formed on grafts with the E151 stock. Thus nodulation in E151 appeared to be root-controlled.

IV. DISCUSSION

A number of pleiotropic pea mutants from Tom LaRue's collection were found to exhibit altered nodulation in comparison to the WT (Guinel and LaRue, 1991; Guinel and Sloetjes, 2000; Kneen, Weeden, and LaRue, 1994; Markwei and LaRue, 1997). Here, the pleiotropic pea mutant E151 (*sym15*) with its short primary and lateral roots, reduced epicotyl, and low nodulation was partially characterized. When looking at some physiological parameters it was found that:

- E151 seeds retain more water than those of Sparkle.
- There is no difference in pigment concentrations between Sparkle and E151.
- When grown in the dark, E151 behaves like Sparkle.

The physiological characteristics measured did not exhibit any significant differences between Sparkle and E151. Therefore, the findings pertaining to the nodulation phenotype of the E151 mutant will be the main focus of the discussion as a number of interesting differences were found when comparing E151 to Sparkle as far as nodulation is concerned:

- Up to 21 DAI, E151 exhibits a block in nodule organogenesis at stage C (i.e., IT associated with cortical cell divisions) but this block is overcome as the plant matures to 42 DAI.

- The total number of infections did not significantly differ between Sparkle and E151 through the entire developmental study.
- In contrast to Sparkle, E151 responds differently to certain rhizobial strains. When E151 is inoculated with strain 128C53K, it is a low nodulator in comparison to Sparkle but when it is inoculated with strain 8401, it forms as many nodule lobes as Sparkle.
- Nodule formation in E151 is root-controlled.
- The rate of nitrogen fixation does not differ between Sparkle and E151 at the various ages, nor does it significantly change as the plants from each line mature.

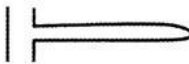




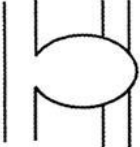
A. Nodule organogenesis in the two plant lines

Using the rhizobial strain 8401 containing the plasmid pXLGD4 (which contains a *lacZ* marker and constitutively expresses β -galactosidase) and a light microscope, nodule organogenesis over a period of 21 days was characterized in Sparkle and E151. In Sparkle, nodule organogenesis was normal, as all nodulation events described in Guinel and Sloetjes (2000) were spotted. E151 plants, however, exhibited a block at stage C (i.e., IT associated with cortical cell divisions) of nodule organogenesis. In addition, a comparison of the total number of infections between the two plant lines revealed that they were similar throughout the entire developmental study. Using a different strain, 128C53K, and a different approach, Delanghe (2007) found that E151 displayed a block at stage D (i.e., nodule primordium). Whatever the results of the studies, it can be concluded that a block exists in the nodule organogenesis of E151 and that the IT grows without any difficulties in the mutant line since it is able to reach the inner cortex. However, a discrepancy exists between the two studies regarding the location of the block. In my study, I

deduced that inner cortical cells in E151 could partake in anticlinal and periclinal divisions but could not develop into a nodule primordium, whereas Delanghe (2007) determined that E151 could form a nodule primordium but not a nodule meristem. To study nodule organogenesis Delanghe (2007) used toluidine blue and hand-sections, whereas I used rhizobia containing a *lacZ* marker and cleared whole root segments. It is likely that the different techniques resulted in differing interpretations of the location of the block in E151. Furthermore, because the definition of a nodule primordium in the literature is not clear (Beveridge et al., 2007) and is subject to interpretation, it is possible that the block found in E151 is at the same stage of nodule development according to my study and the one of Delanghe (2007).

As illustrated in Figure 4.1, the low nodulation pea mutants used in our lab exhibit defects in nodulation at various points during nodule organogenesis (Guinel and Sloetjes, 2000). In relation to the other pea mutants, I propose that E151 (*sym15*) be placed after R50 (*sym16*) but before E132 (*sym21*). The R50 (*sym16*) mutant has ITs which are arrested in the inner cortex and have lost their directional growth towards the stele. In addition, the nodule primordium in the R50 mutant is flat and composed of cells which have only divided anticlinally (Guinel and Sloetjes, 2000). In E151, the IT growth towards the inner cortex is normal and it is associated with the divisions of cortical cells, which are both anticlinal and periclinal, suggesting that the defect is slightly later in development than in R50. Since E151 did not appear to develop a nodule primordium, it is placed before E132, as E132 is capable of forming a nodule meristem (Guinel and Sloetjes, 2000).

Figure 4.1. Nodulation pea mutants in Dr. Guinel's collection, their defects, and E151's location amongst the mutants.

	LOCATION OF DEFECT IN NODULATION	MUTANT GENE	MUTANT LINES (REFERENCES)
	Root Hair Deformation	<i>sym8</i>	R25 (Markwei and LaRue, 1992)
	Infection Thread Formation	<i>sym9</i>	R72 (Markwei and LaRue, 1992)
	Epidermis	<i>brz</i>	E107 (Guinel and LaRue, 1992)
	Cortex (Few Divisions)	<i>sym5</i>	E2 (Guinel and LaRue, 1991)
	Primordium Formation	<i>sym16</i>	R50 (Guinel and Sloetjes, 2000)
	Nodule Meristem Emergence	<i>sym21</i>	E132 (Markwei and LaRue, 1997)

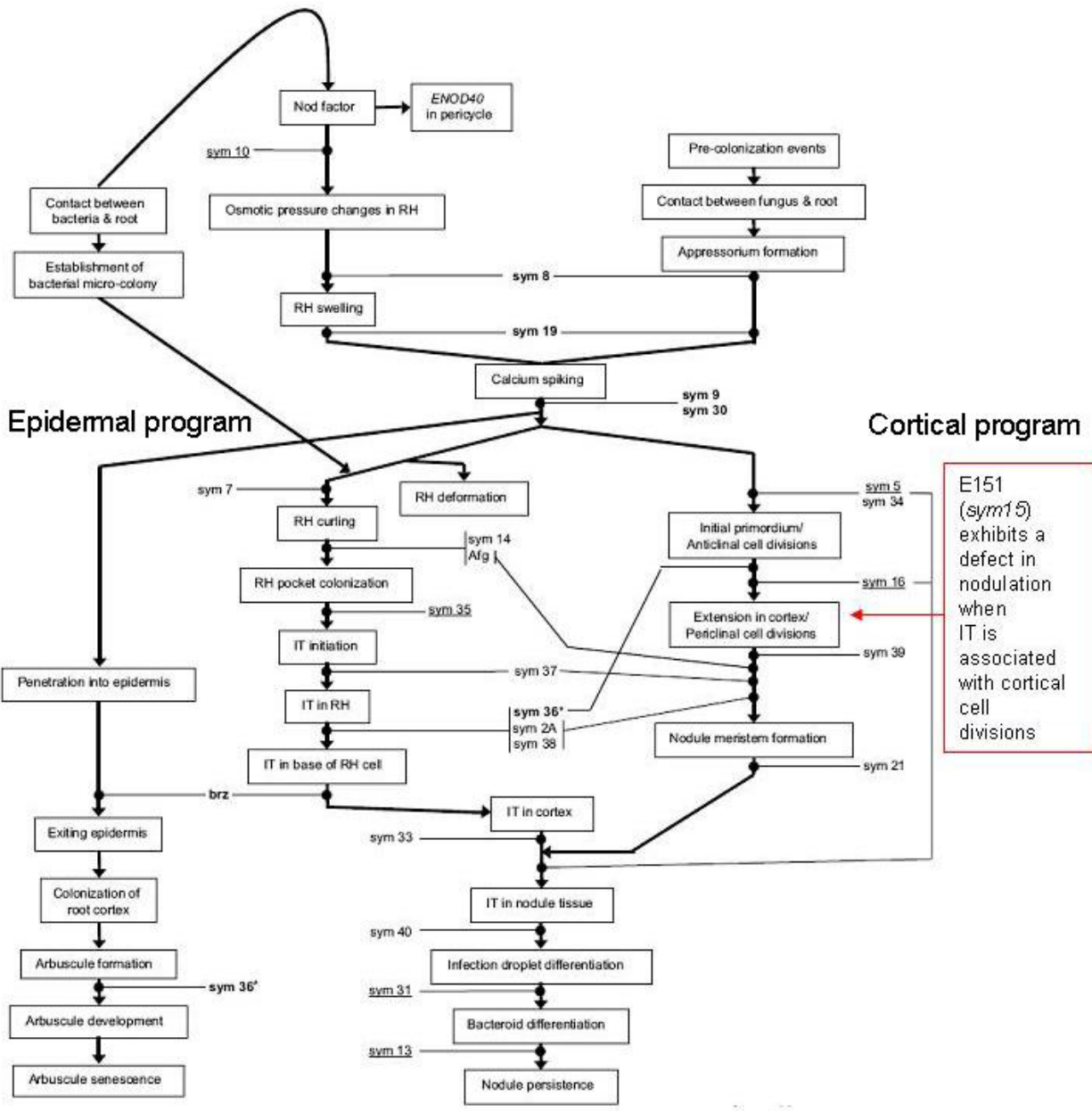
E151 (*sym15*) exhibits a defect in nodulation when IT is associated with cortical cell divisions



Based on an extensive review performed by Guinel and Geil (2002), it was proposed by these authors that the process of nodulation consists of one epidermal and one cortical program. These programs are thought to be independent of each other but not uncoupled from each other, as shown in Figure 4.2. The presence of NFs alone is capable of triggering the cortical program and producing pseudo-nodules devoid of bacteria (Guinel and Geil, 2002). However, the epidermal program can only be triggered in the presence of host-specific bacteria (Guinel and Geil, 2002). The high integrative regulation of the two programs allows nodules to develop that have the capability to fix atmospheric nitrogen. Based on the review by Guinel and Geil (2002), I am hypothesizing that the mutation in E151 affects the cortical cell program, since nodule organogenesis is blocked at stage C (i.e., IT associated with cortical cell divisions).

The mutants used in our lab represent only a small portion of all the pea mutants that are used around the globe to study the process of nodulation. The model proposed by Guinel and Geil (2002), including most of the symbiosis (*sym*) pea mutants studied today, depicts which locus might be responsible for controlling a specific nodulation event in the complex process of nodule organogenesis (Fig. 4.2). A close look at some of the mutants hindered in their cortical program reveals that in the “Afghanistan” cultivar, nodule meristem initiation occurred, however, the cortical cells surrounding the meristem were abnormal in that they were devoid of starch grains (Le Gal and Hobbs, 1989). Further along, the pea mutants RisNod4 (*sym37*) and RisFixF/SGENod⁻⁴ (*sym38*) were both arrested at the stage of nodule meristem development (Tsyganov et al., 2002). Finally, the P57 (*sym39*) mutant exhibited all of the stages of nodule development (i.e., cortical cell division to emerged nodules) but the frequency of these events was decreased (Sagan et al., 1994). Since the block in E151 occurs earlier than at the stage of

Figure 4.2. A model proposed by Guinel and Geil (2002) depicting nodule organogenesis, specifically the epidermal and cortical cell programs. All the pea mutants that had been characterized at that time have been placed onto the model. The potential location of E151 is shown. RH, root hair; IT, infection thread.



nodule meristem development, it appears that E151 could be placed between R50 (*sym16*) and P57 (*sym39*) in Figure 4.2.

Numerous mutants that have defects in nodulation can be found in other legume species. Some species exhibit blocks in both the epidermal and cortical programs. For example, the alfalfa mutant MnNC-1008 is unable to undergo RH curling or cell division in the inner cortex when inoculated with *S. meliloti* (Dudley and Long, 1989). Other species, such as sweetclover, can display a block in either the epidermal or the cortical program. Utrup, Cary, and Norris (1993) looked at the nodulation phenotypes of numerous white sweetclover (*Melilotus alba*) mutants. Some mutated at the *sym-1* and *sym-5* loci exhibited RH deformation in response to inoculation with *S. meliloti* but ITs were not present. These mutants produced white nodules that were unable to fix atmospheric nitrogen (Utrup, Cary, and Norris, 1993); likely demonstrating that the epidermal program was hindered in these mutants but the cortical program had been triggered. However, I would like to focus on those mutants in which the mutation affected only the cortical program. *sym-3* and *sym-4* mutants underwent RH deformation and IT formation (Utrup, Cary, and Norris, 1993) which is controlled by the epidermal program (Guinel and Geil, 2002); however, in *sym-3* and *sym-4* the cortical program never became triggered (Guinel and Geil, 2002) and as a result nodule formation became blocked (Utrup, Cary, and Norris, 1993). Since the stages at which nodule formation became blocked in these two sweetclover mutants are not described in great detail, it is difficult to compare E151 (*sym15*) to these mutants.

The total number of infections between Sparkle and E151 did not significantly differ; this is true for the entire developmental study. Similar results were found in other studies, whereby Sparkle

was compared to E2 (*sym5*) (Guinel and LaRue, 1991) and R50 (*sym16*) (Guinel and Sloetjes, 2000) mutants. That the numbers of total infections were similar between the two plant lines in this study further supports my hypothesis that E151 does not have a defect in its epidermal program but has one in its cortical cell program. A mutant such as E107 (*brz*) displays only one-third the number of infections in comparison to Sparkle because it is rarely capable of undergoing RH curling, as its epidermal program is affected (Fig. 4.2) (Guinel and LaRue, 1992).

Based on the studies mentioned, it can be concluded that the block at stage C (i.e., IT associated with cortical cell divisions) of nodule organogenesis in E151 and the similarity in the total number of infections between Sparkle and E151 supports my hypothesis that the E151 has no hindrance in its epidermal program but does have an obstruction in its cortical cell program.

B. Plant behaviour towards different rhizobial strains

In our lab I was the first person to examine how Sparkle and E151 behaved when inoculated at the same age, with the same concentration of bacteria, but with two different rhizobial strains. During the experiment, the plant lines were inoculated with one rhizobial strain at a time and the nodule lobes were counted at specified times (i.e., 21, 28, 35, and 42 DAI) later than for the organogenesis study. If it is assumed that each nodule has approximately the same number of lobes and that both strains produce the same number of lobes per nodule, then the number of lobes represents an estimation of the number of nodules. Based on this assumption, Sparkle inoculated with either strain 128C53K or the strain carrying a *lacZ* marker in a 8401 background

formed a similar number of nodules (i.e., approximately 300) at all times studied. Furthermore, Sparkle and E151 plants inoculated with the *lacZ* strain developed a similar number of nodules at all ages considered. However, the two plant lines differ when it comes to nodules formed with the strain 128C53K. Indeed, Sparkle produced twice as many nodules as E151 at all times. In addition to the 128C53K (HUP⁺) and *lacZ* strains, Sparkle and E151 were inoculated with strain 128C53K (HUP⁻), and upon examination no conspicuous differences could be seen in the gross morphology of the nodules. Nodules that formed on both plant lines were pink and no statistically significant differences were found in the N₂ fixation capacity of inoculated Sparkle and E151 plants based on the Qubit assay data presented in Table 3.5. However, there was a consistency in the delay of nodule development in E151 and the rate of N₂ fixation. While increasing the sample size would perhaps add more confidence in the statistical analysis and reveal a difference in the rate, the time required to process each sample for Qubit testing makes this next to impossible. Thus, future tests of E151 N₂ fixation should utilize the acetylene reduction assay. This conclusion is consistent with the results of other nodulation researchers who have also recognized this limitation of the Qubit assay and propose the acetylene assay to be more appropriate (Vessey, 1994). Based on the number of nodules produced on E151 when inoculated with the *lacZ* strain it can be concluded that nodulation in E151 is delayed.

In an early study, Skøt (1983) compared how various *R. leguminosarum* strains interacted with various pea cultivars. He found that certain rhizobial strains produce nodules that vary in size and also affect the development of the plant; indeed the *R. leguminosarum* bv. *viciae* strain 128C53 produced large nodules that were associated with a reduced root and shoot biomass, whereas strain 1045 was associated with a high root and shoot biomass (Skøt, 1983). In a very

recent study, Laguerre et al. (2007) classified 42 *R. leguminosarum* bv. *viciae* strain genotypes using their *nodD* gene region and looked at the impact these various strains had on pea cultivars Austin (i.e. semi-leafless spring cultivar) and Frisson (i.e. leafy winter cultivar). The two different pea cultivars were used to determine whether strain and cultivar interactions differ quantitatively (Laguerre et al., 2007). The researchers found that strains with different genotypes formed different sizes and morphology of nodules. For example, some rhizobial genotypes produced nodules that were large in size, had a high total biomass, had a branched shape with multiple nodule meristems (i.e., were lobed), and were mostly located in the upper region of the root system. Other rhizobial genotypes formed nodules that were small, cylindrical in shape, and present along the whole root system (Laguerre et al., 2007). In addition, it was determined that plants that formed large nodules had a lower mean nodule count, and a reduced root and shoot biomass in comparison to plants that developed small nodules (Laguerre et al., 2007). According to the findings of Laguerre et al. (2007), strain 128C53K, which was developed from the ancestor strain 128C53, produces fewer and larger nodules on pea. Thus, I am proposing that when E151 is inoculated with strain 128C53K fewer and larger nodules develop whereas the *lacZ* strain forms numerous small nodules on E151. Sparkle inoculated with either strain 128C53K or the strain carrying a *lacZ* marker in an 8401 background forms a similar number of nodules at all times studied because this plant line likely demonstrates a tighter control of the auto-regulation of nodulation. Finally, the delayed nodulation exhibited by E151 when inoculated with *lacZ* marker strain could be attributed to the fact that the *lacZ* strain produces numerous infections along the whole root system and it likely takes a longer time for all these infections to produce mature nodules. In future studies, the nodule DW, the number of nodules and nodule lobes, and the nodule size and shape should be determined for each rhizobial strain

that is used to inoculate Sparkle or E151. Also, the shoot and root DWs of the inoculated plants should be taken. Measurement of all these parameters will allow our lab to characterize various rhizobial strains properly and will us to determine the affects that the strains have on the development of the pea plant.

C. Nodulation control

In order to determine whether the shoot or root was responsible for controlling nodulation in E151, grafts were performed. The grafts were inoculated with strain 128C53K and the plants were harvested 21 DAI. The reciprocal graft with the Sparkle stock formed an abundant number of nodule lobes whereas only a few nodule lobes formed on the reciprocal graft with the E151 stock. Based on the former assumption that the number of lobes is representative of the number of nodules, the control and reciprocal grafts indicate that nodulation in E151 is root-controlled. Numerous studies have shown that a link exists between the nodulation phenotype (Nod⁺, low Nod, etc.) and the organ responsible for controlling nodule development, where the vast majority of low nodulation mutants are root-controlled and the hypernodulation or supernodulation mutants are shoot-controlled (Table 4.1) (Kinkema, Scott, and Gresshoff, 2006). The E151 mutant can also be placed amongst the various root-controlled low nodulation mutants since it was characterized by Kneen, Weeden, and LaRue (1994) as a low nodulator when inoculated with strain 128C53K and I determined it to be root-controlled when inoculated with the same strain (i.e., 128C53K). It should be noted that some studies have shown that not all low nodulators are root-controlled. For example, the pea mutants E132 (*sym21*) (Markwei and LaRue, 1997) and E107 (*brz*) (Resendes, Geil, and Guinel, 2001) are classified as low nodulators

Table 4.1. Examples of some root-controlled and shoot-controlled pea mutants, along with the genes responsible for the mutation, their orthologs, and gene products. *Mt*= *Medicago truncatula*, *Lj*= *Lotus japonicus*, *Gm*= *Glycine max*.

Root-controlled nodulation phenotype				
Pea gene	Orthologue	Gene product	Other characteristics	Reference
<i>nod49</i>			-Mutation is allelic to the naturally occurring mutation <i>rj1</i> . Plant expresses inducible and constitutive nitrate reductase activity that is similar to the WT soybean Bragg.	Delves et al., 1986 Mathews, Carroll, and Gresshoff, 1992
<i>sym9=</i> <i>sym30</i>	<i>MtDMI3</i>	-encodes a calcium/calmodulin dependent kinase.	-Mutant (e.g. R72) cannot undergo root hair curling (Hac ⁻) and proper cortical cell division (Ccd ⁻) in the inner root cortex.	Duc and Messenger, 1989 Markwei and LaRue, 1992 Ovtsyna et al., 2005 Mitra et al., 2004
<i>sym8=</i> <i>sym20</i>	<i>MtDMI1</i> <i>LjPOLLUX</i>	-encodes a protein that has similarity to a ligand-gated cation channel.	-Mutant (e.g. R25) has difficulties undergoing root hair curling (Hac ⁻) and nodule meristem initiation (Ccd ⁻) in the inner root cortex.	Kneen and LaRue, 1984 Novak, 2003 Markwei and LaRue, 1992 Ané et al., 2004 Imaizumi-Anraku, 2005
Shoot-controlled nodulation phenotype				
Pea gene	Orthologue	Gene product	Other characteristics	Reference
<i>sym29</i>	<i>LjHAR1</i> <i>GmNARK</i> <i>MtSUNN</i>	- <i>sym29</i> encodes a putative serine/threonine receptor kinase.	-Plants that have their <i>sym29</i> gene mutated are nitrate tolerant.	Sagan and Duc, 1996 Krusell et al., 2004 Nishimura et al., 2002 Oka-Kira and Kawaguchi, 2006 Schnabel et al., 2005
<i>sym28</i>	<i>LjKLV</i>	-KLV encodes a shoot-derived signal for nodule differentiation.	-The phenotype of the <i>L. japonicus klavier</i> mutant is similar to the <i>sym28</i> and <i>nod4 P. sativum</i> mutants.	Sagan and Duc, 1996 Sidorova and Shumnyi, 2003 Oka-Kira et al., 2005

but are shoot-controlled. Likewise, the *P. sativum* mutant K24 is considered to be a low nodulating mutant but is controlled by both the shoot and the root (Postma et al., 1988). When reciprocal grafts were performed using K24, a similar number of nodules formed on the two types of reciprocal grafts (Postma et al., 1988).

In contrast to root-controlled low nodulators, large varieties of shoot-controlled hypernodulating mutants from such species as *L. japonicus* (*har1*, *astray*), *M. truncatula* (*sickle*, *sun*), *P. sativum* (*sym29*), and *G. max* (*nark*) exhibit altered zones of nodulation in comparison to their WTs (Table 4.1). For example, the *har1*, *sym29*, *sun*, and *nark* mutants have root systems with nodules densely covering their entire lengths (Oka-Kira and Kawaguchi, 2006). It is suggested that the HAR1 (Krusell et al., 2002; Nishimura et al., 2002), SYM29 (Krusell et al., 2002), SUNN (Schnabel et al., 2005), and NARK (Nishimura et al., 2002) orthologues encode for a serine/threonine receptor kinase which is located in the shoot and root, and is required for shoot-controlled regulation of nodule formation and nitrate sensitivity (i.e., nitrogen compounds normally inhibit nodule development) (Schnabel et al., 2005). In the *M. truncatula sickle* mutant, nodules densely cover the upper region of the root which is close to the cotyledons, whereas in the *L. japonicus astray* mutant, the entire root length is covered by nodules but these are not densely packed (Oka-Kira and Kawaguchi, 2006). The increased nodule production in the *sickle* mutant is linked to an increase in the magnitude of rhizobial infections and insensitivity to ethylene, which has been shown to regulate nodulation by blocking the path of the IT either in the basal epidermal cell or the outer cortical cells (Lee and LaRue, 1992b). In the *astray* mutant, the hypernodulation phenotype is proposed to be a result of an increase in the formation of nodule primordia and the lack of nodule auto-regulation which leads to the development of more

nodules (Nishimura, Ohmori, and Kawaguchi, 2002). In general, the E151 mutant and its root-controlled phenotype fits well with most of the root-controlled mutants described in Table 4.1, with the exception of E132 (*sym21*) and E107 (*brz*) which are shoot-controlled low nodulation mutants.

D. Model

Before I can talk about the model that explains the possible root and shoot auto-regulatory signal interactions occurring in Sparkle and E151 during nodule formation I would like to talk about the zone of susceptibility and auto-regulation of nodulation.

D1. Zone of Susceptibility

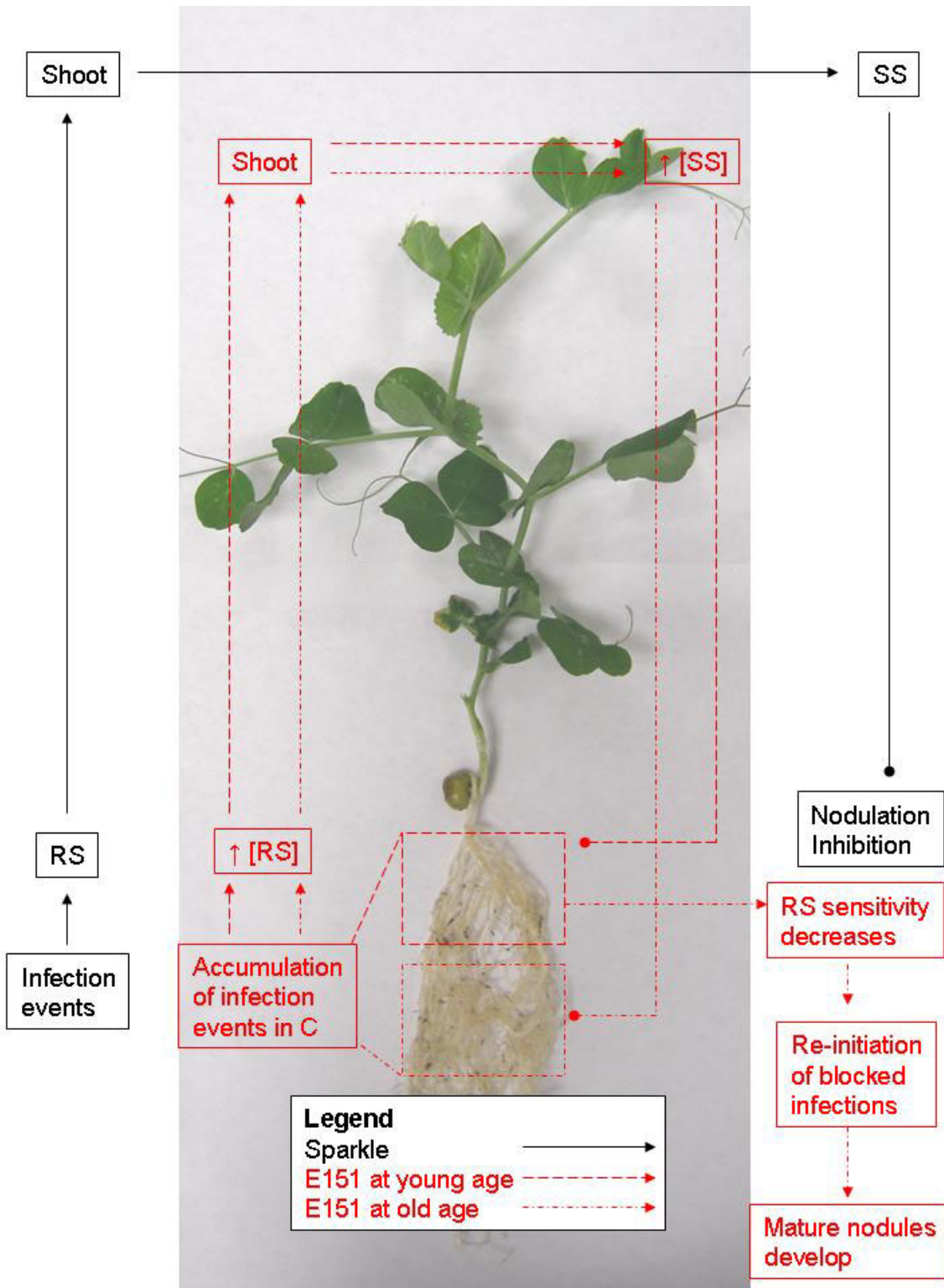
Not every epidermal cell (i.e., root hair) can become infected. The region of the root with the cells capable of rhizobial entry is very restricted and is referred to as the zone of susceptibility. In studies performed by Bhuvanewari, Bhagwat, and Bauer (1981) and Bhuvanewari, Turgeon, and Bauer (1980), the roots of various legumes (e.g., soybean, cowpea, alfalfa, and peanut) were divided into three zones (i.e. zone of no RHs, zone of developing RHs, and zone of mature RHs) by marking the position of the zones with a waterproof pen. Specifically marked points in the zones were then inoculated with rhizobia specific to the host plant using the droplet technique and later on scored for infection. It was determined that the zones of the root that had either no RHs or developing RHs at the time of inoculation were the most susceptible to infection (Bhuvanewari, Turgeon, and Bauer, 1980) because the cells in these zones are still plastic and

capable of growing. Furthermore, no legume species were infected in the zone that contained mature RHs (Bhuvanewari, Bhagwat, and Bauer, 1981; Bhuvanewari, Turgeon, and Bauer, 1980), as these RHs had fully developed cell walls that prevented the RHs from curling and entrapping bacteria. An experiment was also performed whereby two groups of plants (e.g., A and B) were inoculated in the exact same spot along the root that is susceptible to infection, but in the one group (e.g., B) the inoculation was delayed up to 4 hours (Bhuvanewari, Turgeon, and Bauer, 1980). By delaying the inoculation, the researchers found the zones of the root once susceptible to infection were no longer capable of being infected, and it was deduced that there was a transient window of opportunity during which infections had to occur in the zone of susceptibility for nodules to form (Bhuvanewari, Bhagwat, and Bauer, 1981; Bhuvanewari, Turgeon, and Bauer, 1980). Based on the work of Bhuvanewari, Turgeon, and Bauer (1980), it is known that in WT plants the majority of rhizobial infections and mature nodules are located in the upper region of the root system, slightly below the cotyledons of the plant. Nodules develop on the upper portion of the root system because in plants the zones of the root with no RHs or developing RHs are more sensitive to infection (Bhuvanewari, Turgeon, and Bauer, 1980); as the plant develops and the root lengthens, most of the infections in those zones develop into mature nodules and the transient zone of susceptibility shifts downwards.

D2. Auto-regulation signal

As previously mentioned in the Introduction, in WT plants the accumulation of infection events in the root leads to the production of a root-derived auto-regulatory signal (RS) which is sent towards the shoot. Once this root signal reaches the shoot, a shoot-derived auto-regulatory signal

Figure 4.3. A model explaining the root and shoot auto-regulatory signal interactions occurring in Sparkle and E151 during nodule formation. Solid black lines represent the pathway of the auto-regulation signal in Sparkle. Red lines with long solid dashes represent the pathway of the auto-regulation signal in young E151 plants. Red dotted lines represent the pathway of the auto-regulation signal in old E151 plants. RS= root-derived auto-regulatory signal; SS= shoot-derived auto-regulatory signal. Inhibition depicted as a dot.



(SS) is produced and is sent to the roots to inhibit any further nodulation (Fig. 4.3). However, hypernodulating and supernodulating mutant's exhibit increased nodulation because of an impairment in either the perception of a root-derived auto-regulation signal or the transmission of the shoot-derived auto-regulation signal (Oka-Kira and Kawaguchi, 2006).

D3. The Model

The varied nodulation exhibited by E151 in either the nodule organogenesis study or the study that looked at nodule development over time when inoculated with *lacZ* marker strain (i.e. 8401) can be explained using a model that focuses on the auto-regulatory signaling occurring in Sparkle and E151 (Fig. 4.3). I am hypothesizing that in young E151 plants (i.e., 21 DAI) a similar signaling pathway occurs as in the WT Sparkle. Rhizobia infect the zone of the root system that is susceptible to infection (i.e., emerging and developing RHs). Then some unknown signal in the root cortex prevents the progression of the rhizobial infection; the block in nodule development results in a root-derived auto-regulatory signal which is higher in concentration (Fig. 4.3). The root-derived signal acts on the shoot causing the production of a concentrated shoot-derived auto-regulatory signal which is then sent towards the root zone being infected and prevents further nodulation in E151 (Fig. 4.3). However, the formation of numerous mature nodules in E151 as the plant ages is attributed to the fact that as the plant develops the zone of the root system that is susceptible to infection shifts downward. As E151 develops, the root system lengthens, and a lower portion of the root system becomes susceptible to the rhizobia. The infections in the lower zone of nodulation become blocked because of the mutation (direct or indirect effect) and the plant produces concentrated root and shoot-derived signals to inhibit

further nodulation in this lower region (Fig. 4.3). Since the plant has allocated a majority of the auto-regulatory signal towards preventing new infections from developing in the lower zone of susceptibility, the sensitivity to the auto-regulatory signal in the older upper zone of the root system has decreased. The infections that were once blocked in the upper zone are re-initiated and are able to continue developing and will eventually produce mature nodules (Fig. 4.3) (Kinkema, Scott, and Gresshoff, 2006).

In a manner similar to Wasson, Pellerone, and Mathesius (2006), it would be valuable to divide the root system of Sparkle and E151 plants of the same age into specific segments (e.g., root segments that are 5 cm in length) and count the number of nodules and *lacZ* ITs present in each segment. Then the total number of nodules and *lacZ* ITs present in each of the segments of the WT and mutant root systems could be compared. This type of experiment would confirm that this proposed interaction (i.e., re-initiation) between the rhizobia and the host plant is occurring.

In conclusion, the model proposed can be applied to both of the strains (i.e., 128C53K and 8401) used to inoculate E151, as both strains produce a lower number of nodules on E151 at an early stage of development of the plant (i.e., 21 DAI) and an increased number of nodules at a later stage of development of the plant (i.e., 42 DAI). However, even though the two strains fit the model, I am still unable to explain why the *lacZ* strain produces significantly more nodules than the 128C53K strain on E151. Further studies need to be performed to determine whether one strain is capable of infecting a greater portion of the zone of susceptibility and producing more nodules.

REFERENCES

- Ané, J.-M., Kiss, G.B., Riely, B.K., Penmetsa, R.V., Oldroyd, G.E., Ayax, C., Levy, J., Debelle, F., Baek, J.M., Kalo, P., Rosenberg, G., Roe, B.A., Long, S.R., Denarie, J., and Cook, D.R. 2004. *Medicago truncatula DMII* Required for Bacterial and Fungal Symbioses in Legumes. *Science*. 303: 1364-1367.
- Ardourel, M., Demont, N., Debellé, F.D., Maillet, F., Debilly, F., Prome, J.C., Denarie, J., and Truchet, J. 1994. *Rhizobium-Meliloti* lipooligosaccharide nodulation factors – different structural requirements for bacterial entry into target root hair cells and induction of plant symbiotic developmental responses. *Plant Cell*. 6: 1357 -1374.
- Arianoutsou, M. and Thanos, C.A. 1996. Legumes in the fire-prone Mediterranean regions: an example from Greece. *Int. J. Wildland Fire*. 6: 77-82.
- Arnon, D.I. 1949. Copper enzymes in isolated chloroplasts: polyphenoloxidase in *Beta vulgaris*. *Plant Physiol*. 24: 1-15.
- Baginsky, C., Brito, B., Imperial, J., Palacios, J.M., and Ruiz-Argueso, T. 2002. Diversity and evolution of hydrogenase systems in rhizobial. *App. Environ. Micro*. 68: 4915-4924.
- Barker, D.G., Bianchi, S., Blondon, F., Dattée, Y., Duc, G., Essad, S., Flament, P., Gallusci, P., Génier, G., Guy, P., Muel, X., Tourneur, J., Dénarié, J., and Huguet, T. 1990. *Medicago truncatula*, a model plant for studying the molecular genetics of the *Rhizobium* -legume symbiosis. *Plant Mol. Bio. Rep*. 8: 40-49.
- Begum, A.A., Leibovitch, S., Migner, P., and Zhang, F. 2001. Specific flavonoids induce *nod* gene expression and pre-activated *nod* genes of *Rhizobium leguminosarum* increased pea (*Pisum sativum* L.) and lentil (*Lens culinaris* L.) nodulation in controlled growth chamber environments. *J. Exp. Bot*. 52: 1537-1543.
- Ben Amor, B., Shaw, S.L., Oldroyd, G.E.D., Maillet, F., Penmetsa, R.V., Cook, D., Long, S.R., Dénarié, J., and Gough, C. 2003. The *NFP* locus of *Medicago truncatula* controls an early step of Nod factor signal transduction upstream of a rapid calcium flux and root hair deformation. *Plant J*. 34: 495–506.
- Beveridge, C.A., Mathesius, U., Rose, R.J., and Gresshoff, P.M. 2007. Common regulatory themes in meristem development and whole-plant homeostasis. *Curr. Opin. Plant Biol*. 10: 44-51.
- Bhuvanewari, T.V., Bhagwat, A.A., and Bauer, W.D. 1981. Transient Susceptibility of Root Cells in Four Common Legumes to Nodulation by Rhizobia. *Plant Physiol*. 68: 1144-1149.
- Bhuvanewari, T.V., Turgeon, B.G., and Bauer, W.D. 1980. Early Events in the Infection of

- Soybean (*Glycine max* L. Merr) by *Rhizobium japonicum*. *Plant Physiol.* 66: 1027-1031.
- Bishop, G.J., Nomura, T., Yokota, T., Harrison, K., Noguchi, T., Fujioka, S., Takatsuto, S., Jones, J.D.G., and Kamiya, Y. 1999. The tomato DWARF enzyme catalyses C-6 oxidation in brassinosteroid biosynthesis. *Proc. Natl. Acad. Sci.* 96:1761–1766.
- Bonfante, P., Genre, A., Faccio, A., Martini, I., Schauser, L., Stougaard, J., Webb, J., and Parniske, M. 2000. The *Lotus japonicus* *LjSym4* gene is required for the successful symbiotic infection of root epidermal cells. *Mol. Plant–Microbe Interact.* 13: 1109–1120.
- Borisov, A.Y., Barmicheva, E.M., Jacobi, L.M., Tsyganov, V.E. Voroshilova, V.A., and Tikhonovich, I.A. 2000. Pea (*Pisum sativum* L.) mendelian genes controlling development of nitrogen-fixing nodule and arbuscular mycorrhiza. *Czech J. Gen. Plant Breeding.* 36: 106-110.
- Bradbury, S.M., Peterson, R.L., and Bowley, S.R. 1991. Interactions between 3 *Alfalfa* nodulation genotypes and 2 *Glomus* species. *New Phyto.* 119: 115-120.
- Bras, C.P., Spaink, H.P., and Stuurman, N. 2000. Structure and function of nod factors. In: *Prokaryotic Nitrogen Fixation: A model system for analysis of a biological process.* Wymondham, UK: Horizon Scientific Press. pp 365-383.
- Brewin, N.J. 1991. Development of the legume root nodule. *Annu. Rev. Cell Biol.* 7: 191-226.
- Brewin, N.J., Ambrose, M.J., and Downie, J.A. 1993. Root nodules, *Rhizobium* and nitrogen fixation. In: *Pea: Genetics, Molecular Biology and Biotechnology.* Wallingford: CAB International. pp 237-290.
- Caba, J.M., Poveda, J.L., Gresshoff, P.M., and Ligeró, F. 1999. Differential sensitivity of nodulation to ethylene in soybean cv. Bragg and a supernodulating mutant. *New Phyto.* 142: 233-242.
- Caetano-Anollés, G., Papparozzi, E.T., and Gresshoff, P.M. 1991. Mature nodules and root tips control nodulation in soybean. *J. Plant Physiol.* 137: 389–396.
- Cárdenas, L., Vidali, L., Dominguez, J., Perez, H., Sanchez, F., Hepler, P.K., and Quinto, C. 1998. Rearrangement of actin microfilaments in plant root hairs responding to *Rhizobium etli* nodulation signals. *Plant Phys.* 116: 871-877.
- Carroll, B.J., McNeil, D.L., and Gresshoff, P.M. 1985. Isolation and properties of soybean [*Glycine max* (L.) Merr.] mutants that nodulate in the presence of high nitrate concentrations. *PNAS.* 82: 4162-4166.
- Catoira, R., Timmers, A.C.J., Maillet, F., Galera, C., Penmetsa, R.V., Cook, D., Denarie,

- J., and Gough, C. 2001. The HCL gene of *Medicago truncatula* controls *Rhizobium*-induced root hair curling. *Development*. 128: 1507-1518.
- Chory, J., Chatterjee, M., Cook, R.K., Elich, T., Frankhauser, C., Li, J., Nagpal, P., Neff, M., Pepper, A., Poole, D., Reed, J., and Vitart, V. 1996. From seed germination to flowering, light controls plant development via the pigment phytochrome. *Proc. Natl. Acad. Sci.* 93:12066–12071.
- Chovanec, P., and Novak, K. 2005. Visualization of nodulation gene activity on the early stages of *Rhizobium leguminosarum* bv. *viciae* symbiosis. *Folia Micro.* 50: 323-331.
- Cohn, J., Day, R.B., and Stacey, G. 1997. Legume nodule organogenesis. *Tr. Pl. Sci.* 3: 105-110.
- Cook, D.R., Gualtieri, G., Kulikova, O., Limpens, E., Kim, D.J., and Bisseling, T. 2002. Microsynteny between pea and *Medicago truncatula* in the *SYM2* region. *Plant Mol. Biol.* 50: 225-235.
- Delanghe, S.D. 2007. Investigation of the nodule development in the low nodulating pea mutant E151 (*sym 15*). Waterloo, ON. Wilfrid Laurier University. pp 14-51.
- Delves, A.C., Mathews, A., Day, D.A., Carter, A.S., Carroll, B.J., and Gresshoff, P.M. 1986. Regulation of the soybean-rhizobium nodule symbiosis by shoot and root factors. *Plant Physiol.* 82: 588-590.
- Dennis, D.T., Turpin, D.H., Lefebvre, D.D., and Layzell, D.B. 1997. The physiology and biochemistry of legume N₂ fixation. In: *Plant Metabolism* (2nd Ed.). Essex, England. Addison Wesley Longman Ltd. pp 495-506.
- D'Haeze, W., and Holsters, M. 2002. Nod factor structures, responses, and perception during initiation of nodule development. *Glycobiology*. 12: 79R -105R.
- Dong, Z., Hunt, S., Dowling, A.N., Winship, L.J., and Layzell, D.B. 2000. Rapid measurement of hydrogen concentration and its use in the determination of nitrogenase activity of legume plants. *Symbiosis*. 29: 71-81.
- Downie, J.A. 2007. Infectious Heresy. *Plant Sci.* 316: 1296-1297.
- Duc, G., and Messenger, A. 1989. Mutagenesis of pea (*Pisum-sativum*-L.) and the isolation of mutants for nodulation and nitrogen-fixation. *Plant Sci.* 60: 207-213.
- Duc, G., Trouvelot, A., Gianinazzi-Pearson, V., and Gianinazzi, S. 1989. First report of non-mycorrhizal plant mutants (Myc-) obtained in pea (*Pisum sativum* L.) and fababean (*Vicia faba* L.). *Plant Sci.* 60: 215–222.
- Dudley, M.E., and Long, S.R. 1989. A Non-nodulating Alfalfa Mutant Displays neither Root

- Hair Curling nor Early Cell Division in Response to *Rhizobium meliloti*. *Plant Cell*. 1: 65-72.
- Edwards, A., Heckmann, A.B., Yousafzai, F., Duc, G., and Downie, J.A. 2007. Structural Implications of Mutations in the Pea *SYM8* Symbiosis Gene, the *DMII* Ortholog, Encoding a Predicted Ion Channel. *MPMI*. 20: 1183-1191.
- Ehrhardt, D.W., Wais, R., and Long, S.R. 1996. Calcium spiking in plant root hairs responding to *Rhizobium* nodulation signals. *Cell*. 85: 673-681.
- Ellis, T.H.N. and Poyser, S.J. 2002. An integrated and comparative view of pea genetic and cytogenetic maps. *New Phytol*. 153: 17-25.
- Emons, A.M.C., and De Ruijter, N.C.A. 2000. Actin: a target for signal transduction in root hairs. In: Staiger C, Baluska F, Volkmann D, Barlow P, eds. *Actin: a dynamic framework for multiple plant cell functions*. Dordrecht: Kluwer Academic Publishers. 373-390.
- Endre, G., Kalo, P., Kevei, Z., Kiss, P., Mihacea, S., Szakal, B., Kereszt, A., and Kiss, G.B. 2002. Genetic mapping of the non-nodulation phenotype of the mutant MN-1008 in tetraploid alfalfa (*Medicago sativa*). *Mol. Gen. Genom.*266: 1012-1019.
- Fearn, J.C., and LaRue, T.A. 1991. A temperature-sensitive nodulation mutant (*sym 5*) of *Pisum-sativum* L. *Plant, Cell, and Environ.* 14: 221-227.
- Fearn, J.C., and LaRue, T.A. 1991b. Ethylene inhibitors restore nodulation to *sym 5* mutants of *Pisum-sativum* L. cv. Sparkle. *Plant Physiol*. 96: 239-244.
- Felle, H.H., Kondorosi, E., Kondorosi, A., and Schultze, M. 1998. The role of ion fluxes in nod factor signalling in *Medicago sativa*. *Plant J*. 13: 455-463.
- Ferguson, B.J., Wiebe, E.M.K., Emery, R.J.N., and Guinel, F.C. 2005. Cytokinin accumulation and an altered ethylene response mediate the pleiotropic phenotype of the pea nodulation mutant R50 (*sym16*). *Can. J. Bot.* 83: 989-1000.
- Finch-Savage, W.E. and Leubner-Metzger, G. 2006. Seed dormancy and the control of germination. *New Phyt.* 171: 501-523.
- Fisher, R.F., and Long, S.R. 1992. *Rhizobium* – plant signal exchange. *Nature*. 357: 655 -660.
- Gage, D.J. 2004. Infection and invasion of roots by symbiotic, nitrogen-fixing rhizobia during nodulation of temperate legumes. *Micro. Mol. Biol. Review.* 68: 280-300.
- Gage, D.J., Bobo, T., and Long, S.R. 1996. Use of green fluorescent protein to visualize the early

- events of symbiosis between *Rhizobium meliloti* and alfalfa (*Medicago sativa*). J. Bacteriol. 178: 7159-7166.
- Gathumbi, S.M., Ndufa, J.K., Giller, K.E., and Cadisch, G. 2002. Do species mixtures increase above- and below-ground resource capture in woody and herbaceous tropical legumes? Agron. J. 94: 518-526.
- Geurts, R., Heidstra, R., Hadri, A.E., Downie, J.A., Franssen, H., vanKammen, A., and Bisseling, T. 1997. Sym2 of pea is involved in a nodulation factor-perception mechanism that controls the infection process in the epidermis. Plant Physiol. 115: 351-359.
- Goedhart, J., Rohrig, H., Hink, M.A., van Hoek, A., Visser, A.J.W.G., Bisseling, T., and Gadella, T.W.J. 1999. Nod factors integrate spontaneously in biomembranes and transfer rapidly between membranes and to root hairs, but transbilayer flip-flop does not occur. Biochemistry. 38: 10898-10907.
- Gonzalez, J.E., York, G.M., and Walker, G.C. 1996. *Rhizobium meliloti* exopolysaccharides: Synthesis and symbiotic function. Gene. 179: 141-146.
- Goodlass, G., and Smith, K.A. 1979. Effects of ethylene on root extension and nodulation of pea (*Pisum-sativum*-L.) and white clover (*Trifolium-repens* L.). Plant Soil. 51: 387-395.
- Graham, P.H. and Vance, C.P. 2003. Legumes: Importance and constraints to greater use. Plant Physiol. 131: 872-877.
- Gresshoff, P.M. 1993. Analysis of nodulation controlling genes in soybean. In: Current Developments in Soybean-*Rhizobium* Symbiotic Nitrogen Fixation. Harbin, China: Heilongjiang Science & Technology Publishers. pp 3-32.
- Gresshoff, P.M., Wopereis, J., Pajuelo, E., Dazzo, F.B., Jiang, Q., and de Bruijn, F.J. 2000. Short root mutant of *Lotus japonicus* with a dramatically altered symbiotic phenotype. Plant J. 23: 97-114.
- Guinel F.C. and Geil, R.D. 2002. A model for the development of the rhizobial and arbuscular mycorrhizal symbioses in legumes and its use to understand the roles of ethylene in the establishment of these two symbioses. Can. J. Bot. 80: 695-720.
- Guinel, F.C. and LaRue, T.A. 1991. Light-microscopy study of nodule initiation in *Pisum-sativum* L. cv. Sparkle and its low-nodulating mutant E2 (*sym* 5).
- Guinel, F.C., and LaRue, T.A. 1992. Ethylene inhibitors partly restore nodulation to pea mutant E107 (*brz*). Plant Physiol. 99: 515-518.
- Guinel, F.C., and LaRue, T.A. 1993. Excessive aluminum accumulation in the pea mutant E107 (*brz*). Plant Soil. 157: 75-82.

- Guinel, F.C. and Sloetjes, L.L. 2000. Ethylene is involved in the nodulation phenotype of *Pisum sativum* R50 (*sym 16*), a pleiotropic mutant that nodulates poorly and has pale green leaves. *J. Exp. Bot.* 51: 885-894.
- Guo, H.W., and Ecker, J.R. 2004. The ethylene signaling pathway: new insights. *Curr. Op. Plant Biol.* 7: 40-49.
- Handberg, K., and Stougaard, J. 1992. *Lotus-japonicus*, an autogamous, diploid legume species for classical and molecular-genetics. *Plant J.* 2: 487-496.
- Hardy, R.W.F., Holsten, R.D., Jackson, E.K., and Burns, R.C. 1968. Acetylene-ethylene assay for N₂ fixation – Laboratory and field evaluation. *Plant Physiol.* 43: 1185-1207.
- Hirsch, A.M. 1992. Developmental biology of legume nodulation. *New Phytol.* 122: 211-237.
- Hopkins, W.G. 1999. Introduction to plant biology (2nd Ed.). New York, NY. John Wiley & Sons.
- Hunt, Stephen. 2005. An open flow gas exchange system for measurement of nitrogenase activity in legumes. Kingston, ON. Qubit Systems Inc. pp 1-36.
- Hunter, W.J. 1993. Ethylene production by root-nodules and effect of ethylene on nodulation in *Glycine-max*. *App. Environ. Micro.* 59: 1947-1950.
- Imaizumi-Anraku, H., Takeda, N., Charpentier, M., Perry, J., Miwa, H., Umehara, Y., Kouchi, H., Murakami, Y., Mulder, L., Vickers, K., Pike, J., Downie, J.A., Wang, T., Sato, S., Asamizu, E., Tabata, S., Yoshikawa, M., Murooka, Y., Wu, G.J., Kawaguchi, M., Kawasaki, S., Parniske, M., and Hayashi, M. 2005. Plastid proteins crucial for symbiotic fungal and bacterial entry into plant roots. *Nature.* 433: 527 -531.
- Kantar, F., Pilbeam, C.J., and Hebblethwaite, P.D. 1996. Effect of tannin content of faba bean (*Vicia faba*) seed on seed vigour, germination and field emergence. *Ann. App. Biol.* 128: 85-93.
- Karas, B., Murray, J., Gorzelak, M., Smith, A., Sato, S., Tabata, S., and Szczyglowski, K. 2005. Invasion of *Lotus japonicus* root hairless 1 by *Mesorhizobium loti* involves the nodulation factor-dependent induction of root hairs. *Plant Physiol.* 137: 1331-1344.
- Kawaguchi, M., Imaizumi-Anraku, H., Koiwa, H., Niwa, S., Ikuta, A., Syono, K., and Akao, S. 2002. Root, root hair, and symbiotic mutants of the model legume *Lotus japonicus*. *MPMI.* 15: 17-26.
- Kinkema, M., Scott, P.T., and Gresshoff, P.M. 2006. Legume nodulation: successful symbiosis through short- and long-distance signaling. *Fun. Plant Biol.* 33: 707-721.

- Kneen, B.E. and LaRue, T.A. 1984. Nodulation resistant mutant of *Pisum sativum*. J. Heredity. 75: 238-240.
- Kneen, B.E., and LaRue, T.A. 1988. Induced symbiosis mutants of pea (*Pisum-sativum*) and sweetclover (*Melilotus-alba-annua*). Plant Sci. 58: 177-182.
- Kneen, B.E., Weeden, N.F., and LaRue, T.A. 1994. Non-nodulating mutants of *Pisum sativum* (L.) cv. Sparkle. J. Heredity. 85: 129-133.
- Krusell, L., Madsen, L.H., Sato, S., Aubert, G., Genua, A., Szczyglowski, K., Duc, G., Kaneko, T., Tabata, S., de Bruijn, F., Pajuelo, E., Sandal, N., and Stougaard, J. 2002. Shoot control of root development and nodulation is mediated by a receptor-like kinase. Nature. 420: 422–426.
- Kuppusamy, K.T., Endre, G., Prabhu, R., Penmetsa, R.V., Veereshlingam, H., Cook, D.R., Dickstein, R., and VandenBosch, K.A. 2004. LIN, a *Medicago truncatula* gene required for nodule differentiation and persistence of rhizobial infections. Plant Physiol. 136: 3682-3691.
- Kusnetsov, V.V., Herrmann, R.G., and Kulaeva, O.N. 1998. Cytokinins stimulates and abscisic acid inhibits greening of etiolated *Lupinus luteus* cotyledons by affecting the expression of the light-sensitive protochlorophyllide oxidoreductase. Mol. Gener. Gen. 259: 21-28
- Laguerre, G., Depret, G., Bourion, V., and Duc, G. 2007. *Rhizobium leguminosarum* bv. *viciae* genotypes interact with pea plants in developmental responses of nodules, roots and shoots. New Phytol. 176: 680-690.
- Lambers, H., Chapin III, F.S., and Pons, T.L. 1998. Symbiotic Association. In: Plant Physiological Ecology. New York, NY: Springer-Verlag. pp 378-405.
- Lee, K.H., and LaRue, T.A. 1992. Ethylene as a possible mediator of light-induced and nitrate-induced inhibition of nodulation of *Pisum-sativum* L. cv. Sparkle. Plant Physiol. 100: 1334-1338.
- Lee, K.H., and LaRue, T.A. 1992b. Exogenous ethylene inhibits nodulation of *Pisum-sativum* L. cv. Sparkle. Plant Physiol. 100: 1759-1763.
- Le Gal, M.F., and Hobbs, S.L.A. 1989. Cytological studies of the infection process in nodulating and non-nodulating pea genotypes. Can. J. Bot. 67: 2435–2443.
- Leigh, J.A., and Coplin, D.L. 1992. Exopolysaccharides in plant-bacterial interactions. Ann. Rev. Micro. 46: 307-346.
- Leong, S. A., Williams, P. H., and Ditta, G. S. 1985. Analysis of the 5' regulatory region of the

- gene for δ -aminolevulinic acid synthetase of *Rhizobium meliloti*. *Nucleic Acids Res.* 13:5965-5976.
- Levy, J., Bres, C., Geurts, R., Chalhoub, B., Kulikova, O., Duc, G., Journet, E.P., Ane, J.M., Lauber, E., Bisseling, T., Denarie, J., Rosenberg, C., and Debelle, F. 2004. A putative Ca^{2+} and calmodulin-dependent protein kinase required for bacterial and fungal symbioses. *Science.* 303: 1361-1364.
- Lhuissier, F.G.P., De Ruijter, N.C.A., Sieberer, B.J., Esseling, J.J., and Emons, A.M.C. 2001. Time course of cell biological events evoked in legume root hairs by *Rhizobium* Nod factors: State of the art. *Ann. Bot.* 87: 289 -302.
- Li, J., Nagpal, P., Vitart, V., McMorris, T.C., and Chory, J. 1996. A role for brassinosteroids in light-dependent development of *Arabidopsis*. *Science.* 272: 398–401.
- Lichtenthaler, H.K. 1987. Chlorophylls and carotenoids: pigments of photosynthetic biomembranes. *Methods in Enzymology.* 148: 350-382.
- Ligero, F., Caba, J.M., Lluch, C., and Olivares, J. 1991. Nitrate inhibition of nodulation can be overcome by the ethylene inhibitor aminoethoxyvinylglycine. *Plant Physiol.* 97: 1221-1225.
- Madsen, E.B., Madsen, L.H., Radutoiu, S., Olbryt, M., Rakwalska, M., Szczyglowski, K., Sato, S., Kaneko, T., Tabata, S., Sandal, N., and Stougaard, J. 2003. A receptor kinase gene of the LysM type is involved in legume perception of rhizobial signals. *Nature.* 425: 637 -640.
- Malik, N.S.A., Calvert, H.E., and Bauer, W.D. 1987. Nitrate induced regulation of nodule formation in soybean. *Plant Physiol.* 84: 266-271.
- Markwei, C.M., and LaRue, T.A. 1992. Phenotypic characterization of *sym8* and *sym9*, two genes conditioning non-nodulation in *Pisum sativum* 'Sparkle'. *Can. J. Microbiol.* 38: 548–554.
- Markwei, C.M., and LaRue, T.A. 1997. Phenotypic characterization of *sym21*, a gene conditioning shoot-controlled inhibition of nodulation in *Pisum sativum* cv. Sparkle. *Physiol. Plant.* 100: 927–932.
- Mateos, P.F., Baker, D.L., Petersen, M., Velazquez, E., Jimenez-Zurdo, J.I., Martinez-Molina, E., Squartini, A., Orgambide, G., Hubbell, D.H., and Dazzo, F.B. 2001. Erosion of root epidermal cell walls by *Rhizobium* polysaccharide-degrading enzymes as related to primary host infection in the *Rhizobium*-legume symbiosis. *Can. J. Micro.* 47: 475-487.
- Mathews, A., Carroll, B.J., and Gresshoff, P.M. 1992. Studies on the root control of non-nodulation and plant-growth of nonnodulating mutants and a supernodulating mutant of soybean (*Glycine-max* (L.) Merr.). *Plant Science:* 83: 35-43.

- McLearn, N., and Dong, Z.M. 2002. Microbial nature of the hydrogen-oxidizing agent in hydrogen-treated soil. *Biol. Fert. Soils*. 35: 465-469.
- Mergaert, P., Uchiumi, T., Alunni, B., Evanno, G., Cheron, A., Catrice, O., Mausset, A.E., Barloy-Hubler, F., Galibert, F., Kondorosi, A., and Kondorosi, E. 2006. Eukaryotic control on bacterial cell cycle and differentiation in the *Rhizobium*-legume symbiosis. *PNAS*. 13: 5230-5235.
- Messina, M.J. 1999. Legumes and soybeans: overview of their nutritional profiles and health effects. *Am. Soc. Nutrition*. 70: 439S-450S.
- Miller, D.D., De Ruijter, N.C.A., and Emons, A.M.C. 1997. From signal to form: aspects of the cytoskeleton-plasma membrane-cell wall continuum in root hair tip. *J. Exp. Bot.* 316: 1881-1896.
- Mitra, R.M., Gleason, C.A., Edwards, A., Hadfield, J., Downie, J.A., Oldroyd, G.E.D., and Long, S.R. 2004. A Ca²⁺/calmodulin-dependent protein kinase required for symbiotic nodule development: Gene identification by transcript-based cloning. *PNAS*. 101: 4701-4705.
- Morris, J.B. 1997. Special purpose legume genetic resources conserved for agricultural, industrial, and pharmaceutical use. *Econ. Bot.* 51: 251-263.
- Murphy, J.B., and Noland, T.L. 1982. Temperature effects on seed imbibition and leakage mediated by viscosity and membranes. *Plant Physiol.* 69: 428-431.
- Mylona, P., Pawlowski, K., and Bisseling, T. 1995. Symbiotic nitrogen fixation. *Plant Cell*. 7: 869-885.
- Nakagawa, T., and Kawaguchi, M. 2006. Shoot-applied MeJA suppresses root nodulation in *Lotus japonicus*. *Plant Cell Physiol.* 47: 176-180.
- Nazaryuk, V.M., Sidorova, K.K., Shumny, V. K., Kalimullina, F. R., and Klenova, M.I. 2006. Physiological and agrochemical properties of different symbiotic genotypes of pea (*Pisum sativum* L.). *Biol. Bulletin*. 33: 559-567.
- Newcomb, W. 1976. Correlated light and electron-microscopic study of symbiotic growth and differentiation in *Pisum-sativum* root-nodules. *Can. J. Bot.* 54: 2163-2185.
- Niebel, A., Bono, J.J., Ranjeva, R., and Cullimore, J.V. 1997. Identification of a high affinity binding site for lipo-oligosaccharidic NodRm factors in the microsomal fraction of *Medicago* cell suspension cultures. *MPMI*. 10: 132-134.
- Nishimura, R., Hayashi, M., Wu, G.J., Kouchi, H., Imaizumi-Anraku, H., Murakami, Y.,

- Kawasaki, S., Akao, S., Ohmori, M., Nagasawa, M., Harada, K., and Kawaguchi, M. 2002. HAR1 mediates systemic regulation of symbiotic organ development. *Nature*. 420: 426-429.
- Nishimura, R., Ohmori, M., and Kawaguchi, M. 2002. The novel symbiotic phenotype of enhanced-nodulating mutant of *Lotus japonicus astray* mutant is an early nodulating mutant with wider nodulation zone. *Plant Cell Physiol*. 43: 853-859.
- Novák, K. 2003. Allelic relationships of pea nodulation mutants. *J. Her.* 94: 191-193.
- Oka-Kira, E., and Kawaguchi, M. 2006. Long-distance signaling to control root nodule number. *Curr. Opin. Plant Biol.* 9: 496-502.
- Oka-Kira, E., Tateno, K., Miura, K., Haga, T., Hayashi, M., Harada, K., Sato, S., Tabata, S., Shikazono, N., Tanaka, A., Watanabe, Y., Fukuhara, I., Nagata, T., and Kawaguchi, M. 2005. *klavier (klv)*, A novel hypernodulation mutant of *Lotus japonicus* affected in vascular tissue organization and floral induction. *Plant J.* 44: 505-515.
- Oláh, B., Brière, C., Bécard, G., Dénarié, J., and Gough, C. 2005. Nod factors and a diffusible factor from arbuscular mycorrhizal fungi stimulate lateral root formation in *Medicago truncatula* via the DMI1/DMI2 signalling pathway. *Plant J.* 44: 195-207.
- Oldroyd, G.E.D., Ben Amor, B., Shaw, S.L., Maillet, F., and Penmetsa, RV. 2003. The *NFP* locus of *Medicago truncatula* controls an early step of Nod factor signal transduction upstream of a rapid calcium flux and root hair deformation. *Plant J.* 34: 495-506.
- Oldroyd, G.E.D., Harrison, M.J., and Udvardi, M. 2005. Peace Talks and Trade Deals. Keys to Long-Term Harmony in Legume-Microbe Symbioses. *Plant Physiol.* 137: 1205-1210.
- Olsson, J.E., Nakao, P., Bohlool, B.B., and Gresshoff, P.M. 1989. Lack of systemic suppression of nodulation in split root systems of supernodulating soybean (*Glycine max* [L.] merr.) mutants. *Plant Physiol.* 90: 1347-1352.
- Ovtsyna, A.O., Dolgikh, E.A., Kilanova, A.S., Tsyganov, V.E., Borisov, A.Y., Tikhonovich, I.A., and Staehelin, C. 2005. Nod Factors Induce Nod Factor Cleaving Enzymes in Pea Roots. Genetic and Pharmacological Approaches Indicate Different Activation Mechanisms. *Plant Physiol.* 139: 1051-1064.
- Paetau, I., Chen, C.Z., and Jane, J.L. 1994. Biodegradable plastic made from soybean products: 1. Effect of preparation and processing on mechanical properties and water absorption. *Indust. Eng. Chem. Res.* 33: 1821-1827.
- Peck, M.C., Fisher, R.F., and Long, S.R. 2006. Diverse flavonoids stimulate NodD1 binding to *nod* gene promoters in *Sinorhizobium meliloti*. *J. Bact.* 188: 5417-5427.

- Penmetsa, R.V., and Cook, D.R. 1997. A legume ethylene-insensitive mutant hyperinfected by its rhizobial symbiont. *Science*. 275: 527-530.
- Pepper, A.N., Morse, A.P., and Guinel, F.C. 2007. Abnormal root and nodule vasculature in R50 (*sym16*), a pea nodulation mutant which accumulates cytokinins. *Ann. Bot.* 99: 765-776.
- Peterson, T.A. and Russell, M.P. 1991. Alfalfa and the nitrogen cycle in the corn belt. *J. Soil Water Conserv.* 46: 229-235.
- Postma, J.G., Jacobsen, E., and Feenstra, W.J. 1988. 3 Pea mutants with an altered nodulation studied by genetic-analysis and grafting. *J. Plant Physiol.* 132: 424-430.
- Provorov, N.A., Yu, A., Tikhonovich, B.A., and Tikhonovich, I.A. 2002. Developmental genetics and evolution of symbiotic structures in nitrogen-fixing nodules and arbuscular mycorrhiza. *J. Theor. Biol.* 214: 215-232.
- Rae, A.L., Bonfantefasolo, P., and Brewin, N.J. 1992. Structure and growth of infection threads in the legume symbiosis with *Rhizobium-leguminosarum*. *Plant J.* 2: 385-395.
- Raven, P.H., Evert, R.F., and Eichhorn, S.E. 1999. Nitrogen and the Nitrogen Cycle. In: *Biology of Plant* (6th Ed.). New York, NY: W.H. Freeman and Company. pp 736-742.
- Reich, P.B., Tilman, D., Craine, J., Ellsworth, D., Tjoelker, M.G., Knops J, Wedin, D., Naeem, S., Bahauddin, D., Goth J., et al. 2001. Do species and functional groups differ in acquisition and use of C, N and water under varying atmospheric CO₂ and N availability regimes? A field test with 16 grassland species. *New Phytol.* 150:435 -448.
- Reid, J. 2005. Is there a shoot organic molecule that inhibits root nodulation in the pea mutant E107?. Waterloo, ON. Wilfrid Laurier University.
- Reiss, H-D., and Herth, W. 1985. Nifedipine-sensitive calcium channels are involved in polar growth of lily pollen tubes. *Cell Sci.* 76: 247-54.
- Resendes, C.M., Geil, R.D., and Guinel, F.C. 2001. Mycorrhizal development in a low nodulation pea mutant. *New Phytol.* 150: 563-572.
- Russell, M. 2001. Alfalfa. *Am. Sci.* 89: 252-259.
- Sagan, M., and Duc, G. 1996. *Sym28* and *Sym29*, two new genes involved in regulation of nodulation in pea (*Pisum sativum* L.). *Symbiosis.* 20:229-245.
- Sagan, M., Huguet, T., and Duc, G. 1994. Phenotypic characterization and classification of nodulation mutants of pea (*Pisum sativum* L.). *Plant Sci.* 100: 59-70.
- Sagan, M., Morandi, D., Tarenghi, E., and Duc, G. 1995. Selection of nodulation and

- mycorrhizal mutants in the model plant *Medicago truncatula* (Gaertn.) after γ -ray mutagenesis. *Plant Sci.* 111: 63–71.
- Sanchez, P.A. 1999. Improved fallows come of age in the tropics. *Agrofor. Syst.* 47: 3-12.
- Sanchez, P.A. 2002. Soil fertility and hunger in Africa. *Science.* 295: 2019-2020.
- Schiefelbein, J.W., Shipley, A., and Rowse, P. 1992. Calcium influx at the tip of growing root-hair cells of *Arabidopsis thaliana*. *Planta* 187: 455-459.
- Schmidt, J.S., Harper, J.E., Hoffman, T.K., and Bent, A.F. 1999. Regulation of soybean nodulation independent of ethylene signaling. *Plant Physiol.* 119: 951-959.
- Schnabel, E., Journet, E.P., de Carvalho-Niebel, F., Duc, G., and Frugoli, J. 2005. The *Medicago truncatula* *SUNN* gene encodes a CLV1-like leucine-rich repeat receptor kinase that regulates nodule number and root length. *Plant Mol Biol.* 58: 809–822.
- Sheng, C., and Harper, J.E. 1997. Shoot versus root signal involvement in nodulation and vegetative growth in wild-type and hypernodulating soybean genotypes. *Plant Physiol.* 113: 825-831.
- Shirliffe, S.J., and Vessey, J.K. 1996. A nodulation (Nod+)/Fix- mutant of *Phaseolus vulgaris* L. has nodule-like structures lacking peripheral vascular bundles (Pvb-) and is resistant to mycorrhizal infection (Myc-). *Plant Sci.* 118: 209-220.
- Shirliffe, S.J., Vessey, J.K., Buttery, B.R., and Park, S.J. 1996. Comparison of growth and N accumulation of common bean (*Phaseolus vulgaris* L.) cv. OAC Rico and its two nodulation mutants, R69 and R99. *Can. J. Plant. Sci.* 76: 73-83.
- Shugarman, P.M., and Appleman, D. 1966. Chlorophyll synthesis in *Chlorella* II. effect of glucose and light intensity on the lag phase. *Plant Physiol.* 41: 1701-1708.
- Sidorova, K.K., and Shumnyi, V.K. 2003. A collection of symbiotic mutants in pea *Pisum sativum* L.: Creation and genetic study. *Russian J. Gen.* 39: 406-413.
- Singh, O., Vanrheenen, H.A., and Rupela, O.P. 1992. Inheritance of a new nonnodulation gene in chickpea. *Crop Sci.* 32: 41-43.
- Skøt, L. 1983. Cultivar and *Rhizobium* strain effects on the symbiotic performance of pea (*Pisum sativum*). *Physiologia Plantarum.* 59: 585–589.
- Smil, V. 1999. Nitrogen in crop production. *Global Biogeochem. Cycles.* 13: 647-662.
- Spaink, H.P. 2000. Root nodulation and infection factors produced by rhizobial bacteria. *Ann. Rev. Micro.* 54: 257-288.

- Stacey, G., McAlvin, C.B., Kim, S.Y., Olivares, J., and Soto, M.J. 2006. Effects of endogenous salicylic acid on nodulation in the model legumes *Lotus japonicus* and *Medicago truncatula*. *Plant Physiol.* 141: 1473-1481.
- Suzuki, A., Akune, M., Kogiso, M., Imagama, Y., Osuki, K., Uchiumi, T., Higashi, S., Han, S., Yoshida, S., Asami, T., and Abe, M. 2004. Control of nodule number by the phytohormone abscisic acid in the roots of two legume species. *Plant Cell Physiol.* 45: 914-922.
- Taiz, L., and Zeiger, E. 1998. Assimilation of Mineral Nutrients. In: *Plant Physiology* (2nd Ed.). Sunderland, Massachusetts. Sinauer Associates, Inc. pp 323-346.
- Terakado, J., Fujihara, S., Goto, S., Kuratani, R., Suzuki, Y., Yoshida, S., and Yoneyama, T. 2005. Systemic effect of a brassinosteroid on root nodule formation in soybean as revealed by the application of brassinolide and brassinazole. *Soil Sci. Plant Nutr.* 51: 389-395.
- Thomas, D. and Sumberg, J.E. 1995. A review of the evaluation and use of tropical forage legumes in sub-Saharan Africa. *Agric. Ecosyst. Environ.* 54: 151-163.
- Timmers, A.C.J., Auriac, M.C., and Truchet, G. 1999. Refined analysis of early symbiotic steps of the *Rhizobium-Medicago* interaction in relationship with microtubular cytoskeleton rearrangements. *Development.* 126: 3617-3628.
- Timmers, A.C.J., Soupene, E., Auriac, M.C., de Billy, F., Vasse, J., Boistard, P., and Truchet, G. 2000. Saprophytic intracellular rhizobia in Alfalfa nodules. *MPMI.* 13: 1204-1213.
- Tirichine, L., Imaizumi-Anraku, H., Yoshida, S., Murakami, Y., Madsen, L.H., Miwa, H., Nakagawa, T., Sandal, N., Albrechtsen, A.S., Kawaguchi, M., et al. 2006. Deregulation of a Ca²⁺/calmodulin-dependent kinase leads to spontaneous nodule development. *Nature.* 441: 1153-1156.
- Tsyganov, V.E., Morzhina, E.V., Stefanov, S.Y., Borisov, A.Y., Lebsky, V.K., and Tikhonovich, I.A. 1998. The pea (*Pisum sativum* L.) genes *sym33* and *sym40* control infection thread formation and root nodule function. *Mol. General Gen.* 259: 491-503.
- Tsyganov, V.E., Voroshilova, V.A., Priefer, U.B., Borisov, A.Y., and Tikhonovich, I.A. 2002. Genetic dissection of the initiation of the infection process and nodule tissue development in the *Rhizobium-pea* (*Pisum sativum* L.) symbiosis. *Ann. Bot.* 89: 357-366.
- Udvardi, M.K., and Scheible, W-R. 2005. GRAS Genes and the Symbiotic Green Revolution. *Science.* 17: 1749-1750.
- Utrup, L.J., Cary, A.J., and Norris, J.H. 1993. 5 Nodulation mutants of white sweetclover

- (*Melilotus-alba Desr.*) exhibit distinct phenotypes blocked at root hair curling, infection thread development, and nodule organogenesis. *Plant Physiol.* 103: 925-932.
- van Brussel, A.N.N., Bakhuizen, R., van Spronsen, P.C., Spaink, H.P., Tak, T., Lugtenberg, B.J.J., and Kijne, J.W. 1992. Induction of pre-infection thread structures in the leguminous host plant by mitogenic lipo-oligosaccharides of *Rhizobium*. *Science*. 257: 70-72.
- Van Spronsen, P.C., Bakhuizen, R., van Brussel, A.A., Kijne, J.W. 1994. Cell wall degradation during infection thread formation by the root nodule bacterium *Rhizobium leguminosarum* is a two-step process. *Eur. J. Cell Biol.* 64: 88-94.
- Van Spronsen, P.C., Tak, T., Rood, A.M.M., van Brussel, A.A.N., Kijne, J.W., Boot, K.J.M. 2003. Salicylic acid inhibits indeterminate-type nodulation but not determinate-type nodulation. *MPMI.* 16: 83-91.
- Vance, C.P., Graham, P.H., and Allan, D.L. 2000. Biological nitrogen fixation. In: *Nitrogen Fixation: From Molecules to Crop Productivity*. Dordrecht, The Netherlands: Kluwer Academic Publishers. pp 506-514.
- Veselova, T., and Veselovsky, V. 2006. Possible involvement of aquaporins in water uptake by pea seeds differing in quality. *Russ. J. Plant Physiol.* 53: 96-101.
- Vessey, J.K. 1994. Measurement of nitrogenase activity in legume root-nodules - In defense of the acetylene-reduction assay. *Plant Soil.* 158: 151-162.
- Walker, S.A., and Downie, J.A. 2000. Entry of *Rhizobium leguminosarum* bv. *viciae* into root hairs requires minimal nod factor specificity, but subsequent infection thread growth requires *nodO* or *nodE*. *MPMI.* 13: 754-762.
- Walker, S.A., Viprey, V., and Downie, J.A. 2000. Dissection of nodulation signaling using pea mutants defective for calcium spiking induced by Nod factors and chitin oligomers. *PNAS.* 97: 13413-13418.
- Wasson, A.P., Pellerone, F.I., and Mathesius, U. 2006. Silencing the flavonoid pathway in *Medicago truncatula* inhibits root nodule formation and prevents auxin transport regulation by rhizobia. *Plant Cell.* 18: 1617-1629.
- Wattiaux, M.A. and Howard, T.M. 2001. *Technical Dairy Guide: Nutrition and Feeding*. University of Wisconsin. http://babcock.cals.wisc.edu/de/html/ch6/nutrition_eng_ch6.html. (Accessed 04/14/06).
- Weeden, N.F., Kneen, B.E., and LaRue, T.A. 1990. Genetic analysis of *sym* genes and other nodule-related genes in *Pisum sativum*. In: *Nitrogen Fixation: Achievement and Objectives*. New York, NY: Chapman and Hall. pp 323-330.

- Wegel, E., Schauser, L., Sandal, N., Stougaard, J., and Parniske, M. 1998. Mycorrhiza mutants of *Lotus japonicus* define genetically independent steps during symbiotic infection. *Mol. Plant-Microbe Interact.* 11: 933-936.
- Wei, H., and Layzell, D.B. 2006. Adenylate-coupled ion movement. A mechanism for the control of nodule permeability to O₂ diffusion. *Plant Phys.* 141: 280-287.
- Yokoyama, M., Naito, K., and Suzuki, H. 1981. Benzyladenine-enhanced cell proliferation and -suppressed greening in attached young bean leaves. *Plant Cell Physiol.* 22: 623-627.
- Zettler, L. 1998. A study of pigmentation in R50, a pleiotropic pea mutant. Waterloo, ON, Canada. Wilfrid Laurier University. pp 20.

Appendix A- Chlorophyll pigment raw data and calculations

Below are the average values of the absorbance's, for Sparkle and E151 leaves from the 4th and 6th nodes at 14 and 22 days after planting (DAP).

Spk 4th 14 DAP (647nm)	Spk 4th 14 DAP (663nm)	Spk 4th 14 DAP (470nm)	Spk 4th 14 DAP (710nm)
0.535	1.191	1.343	0.290
0.695	1.287	1.670	0.265
0.714	1.514	1.584	0.333
0.466	1.048	1.221	0.049

E151 4th 14 DAP (647nm)	E151 4th 14 DAP (663nm)	E151 4th 14 DAP (470nm)	E151 4th 14 DAP (710nm)
0.331	0.686	0.888	0.343
0.626	1.157	1.501	0.202
0.465	1.022	1.069	0.345
0.663	1.536	1.417	0.113

Spk 4th 22 DAP (647nm)	Spk 4th 22 DAP (663nm)	Spk 4th 22 DAP (470nm)	Spk 4th 22 DAP (710nm)
0.717	1.435	1.567	0.237
0.687	1.494	1.442	0.264
0.724	1.616	1.512	0.249
0.632	1.364	1.314	0.202
0.433	0.993	1.041	0.410

E151 4th 22 DAP (647nm)	E151 4th 22 DAP (663nm)	E151 4th 22 DAP (470nm)	E151 4th 22 DAP (710nm)
0.669	1.353	1.399	0.207
0.590	1.249	1.223	0.191
0.706	1.521	1.428	0.215
0.733	1.598	1.517	0.258
0.800	1.844	1.665	0.000

Spk 6th 22 DAP (647nm)	Spk 6th 22 DAP (663nm)	Spk 6th 22 DAP (470nm)	Spk 6th 22 DAP (710nm)
0.704	1.553	1.485	0.321
0.768	1.684	1.567	0.301
0.643	1.428	1.382	0.300
0.600	1.440	1.338	0.000

E151 6th 22 DAP (647nm)	E151 6th 22 DAP (663nm)	E151 6th 22 DAP (470nm)	E151 6th 22 DAP (710nm)
0.674	1.444	1.405	0.300
0.725	1.576	1.497	0.263
0.636	1.444	1.395	0.368
0.748	1.777	1.561	0.014

Below are the values obtained for chlorophyll a using the appropriate Lichtenthaler (1987) equation. (A) Chlorophyll $a = 12.25\text{Abs}_{663} - 2.79\text{Abs}_{647}$

Chl a	Chl a w/ dilution	Chl a (mg/g)
13.097	17.419	1.394
13.827	18.389	1.379
16.554	22.017	1.761
11.542	15.351	1.228
Spk 4th 14 DAP	Average ± S.E.	1.441 ± 0.113
Chl a	Chl a w/ dilution	Chl a (mg/g)
7.482	9.951	0.796
12.431	16.533	1.323
11.222	14.925	1.194
16.968	22.567	1.805
E151 4th 14 DAP	Average ± S.E.	1.280 ± 0.208
Chl a	Chl a w/ dilution	Chl a (mg/g)
15.573	20.713	1.636
16.385	21.792	1.743
17.776	23.642	1.820
14.946	19.878	1.570
10.961	14.578	1.166
Spk 4th 22 DAP	Average ± S.E.	1.587 ± 0.114
Chl a	Chl a w/ dilution	Chl a (mg/g)
14.706	19.559	1.565
13.654	18.160	1.580
16.663	22.161	1.751
17.530	23.315	1.842
20.358	27.077	2.166
E151 4th 22 DAP	Average ± S.E.	1.781 ± 0.110
Chl a	Chl a w/ dilution	Chl a (mg/g)
17.060	22.690	1.793
18.486	24.587	1.942
15.699	20.880	1.649
15.962	21.230	1.698
Spk 6th 22 DAP	Average ± S.E.	1.771 ± 0.0645
Chl a	Chl a w/ dilution	Chl a (mg/g)
15.809	21.025	1.682
17.283	22.987	1.793
15.915	21.166	1.672
19.682	26.177	2.094
E151 6th 22 DAP	Average ± S.E.	1.810 ± 0.0985

Below are the values obtained for chlorophyll b using the appropriate Lichtenthaler (1987) equation. (B) Chlorophyll $b = 21.50\text{Abs}_{647} - 5.10\text{Abs}_{663}$

Chl b	Chl b w/ dilution	Chl b (mg/g)
5.431	7.223	0.578
8.371	11.133	0.835
7.630	10.147	0.812
4.679	6.223	0.498
Spk 4th 14 DAP	Average ± S.E.	0.681 ± 0.0842
Chl b	Chl b w/ dilution	Chl b (mg/g)
3.619	4.813	0.385
7.552	10.045	0.804
4.785	6.364	0.509
6.418	8.536	0.683
E151 4th 14 DAP	Average ± S.E.	0.595 ± 0.0925
Chl b	Chl b w/ dilution	Chl b (mg/g)
8.099	10.772	0.851
7.151	9.511	0.761
7.324	9.741	0.750
6.632	8.820	0.697
4.243	5.643	0.451
Spk 4th 22 DAP	Average ± S.E.	0.702 ± 0.0674
Chl b	Chl b w/ dilution	Chl b (mg/g)
7.488	9.959	0.797
6.315	8.399	0.731
7.422	9.871	0.780
7.610	10.121	0.800
7.803	10.378	0.830
E151 4th 22 DAP	Average ± S.E.	0.787 ± 0.0163
Chl b	Chl b w/ dilution	Chl b (mg/g)
7.216	9.597	0.758
7.924	10.538	0.833
6.542	8.700	0.687
5.549	7.381	0.590
Spk 6th 22 DAP	Average ± S.E.	0.717 ± 0.0516
Chl b	Chl b w/ dilution	Chl b (mg/g)
7.127	9.478	0.758
7.550	10.041	0.783
6.310	8.392	0.663
7.025	9.344	0.747
E151 6th 22 DAP	Average ± S.E.	0.738 ± 0.0261

Below are the values obtained for xanthophyll and carotenoid using the appropriate Lichtenthaler (1987) equation.

$$\text{Xanthophyll and carotenoid} = (1000\text{Abs}_{470} - 1.82A - 85.02B)/198$$

x+c	x+c w/ dilution	x+c (mg/g)
4.331	5.760	0.461
4.713	6.268	0.470
4.572	6.080	0.486
4.051	5.388	0.431
Spk 4th 14 DAP	Average ± S.E.	0.462 ± 0.0116
x+c	x+c w/ dilution	x+c (mg/g)
2.862	3.806	0.304
4.224	5.618	0.449
3.241	4.311	0.345
4.244	5.645	0.452
E151 4th 14 DAP	Average ± S.E.	0.388 ± 0.0373
x+c	x+c w/ dilution	x+c (mg/g)
4.294	5.711	0.451
4.062	5.402	0.432
4.328	5.756	0.443
3.651	4.856	0.384
3.336	4.437	0.355
Spk 4th 22 DAP	Average ± S.E.	0.413 ± 0.0187
x+c	x+c w/ dilution	x+c (mg/g)
3.717	4.943	0.395
3.340	4.442	0.386
3.872	5.150	0.407
4.233	5.630	0.445
4.872	6.480	0.518
E151 4th 22 DAP	Average ± S.E.	0.430 ± 0.0241
x+c	x+c w/ dilution	x+c (mg/g)
4.245	5.646	0.446
4.342	5.775	0.456
4.027	5.355	0.423
4.230	5.626	0.450
Spk 6th 22 DAP	Average ± S.E.	0.444 ± 0.00723
x+c	x+c w/ dilution	x+c (mg/g)
3.891	5.174	0.414
4.160	5.533	0.432
4.190	5.573	0.440
4.685	6.231	0.499
E151 6th 22 DAP	Average ± S.E.	0.446 ± 0.0183

Below are the values obtained for total chlorophyll using the appropriate Lichtenthaler (1987) equation. Total chlorophyll = $7.15\text{Abs}_{663} + 18.71\text{Abs}_{647}$

Chlorophyll a+b	Chl a+b w/ dilution	Chl a+b (mg/g)
18.527	24.641	1.971
22.197	29.522	2.214
24.184	32.165	2.573
16.221	21.573	1.726
Spk 4th 14 DAP	Average ± S.E.	2.121 ± 0.181
Chlorophyll a+b	Chl a+b w/ dilution	Chl a+b (mg/g)
11.101	14.765	1.181
19.983	26.578	2.126
16.007	21.290	1.703
23.386	31.103	2.488
E151 4th 14 DAP	Average ± S.E.	1.875 ± 0.281
Chlorophyll a+b	Chl a+b w/ dilution	Chl a+b (mg/g)
23.672	31.484	2.487
23.536	31.303	2.504
25.100	33.384	2.571
21.577	28.698	2.267
15.204	20.222	1.618
Spk 4th 22 DAP	Average ± S.E.	2.289 ± 0.175
Chlorophyll a+b	Chl a+b w/ dilution	Chl a+b (mg/g)
22.194	29.518	2.361
19.969	26.559	2.311
24.084	32.032	2.531
25.140	33.436	2.641
28.162	37.455	2.996
E151 4th 22 DAP	Average ± S.E.	2.568 ± 0.122
Chlorophyll a+b	Chl a+b w/ dilution	Chl a+b (mg/g)
24.276	32.287	2.551
26.410	35.125	2.775
22.241	29.580	2.337
21.512	28.611	2.289
Spk 6th 22 DAP	Average ± S.E.	2.488 ± 0.111
Chlorophyll a+b	Chl a+b w/ dilution	Chl a+b (mg/g)
22.935	30.504	2.440
24.833	33.028	2.576
22.224	29.558	2.335
26.707	35.520	2.842
E151 6th 22 DAP	Average ± S.E.	2.548 ± 0.110

Below are the values obtained for the ratio of chlorophyll *a/b*. The values for the ratio are a combination of the results from chlorophyll *a* and *b*. Chlorophyll *a/b* ratio= chl *a*/chl *b*

Spk 4th 14 DAP

chl <i>a/b</i>	
	2.412
	1.652
	2.170
	2.467
Average ± S.E.	2.175 ± 0.186

E151 4th 14 DAP

chl <i>a/b</i>	
	2.067
	1.646
	2.345
	2.644
Average ± S.E.	2.176 ± 0.212

Spk 4th 22 DAP

chl <i>a/b</i>	
	1.923
	2.291
	2.427
	2.254
	2.583
Average ± S.E.	2.296 ± 0.110

E151 4th 22 DAP

chl <i>a/b</i>	
	1.964
	2.162
	2.245
	2.304
	2.609
Average ± S.E.	2.257 ± 0.105

Spk 6th 22 DAP

chl <i>a/b</i>	
	2.364
	2.333
	2.400
	2.876
Average ± S.E.	2.493 ± 0.128

E151 6th 22 DAP

chl <i>a/b</i>	
	2.218
	2.289
	2.522
	2.802
Average ± S.E.	2.458 ± 0.132

Appendix B- Nodule organogenesis raw data

The number of nodulation events/cm of 3rd lateral root in Sparkle and E151 3 days after inoculation (DAI). Values represent means with standard errors for study #1-4.

Nodulation Event	Spk	E151	Spk S.E.	E151 S.E.
A	4.33	2.83	1.33	1.46
B	1.17	0.42	0.51	0.26
C	0.17	0.00	0.17	0.00
D	0.58	0.00	0.19	0.00
E	0.08	0.00	0.08	0.00
F	0.00	0.00	0.00	0.00

The number of nodulation events/cm of 3rd lateral root in Sparkle and E151 6 days after inoculation (DAI). Values represent means with standard errors for study #1-4.

Nodulation Event	Spk	E151	Spk S.E.	E151 S.E.
A	7.33	4.83	0.99	0.94
B	4.00	2.50	1.18	0.78
C	0.42	0.50	0.23	0.34
D	1.00	0.00	0.41	0.00
E	0.42	0.00	0.15	0.00
F	0.00	0.00	0.00	0.00

The number of nodulation events/cm of 3rd lateral root in Sparkle and E151 9 days after inoculation (DAI). Values represent means with standard errors for study #1-4.

Nodulation Event	Spk	E151	Spk S.E.	E151 S.E.
A	5.25	5.67	1.23	1.46
B	2.50	2.58	0.96	1.25
C	1.08	0.83	0.34	0.35
D	0.75	0.33	0.37	0.19
E	1.00	0.33	0.44	0.33
F	0.33	0.00	0.23	0.00

The number of nodulation events/cm of 3rd lateral root in Sparkle and E151 12 days after inoculation (DAI). Values represent means with standard errors for study #1-4.

Nodulation Event	Spk	E151	Spk S.E.	E151 S.E.
A	6.58	7.75	0.71	1.36
B	2.75	3.75	0.97	0.87
C	0.92	3.75	0.31	1.02
D	0.42	0.25	0.19	0.13
E	1.33	0.17	0.38	0.17
F	1.92	0.00	0.51	0.00

The number of nodulation events/cm of 3rd lateral root in Sparkle and E151 15 days after inoculation (DAI). Values represent means with standard errors for study #1-4.

Nodulation Event	Spk	E151	Spk S.E.	E151 S.E.
A	6.67	7.00	2.17	2.04
B	2.58	3.00	0.78	1.04
C	0.75	3.55	0.43	1.18
D	0.33	0.27	0.14	0.20
E	0.50	0.00	0.20	0.00
F	2.50	0.00	0.63	0.00

The number of nodulation events/cm of 3rd lateral root in Sparkle and E151 18 days after inoculation (DAI). Values represent means with standard errors for study #1-4.

Nodulation Event	Spk	E151	Spk S.E.	E151 S.E.
A	6.58	5.82	1.12	1.45
B	1.83	1.64	0.56	0.58
C	1.08	2.00	0.53	0.65
D	0.17	0.00	0.17	0.00
E	0.50	0.18	0.20	0.12
F	2.33	0.00	0.77	0.00

The number of nodulation events/cm of 3rd lateral root in Sparkle and E151 21 days after inoculation (DAI). Values represent means with standard errors for study #1-4.

Nodulation Event	Spk	E151	Spk S.E.	E151 S.E.
A	9.83	4.42	2.53	0.76
B	2.08	3.00	0.68	0.80
C	0.67	1.33	0.43	0.43
D	0.33	0.42	0.26	0.26
E	1.00	0.08	0.33	0.08
F	2.83	0.00	0.74	0.00

The total number of infections per centimetre of 3rd lateral root in Sparkle and E151, at pre-determined days after inoculation (DAI). Values represent means with standard errors for study #1-4.

DAI	Spk	E151	Spk S.E.	E151 S.E.
3	6.25	3.25	1.84	1.66
6	13.17	7.83	2.43	1.69
9	10.92	9.67	2.43	2.27
12	13.92	15.67	1.94	1.84
15	13.33	13.82	2.67	3.09
18	12.50	9.64	2.06	2.14
21	16.75	9.25	4.06	1.53

Sparkle and E151 compared at each nodulation event.

Nodulation Event	Days after inoculation						
	3	6	9	12	15	18	21
A	N	N	N	N	N	N	N
B	N	N	N	N	N	N	N
C	N	N	N	Y (E)	Y (E)	N	N
D	Y (S)	N	N	N	N	N	N
E	N	N	N	Y (S)	N	N	N
F	N	N	N	Y (S)	Y (S)	Y (S)	Y (S)

Significant differences between Sparkle and E151 are denoted by N (No) or Y (Yes). Letters in brackets represent which plant line was significantly greater.

The total number of infection events compared amongst each plant line, and between each plant line.

Sparkle & DAI	Difference (Y or N)	E151 & DAI	Difference (Y or N)	Sparkle vs. E151 & DAI	Difference (Y or N)
3 & 6	Y	3 & 6	Y	3	N
6 & 9	N	6 & 9	N	6	N
9 & 12	N	9 & 12	Y	9	N
12 & 15	N	12 & 15	N	12	N
15 & 18	N	15 & 18	N	15	N
18 & 21	N	18 & 21	N	18	N
				21	N

Significant difference amongst each plant line and between each plant line denoted by N (No) or Y (Yes).

Appendix C- Nitrogenase activity raw data

Values measured for Sparkle and E151 14 days after inoculation (DAI). It should be noted that the control plants formed no nodules, therefore the rates of N₂ fixation could not be measured for these plants.

Plant	H2 [ppm] in N2	H2 [ppm] in Ar	ANA (umol H2/hr)	TNA (umol H2/hr)	EAC	N2 Fix (umol N2/hr)	Nodule Dry Weight (g)	Shoot Dry Weight (g)
Spk 1	9.80	11.41	24.59	28.61	0.141	1.34	0.024	0.23
Spk 2	10.80	13.05	27.09	32.74	0.172	1.88	0.028	0.28
Spk 3	7.75	16.04	19.44	40.24	0.517	6.94	0.028	0.314
Spk 4	5.44	7.48	13.65	18.77	0.273	1.71	0.020	0.173
Spk 5	7.50	3.85	18.81	9.65	-0.949	-3.05	0.022	0.209
Spk 6	0.00	3.02	0.00	7.57	1.288	2.52	0.023	0.2253
Spk 7	0.00	0.00	0.00	0.00	0.000	0.00	0.009	0.12
Spk 8	2.67	12.87	6.70	32.28	0.792	8.53	0.028	0.288
Spk 9	3.16	5.17	7.93	12.96	0.388	1.68	0.034	0.3388
Spk 10	5.75	5.55	14.42	13.92	-0.036	-0.17	0.019	0.1948
Average	5.29	7.84	13.26	19.68	0.446	3.07	0.024	0.237
S.E.	1.20	1.65	3.01	4.14	0.148	1.06	0.002	0.0214
E151 1	2.79	0.00	7.00	0.00	-2.014	-2.33	0.000	0.13
E151 2	1.85	0.00	4.64	0.00	1.074	-1.55	0.000	0.1
E151 3	2.31	0.00	5.79	0.00	2.876	-1.93	0.000	0.026
E151 4	0.00	0.00	0.00	0.00	0.000	0.00	0.000	0.067
E151 5	0.00	0.00	0.00	0.00	0.000	0.00	0.000	0.1303
E151 6	0.00	0.00	0.00	0.00	0.000	0.00	0.004	0.3282
E151 7	0.00	0.32	0.00	0.82	1.000	0.27	0.001	0.322
E151 8	0.00	3.12	0.00	7.82	1.000	2.61	0.003	0.241
E151 9	0.00	22.72	0.00	57.00	1.000	19.00	0.003	0.2412
E151 10	0.00	20.07	0.00	50.35	1.000	16.78	0.002	0.25
Average	0.70	4.62	1.74	11.60	0.571	5.52	0.001	0.184
S.E.	0.36	2.82	0.91	7.07	0.202	3.22	0.000	0.0337

Bold values represent statistically significant differences between the lines. Plants highlighted in grey could not be used in the final calculations because these plants either exhibited abnormally high ANA values in comparison to TNA values or abnormally high EAC values which are associated with non-fixing plants.

Values measured for Sparkle and E151 14 days after inoculation (DAI).

Plant	Root Dry Weight (g)	N2 Fix (umol N2/hr)/NDW(g)	N2 Fix (umol N2/hr)/SDW(g)	N2 Fix (umol N2/hr)/RDW(g)
Spk 1	0.1	56.09	5.83	13.41
Spk 2	0.14	66.50	6.72	13.44
Spk 3	0.151	247.70	22.09	45.93
Spk 4	0.108	85.40	9.87	15.81
Spk 5	0.1195	-139.39	-14.61	-25.54
Spk 6	0.113	108.75	11.20	22.33
Spk 7	0.062	0.00	0.00	0.00
Spk 8	0.108	304.49	29.60	78.94
Spk 9	0.1434	48.75	4.95	11.69
Spk 10	0.0679	-9.07	-0.87	-2.48
Average	0.111	114.71	11.28	25.20
S.E.	0.00941	37.29	3.47	8.97
E151 1	0.1	#DIV/0!	-17.95	-23.34
E151 2	0.14	#DIV/0!	-15.46	-11.04
E151 3	0.151	#DIV/0!	-74.21	-12.78
E151 4	0.108	0.00	0.00	0.00
E151 5	0.1195	0.00	0.00	0.00
E151 6	0.113	0.00	0.00	0.00
E151 7	0.062	271.71	0.84	4.38
E151 8	0.108	869.42	10.82	24.15
E151 9	0.1217	5588.20	78.77	156.12
E151 10	0.1237	8391.78	67.13	135.68
Average	0.115	3024.22	22.51	45.76
S.E.	0.0076	1684.49	13.17	26.15

Bold values represent statistically significant differences between the lines. Plants highlighted in grey could not be used in the final calculations because these plants either exhibited abnormally high ANA values in comparison to TNA values or abnormally high EAC values which are associated with non-fixing plants.

Values measured for Sparkle and E151 21 days after inoculation (DAI).

Plant	H2 [ppm] in N2	H2 [ppm] in Ar	ANA (umol H2/hr)	TNA (umol H2/hr)	EAC	N2 Fix (umol N2/hr)	Nodule Dry Weight (g)	Shoot Dry Weight (g)
Spk 1	3.76	4.82	9.43	12.09	0.220	0.89	0.044	0.508
Spk 2	7.44	13.21	18.66	33.13	0.437	4.82	0.045	0.692
Spk 3	6.55	5.35	16.43	13.43	-0.223	-1.00	0.033	0.344
Spk 4	10.53	22.46	26.41	56.34	0.531	9.98	0.055	0.744
Spk 5	5.78	6.24	14.49	15.65	0.074	0.39	0.044	0.6331
Spk 6	2.34	7.06	5.88	17.70	0.668	3.94	0.030	0.3792
Spk 7	1.24	3.79	3.10	9.51	0.674	2.14	0.042	0.6328
Spk 8	1.92	0.00	4.82	0.00	#DIV/0!	-1.61	0.001	0.081
Spk 9	11.32	36.79	28.40	92.28	0.692	21.29	0.106	1.239
Spk 10	3.83	15.85	9.61	39.76	0.758	10.05	0.088	0.9146
Average	5.47	11.56	13.72	28.99	0.507	6.69	0.049	0.617
S.E.	1.11	3.50	2.78	8.78	0.087	2.47	0.009	0.102
E151 1	3.19	2.60	8.01	6.51	-0.231	-0.50	0.009	0.235
E151 2	3.78	3.33	9.47	8.35	-0.134	-0.37	0.006	0.518
E151 3	0.00	0.00	0.00	0.00	0.000	0.00	0.009	0.372
E151 4	0.00	0.00	0.00	0.00	0.000	0.00	0.009	0.464
E151 5	1.04	1.19	2.62	2.97	0.120	0.12	0.010	0.2959
E151 6	3.44	2.69	8.63	6.74	-0.280	-0.63	0.030	0.4892
E151 7	0.00	1.48	0.00	3.70	1.000	1.23	0.025	0.5755
E151 8	0.00	1.41	0.00	3.54	1.000	1.18	0.020	0.6005
E151 9	3.64	5.59	9.13	14.01	0.348	1.63	0.029	0.784
E151 10	3.04	8.20	7.63	20.56	0.629	4.31	0.044	0.897
Average	1.81	2.65	4.55	6.64	0.442	1.21	0.0191	0.523
S.E.	0.55	0.81	1.37	2.03	0.166	0.58	0.00399	0.0649

Bold values represent statistically significant differences between the lines. Plants highlighted in grey could not be used in the final calculations because these plants either exhibited abnormally high ANA values in comparison to TNA values or abnormally high EAC values which are associated with non-fixing plants.

Values measured for Sparkle and E151 21 days after inoculation (DAI).

Plant	Root Dry Weight (g)	N2 Fix (umol N2/hr)/NDW(g)	N2 Fix (umol N2/hr)/SDW(g)	N2 Fix (umol N2/hr)/RDW(g)
Spk 1	0.166	20.17	1.75	5.35
Spk 2	0.156	107.22	6.97	30.93
Spk 3	0.115	-30.31	-2.91	-8.70
Spk 4	0.187	181.39	13.41	53.35
Spk 5	0.1796	8.74	0.61	2.15
Spk 6	0.1368	131.29	10.39	28.79
Spk 7	0.1653	51.10	3.38	12.92
Spk 8	0.021	-1605.32	-19.82	-76.44
Spk 9	0.287	200.89	17.19	74.20
Spk 10	0.2579	113.70	10.99	38.97
Average	0.167	101.81	8.09	30.83
S.E.	0.0232	25.03	2.09	8.71
E151 1	0.103	-55.64	-2.13	-4.86
E151 2	0.215	-62.15	-0.72	-1.73
E151 3	0.147	0.00	0.00	0.00
E151 4	0.167	0.00	0.00	0.00
E151 5	0.1214	12.37	0.40	0.98
E151 6	0.1948	-21.12	-1.29	-3.23
E151 7	0.2288	49.98	2.15	5.40
E151 8	0.2114	60.24	1.97	5.59
E151 9	0.218	56.13	2.08	7.47
E151 10	0.275	97.96	4.81	15.67
Average	0.188	39.53	1.63	5.01
S.E.	0.0167	13.88	0.65	2.11

Bold values represent statistically significant differences between the lines. Plants highlighted in grey could not be used in the final calculations because these plants either exhibited abnormally high ANA values in comparison to TNA values or abnormally high EAC values which are associated with non-fixing plants.

Values measured for Sparkle and E151 28 days after inoculation (DAI).

Plant	H2 [ppm] in N2	H2 [ppm] in Ar	ANA (umol H2/hr)	TNA (umol H2/hr)	EAC	N2 Fix (umol N2/hr)	Nodule Dry Weight (g)	Shoot Dry Weight (g)
Spk 1	2.29	0.00	5.74	0.00	#DIV/0!	-1.91	0.061	1.579
Spk 2	9.22	6.78	23.14	17.00	-0.361	-2.05	0.070	1.557
Spk 3	11.85	18.05	29.73	45.28	0.343	5.18	0.087	1.504
Spk 4	9.53	21.84	23.91	54.77	0.563	10.29	0.065	1.108
Spk 5	12.87	23.20	32.29	58.19	0.445	8.63	0.092	2.594
Spk6	14.85	34.90	37.26	87.54	0.574	16.76	0.068	1.929
Spk 7	14.49	32.75	36.35	82.15	0.557	15.27	0.188	3.315
Spk 8	15.21	53.07	38.16	133.12	0.713	31.66	0.223	3.949
Spk 9	3.56	15.19	8.92	38.11	0.766	9.73	0.030	0.7272
Spk 10	3.31	16.57	8.31	41.56	0.800	11.08	0.036	0.8274
Average	9.72	22.23	24.38	55.77	0.595	13.57	0.092	1.909
S.E.	1.59	4.78	4.00	11.99	0.056	2.89	0.020	0.337
E151 1	2.44	0.00	6.12	0.00	#DIV/0!	-2.04	0.025	0.779
E151 2	0.91	0.00	2.28	0.00	#DIV/0!	-0.76	0.015	0.689
E151 3	2.38	8.29	5.98	20.80	0.712	4.94	0.034	0.631
E151 4	3.61	11.78	9.07	29.55	0.693	6.83	0.030	0.731
E151 5	3.28	15.21	8.24	38.14	0.784	9.97	0.084	1.005
E151 6	0.00	0.00	0.00	0.00	0.000	0.00	0.014	0.317
E151 7	6.69	22.33	16.79	56.01	0.700	13.07	0.086	1.274
E151 8	0.00	0.31	0.00	0.78	1.000	0.26	0.001	0.203
E151 9	0.00	7.52	0.00	18.86	1.000	6.29	0.009	0.6325
E151 10	3.56	19.35	8.92	48.53	0.816	13.20	0.043	0.6346
Average	2.29	8.48	5.74	21.27	0.713	6.82	0.0341	0.69
S.E.	0.68	2.69	1.70	6.74	0.111	1.81	0.00934	0.0964

Bold values represent statistically significant differences between the lines. Plants highlighted in grey could not be used in the final calculations because these plants either exhibited abnormally high ANA values in comparison to TNA values or abnormally high EAC values which are associated with non-fixing plants.

Values measured for Sparkle and E151 28 days after inoculation (DAI).

Plant	Root Dry Weight (g)	N2 Fix (umol N2/hr/NDW(g)	N2 Fix (umol N2/hr)/SDW(g)	N2 Fix (umol N2/hr)/RDW(g)
Spk 1	0.249	-31.39	-1.21	-7.69
Spk 2	0.225	-29.24	-1.31	-9.10
Spk 3	0.207	59.56	3.45	25.03
Spk 4	0.159	158.26	9.28	64.70
Spk 5	0.379	93.83	3.33	22.78
Spk6	0.242	246.44	8.69	69.25
Spk 7	0.499	81.20	4.61	30.59
Spk 8	0.536	141.95	8.02	59.06
Spk 9	0.1096	323.24	13.38	88.77
Spk 10	0.1219	306.19	13.40	90.93
Average	0.273	176.34	8.02	56.39
S.E.	0.0474	36.44	1.43	9.69
E151 1	0.195	-81.63	-2.62	-10.47
E151 2	0.185	-50.61	-1.10	-4.10
E151 3	0.169	145.29	7.83	29.23
E151 4	0.158	227.58	9.34	43.21
E151 5	0.245	118.66	9.92	40.68
E151 6	0.15	0.00	0.00	0.00
E151 7	0.261	152.02	10.26	50.09
E151 8	0.105	261.09	1.29	2.49
E151 9	0.115	739.50	9.94	54.66
E151 10	0.1421	309.20	20.81	92.91
Average	0.173	244.17	8.67	39.16
S.E.	0.0161	78.35	2.25	10.56

Bold values represent statistically significant differences between the lines. Plants highlighted in grey could not be used in the final calculations because these plants either exhibited abnormally high ANA values in comparison to TNA values or abnormally high EAC values which are associated with non-fixing plants.

Appendix D- Grafting raw data

Grafting results for studies 1-4.

Plant #	Type of graft & # of nodule lobes found			
	Spk/Spk	E151/Spk	Spk/E151	E151/E151
1	232	102	38	56
2	135	116	54	14
3	208	211	0	21
4	3	0	NA	1
5	205	210	13	1
6	185	170	71	49
7	394	236	45	19
8	174	233	8	33
9	12	104	62	12
10	240	58	29	19
11	336	206	NA	82
12	163	223	NA	23
13	227	239	220	190
14	235	152	30	175
15	215	190	9	75
16	219	459	116	118
Mean	198.94	181.81	53.46	55.50
S.E. (+/-)	24.33	25.48	16.41	14.77

NA represents grafts that did not survive.

Grafts were performed 4 DAP.

Grafts were inoculated with 5% HUP⁺ rhizobium (5 DAP).

Grafts were harvested 21 DAI.

Survival rates of the grafts performed.

Type of Graft	Initial # of grafts	Final # of grafts	% Survival
Spk/Spk	16	16	100
E151/Spk	16	16	100
Spk/E151	16	13	81
E151/E151	16	16	100